

Recovery from oxidative stress: insights into stress granule disassembly process

Dissertation
zur Erlangung des akademischen Grades
Doctor rerum naturalium
(*Dr. rer. nat.*)

eingereicht am
Fachbereich Chemie der
Fakultät für Mathematik, Informatik und Naturwissenschaften
der Universität Hamburg

vorgelegt von
Sarada Das, M. Sc.
geboren in West Bengal (Indien)

Hamburg
2022

Die vorgelegte Dissertation wurde von *April 2018 until November 2021* am Institut für Biochemie und Molekularbiologie am Fachbereich Chemie der Fakultät für Mathematik, Informatik und Naturwissenschaften an der Universität Hamburg unter Anleitung von Prof. Dr. Zoya Ignatova angefertigt.

The submitted dissertation was conducted from April 2018 until November 2021 at the Institute of Biochemistry and Molecular Biology at the Department of Chemistry of the Faculty of Mathematics, Informatics, and Natural Sciences at the University of Hamburg under the supervision of Prof. Dr. Zoya Ignatova.

Dissertationsgutachter / *dissertation reviewers:*

1. Gutachterin / *first reviewer:* **Prof. Dr. Zoya Ignatova**, Institute of Biochemistry and Molecular Biology, Universität Hamburg
 2. Gutachter / *second reviewer:* **Prof. Dr. Meliha Karsak**, Center for Molecular Neurobiology, Universität Hamburg
- Date of Disputation : 29-04-2022

Teile dieser Arbeit wurden in folgenden Publikationen veröffentlicht:

Parts of this work were published in the following scientific articles:

Research articles

Amila Zuko, Moushami Mallik, Robin Thompson, Emily L. Spaulding ... **Sarada Das**, Divita Kulshrestha, Robert W. Burgess, Zoya Ignatova, Erik Storkebaum. 2021 tRNA overexpression rescues peripheral neuropathy caused by mutations in tRNA synthetase. *Science* (80-) 373: 1161–1166

Sarada Das, Leonardo Santos, Antonio Virgilio Failla, Zoya Ignatova. 2022. mRNAs sequestered in stress granules recover nearly completely for translation. (*Submitted and currently under revision*)

Sarada Das, Amila Zuko, Robin Thompson, Erik Storkebaum, Zoya Ignatova. 2022. *Immunoprecipitation Assay to Quantify Amounts of tRNA associated with their Interacting Proteins in Tissue and Cell Culture. Bio-protocol (In press)*

Conference proceedings

Das S, Bharti N., Virgilio A. Ignatova Z. Molecular mechanism of stress granule assembly and disassembly. *EMBO: Protein Synthesis and Translational Control*. 4th-7th September 2019; Heidelberg, Germany.

CONTENTS

List of Figures	iv
List of Tables	v
Abbreviation	vii
Zusammenfassung	ix
Abstract	xi
1 Introduction	2
1.1 Cellular Stress: What is the risk?.....	2
1.2 Cellular Stress Response	2
1.2.1 Protein translation upon stress condition.....	3
1.2.2 SG: dynamic cytoplasmic entity formed upon stress.....	4
1.2.2.1 Biochemistry and Function of SG.....	7
1.2.2.2 Protein composition of SGs	8
1.2.2.3 RNA Composition and its role in SGs	9
1.3 Role of RNA modification upon stress.....	10
1.3.1 m ⁶ A RNA and SG formation.	12
1.3.2 m ⁶ A regulator: YTHDF protein and SG formation.	13
1.3.3 SG Assembly and Disassembly.	13
1.4 RNA and Protein Interactions.	15
1.5 Aim of the thesis	17
2 mRNA recovery from SGs and dynamics of m⁶A regulation of its clients	18
2.1 m ⁶ A -RNA assembly and disassembly in SG.....	18
2.2 Material and Methods	18
2.2.1 Cell Lines, Growth Conditions and Immunostaining.....	19
2.2.2 Polysome Profiling, RNA Isolation and RNA-seq Library Preparation.....	20
2.2.3 Sequencing analysis.	20
2.2.4 m ⁶ A peak detection.	21
2.2.5 Data Availability.	21
2.3 Results.	22
2.3.1 Biphasic process of SG Assembly and Disassembly.	22
2.3.2 SG-protected mRNAs recover nearly completely for translation.....	23
2.3.3 Stress induced m ⁶ A profile on mRNA regulates its abundance in SGs.	25

2.3.4 SG clients exhibit only modest effect upon stress induced methylation dysregulation during recovery.	27
2.3.5 Physical Basis of differential m ⁶ A methylation SG-mRNA clients.	28
2.3.6 mRNA is unstructured at m ⁶ A, but more structured in the near vicinity of m ⁶ A modification.	29
2.4 Discussion.	32
3 Influence of YTHDF3 domains on its association with SGs.	33
3.1 m ⁶ A reader YTHDF proteins regulate key features in the cell.	33
3.2 Material and Methods	34
2.2.1 Cell Lines and Growth Conditions	34
2.2.2 Cloning and expression of YTHDF3, YTHDF2, YTHDF3 mutants.	35
2.2.3 Transfection.	35
2.2.4 Immunostaining.	35
3.3 Results	35
2.3.1 YTHDF3 colocalizes to SGs upon arsenite stress condition.	35
2.3.1 Structural analysis of YTHDF3 protein.	36
2.3.1 Reader YTHDF3-domain specificity to SG association.	38
3.4 Discussion.	39
4 Immunoprecipitation Assay to Quantify Amounts of tRNA associated with their Interacting Proteins in Tissue and Cell Culture.	41
4.1 Methods to study RNA and Protein Interactions.	41
4.2 Methods to study tRNA-Protein interaction.	41
4.2.1 tRNA immunoprecipitation approach.	43
4.3 Methodology.	43
4.3.1 Sample Preparation.	43
4.3.2 Preparation of magnetic beads and antibody coupling	45
4.3.3 Immunoprecipitation (IP).	47
4.3.4 Identification and quantification of the bound tRNAs in the IP.	46
4.3.5 Quantification of the GlyRS protein in the IP.	47
4.4 Data analysis.	51
4.5 Discussion.	52
5 General discussion	54
5.1 SG assembly, disassembly with respect to m ⁶ A modified RNA.	54

5.2 Difference in translation recovery of methylated and unmethylated SG clients.....	55
5.3 Method development for tRNA-protein interaction.....	57
References.....	58
List of the hazardous substances used by GHS (hazard symbols, H&P statements).	x
Acknowledgments	xv

List of Figures

Figure 1.1: Translation Initiation Pathway Schematic in Eukaryotes.	3
Figure 1.2: Stress granule dynamics.	5
Figure 1.3: Chart showcasing the diverse pathways by which RNA modifications respond to oxidative stress.	10
Figure 1.4: Classification of RNA–protein interactions, divided into four classes according to the characteristics of their relationships.	15
Figure 2.1: m ⁶ A-signal colocalizes later with SGs and upon stress relief dissipates first followed by clearance of the cores at a later time scale.	22
Figure 2.2: Nearly all mRNAs deposited in SGs are translated upon stress relief.	23
Figure 2.3: Transcription inhibition alters methylation pattern of SG clients and reduces its abundance.	25
Figure 2.4: Abundance of transcripts in translation fraction at different time point after stress relief (30m and 4h) treated and untreated with Actinomycin D.	26
Figure 2.5: Physical basis of differential m ⁶ A methylation of SG mRNAs.	27
Figure 2.6: mRNAs exhibit higher structural propensity in the m ⁶ A vicinity.	29
Figure 3.1: YTH domains of human DF proteins show similar potential at the RNA recognition and high sequence homology.	33
Figure 3.2: Reader protein YTHYTHDF3 co-localizes to SGs upon 500 μM Arsenite stress.	36
Figure 3.3: Structural prediction for potent Prion-like domain in YTHDF3 protein.	37
Figure 3.4: Diagrammatic representation of YTHDF3 (A) and YTHDF2(B) protein structure prediction obtained from MobiDB.	37
Figure 3.5: Visualization of YTHDF3 mutants upon Arsenite stress.	38
Figure 4.1: Schematic for the known RNA centric method to study RNA-protein interactions.	42
Figure 4.1: Schematic of the tRNA-Immunoprecipitation approach.	45
Figure 4.2: Quantification of tRNA bound to GlyRS in HEK cells.	50
Figure 4.3: Quantification of tRNA bound to GlyRS in brain tissue from <i>Gars</i> ^{C201R/+} mice (C201R-IP) and wildtype littermate (WT-IP).	52

List of Tables

Table 4.1: Example of DNA primers for <i>in vitro</i> T7 promoter-driven synthesis of tRNA ^{Gly} GCC.	48
Table 4.2: Sequences of the Atto565-labeled DNA probes used in the Northern blot experiment.	48

Abbreviations

CSR	Cellular Stress Response
SG	Stress Granule
eIF	Eukaryotic initiation factor
LLPS	liquid-liquid phase separation
P bodies	Processing bodies
IDR	Intrinsically disordered region
LCR	Low complexity region
PrLD	Prion like domain
AARS	aminoacyl-tRNA-synthetase
40S	small ribosomal subunit
60S	large ribosomal subunit
PAGE	polyacrylamide gel electrophoresis
TC	ternary complex
UTR	untranslated region
Cds	Coding sequence
WT	wild-type
PIC	43S preinitiation complex
tRNA	Transfer RNA
mRNA	Messenger RNA
IP	Immunoprecipitation
YTHDF	YTH-domain family
CMT	Charcot-Marie-Tooth
RNA	Ribonucleic acid
UV	ultraviolet
CLIP	Crosslinking and immunoprecipitation
RIP	RNA immunoprecipitation
RPKM	Reads per kilobase of transcripts, per million mapped reads

Zusammenfassung

Stressgranula (SG) sind cytoplasmatische Ribonukleoproteine, die als membranlose Kondensate durch Flüssig-Flüssig-Phasentrennung (LLPS) gebildet werden. Sie bilden sich als Reaktion auf Stressreize und werden als eine der wichtigsten zellulären Lösungen gegen Stress angesehen. Ihr vorübergehendes Vorhandensein endet mit dem Stressabbau, aber ein dauerhaftes Vorhandensein kann zu pathologischen Aggregationen und degenerativen Effekten führen. SGs sind komplexe dynamische makromolekulare Ansammlungen aus Proteinen und RNA-Molekülen, die durch additive RNA-Protein-, Protein-Protein- und RNA-RNA-Wechselwirkungen assemblieren.

Jüngste Studien haben gezeigt, dass die m⁶A-Modifikation die Assoziation von mRNAs in SGs durch die Bindung von YTHDF-Proteinen verstärken kann. Sowohl der Zusammenbau als auch der Abbau sind streng kontrollierte Prozesse, doch es bleibt unklar, ob sich die mit SG-assoziierten mRNAs in SGs nach einer Stressentlastung vollständig für die Translation erholen. In dieser Studie haben wir mit Hilfe von RNA-Sequenzierungen der vom Ribosom translatierten Fraktionen in menschlichen Zelllinien die Fraktion der Transkripte, die sich nach Stressabbau vollständig erholen, ermittelt. Die Mehrheit der SG-Transkripte war in dieser Fraktion vorhanden, wobei die methylierten SG-Klienten einen signifikant höheren Anteil hatten. Ein höherer Anteil der m⁶A-modifizierten mRNAs erholte sich für die Translation im Vergleich zu unmodifizierten mRNAs, d.h. 95% gegenüber 84%. Bei der Analyse der mRNA-Strukturen stellten wir fest, dass die m⁶A-Modifikation den Strukturierungsgrad von Nukleotiden in ihrer unmittelbaren Umgebung erhöht. Es wird zum ersten Mal berichtet, dass SG-sequestrierte mRNAs nach Stressabbau fast vollständig disassemblieren und dass sich die m⁶A-Modifikation vorteilhaft auf die Fähigkeit der mRNAs zur Wiederherstellung der Translation auswirkt, vermutlich durch eine m⁶A-getriebene strukturelle Stabilisierung.

Darüber hinaus haben wir die Bindung des YTHDF-Proteins an SGs untersucht, um herauszufinden, wie unterschiedliche Sequenzen und Zusammensetzungen der Prion-ähnlichen Domäne (PrLD) die Bindungsfähigkeit des Proteins verändern und die Phasentrennung der m⁶A-RNA durch YTHDF3 weiter beeinflussen können. Dies unterstreicht die multivalenten homotypischen und heterotypischen Wechselwirkungen, die für den Zusammenbau von SGs erforderlich sind. Der biochemische Assay wurde verwendet, um die Bindung von tRNA^{Gly} an die bei der Charcot-Marie-Tooth-Krankheit betroffene CMT-Mutante Glycin-tRNA-Synthetase

(GlyRS) im Vergleich zum Wildtyp-Synthetaseprotein zu unterscheiden, was zeigt, dass ein großer Teil der zellulären tRNA^{Gly} sequestriert wird und somit für die Translation nicht zur Verfügung steht.

ABSTRACT

Stress granules (SGs) are cytoplasmic ribonucleoproteins composed in membrane less condensates, as a result of liquid-liquid phase separation (LLPS). They assemble in response to stress stimuli and are pivotal in maintaining stress response. Their transient presence ends when stress is relieved but their permanent presence can lead to pathological aggregation and degenerative effects. SGs are complex dynamic macromolecular assemblies composed of proteins and RNA molecules which are targeted due to an additive interaction of potential RNA-protein, protein-protein and RNA-RNA interactions.

Recent studies have shown that the m⁶A modification of mRNAs can increase their partitioning into SGs mediated through binding of YTHDF proteins. Both assembly and disassembly are tightly controlled processes, yet, it remains elusive whether mRNAs in SGs completely recover for translation following stress relief. Here in this study, using RNA-seq of translated fractions in human cell line, we reported the recovery fraction after stress relief. Majority of the SG transcripts were present in this fraction, with a significant advantage harbored by the methylated SG clients. A higher fraction of the m⁶A-modified mRNAs recovered for translation compared to unmodified mRNAs, i.e. 95% vs 84%, respectively. Considering structural mRNA analysis, we found that the m⁶A modification enhances structuring at nucleotides in its close vicinity. We provide evidence that SG-sequestered mRNAs disassemble nearly completely and the m⁶A modification may display some advantage to the mRNAs in their recovery for translation likely by m⁶A-driven structural stabilization.

Additionally, we investigated the binding of YTHDF protein to SGs to examine how distinct sequence and composition of Prion-like-domain (PrLD) could alter its binding capability and may further influence the phase separation of m⁶A-RNA mediated by YTHDF3. This emphasizes on multivalent homotypic and heterotypic interactions required for SG assembly.

The study also covers a new method development, in the field of tRNA-protein interaction studies to decipher the binding affinity between mutant and wild-type tRNA binding protein. The biochemical assay was used to distinguish the binding of tRNA^{Gly} to the CMT disease mutant glycine-tRNA-synthetase (GlyRS) concerned in Charcot-Marie-Tooth disease, compared to wild-type synthetase protein, demonstrating sequestration a large fraction of cellular tRNA^{Gly} and thus depleting them for translation.

1 Introduction

1.1 Cellular stress: What is the risk?

The capability to cope with unfavorable conditions is an essential potential of each organism. The mobile stress response equipment is wide spread and extraordinarily conserved consequently illustrating the critical importance of the defense device to microorganism, flora and animals alike (Kültz, 2004). Since the most important molecular players which might be substantially upregulated as a response to the stressor additionally have important features at everyday physiological situations the conditions of “stress” need to be defined. In step with the Dictionary of Bioscience stress is “a stimulus or succession of stimuli of such magnitude as to tend to disrupt the homeostasis of the organism.” Stress is, however, not only has an affect at the organismic level but additionally at the cellular level. Therefore, cellular stressors can be described as external elements that disturb or upset the homeostasis of the cell (Kültz, 2004; Poljšak & Milisav, 2012).

Most of the stressors are ambivalent in their effects, for example: heavy metals and oxidants play important roles in cellular regulations. But when the critical levels are crossed, a real stress situation is encountered by the cell and during which the heat shock response is elicited. Oxidants in the cell are formed as a product of aerobic metabolism, but it becomes threatening when produced in an elevated level in pathophysiological conditions (Sies, 1997)(Finkel & Holbrook, 2000; Sies, 1997).

The study of mechanisms of adaptation to stressful and extreme environments provides the basis for addressing environmental health problems, performing sound toxicological risk assessment, efficiently utilizing bioindication processes to monitor global environmental change, and clinically utilizing the inherent healing capacity of the adaptive response to stress. Detailed study of the cellular stress response (CSR) has revealed diverse molecular mechanisms.

1.2 Cellular stress response

The evolutionarily conserved principles of the CSR are critical for understanding the molecular mechanisms of cellular adaptation to stress. The CSR was first called the heat shock response because about four decades ago, work with fruit flies revealed that transient heat exposure elicited a unique pattern of chromosomal puffing(Ritossa, 1962). Later, heat-induced changes in chromosomal structure were associated with increased expression of a class of genes called heat shock genes(Lindquist, 1986). Spread among several chromosomes as more than just single family member, these genes contribute to cellular vitality under normal conditions and also during stress.

Even though initial observations were made in fruit flies, heat shock genes are conserved in all living organisms (Voellmy, 1984).

The response is specific that occur during various kinds of stress like: ultraviolet light exposure, oxidant injury, DNA damage, and glucose deprivation. Some of these responses have intersections with the heat shock response, and others have a unique impression. An intriguing aspect is how many divergent factors trigger a common cellular response. The unified result is enhanced cellular protection from otherwise unfavorable and lethal conditions. Curiously, one stressor can lead to cellular protection from other stressors. For example, heavy metal exposure will result in a response that confers protection from heat (Heckathorn *et al*, 2004). Cellular stress induces protein impairment, which signals the cell to shut down usual transcriptional and translational activities and to switch toward expression of heat shock and other stress proteins (Bresson *et al*, 2020; Paschen *et al*, 2007; Vihervaara *et al*, 2018; Aprile-Garcia *et al*, 2019).

When the cellular stress response is triggered, specific transcription factors are activated. Current evidence suggests that two-thirds or more of heat-inducible genes require activation of an intracellular protein called the heat shock factor (HSF1) (Vihervaara & Sistonen, 2014; Dai, 2018). Once HSF1 associates with the promoter region of a stress gene, it binds DNA with other transcription factors so as to amplify RNA polymerase activity. Subsequently, higher levels of messenger RNA (mRNA) encoded by the stress genes are produced and ribosomes preferentially translate these stress mRNAs into stress proteins (Solís *et al*, 2016; Mahat *et al*, 2016; Ananthan *et al*, 1986).

1.2.1 Protein translation at stress

Protein synthesis in eukaryotes is segmented in three broad distinct steps, namely, mRNA translation initiation, elongation and termination (Haselkorn & Rothman-Denes, 1973; Richter & Isono, 1977). All the process is highly regulated by sophisticated machinery out of which the most rate limiting step tends to be translation initiation (Aylett & Ban, 2017; Merrick & Pavitt, 2018). Translation initiation begins with coming together of at-least 10 eukaryotic initiation factors (eIFs) as shown in figure 1.1. Numerous studies have highlighted that the transcriptome and its proteome does not correlate with each other always, especially during variation in physiological conditions of the cell. For example, in cancer cells, the expression and functions of eIFs are hampered, resulting in the inhibition of global translation and enhancement of translation of subsets of

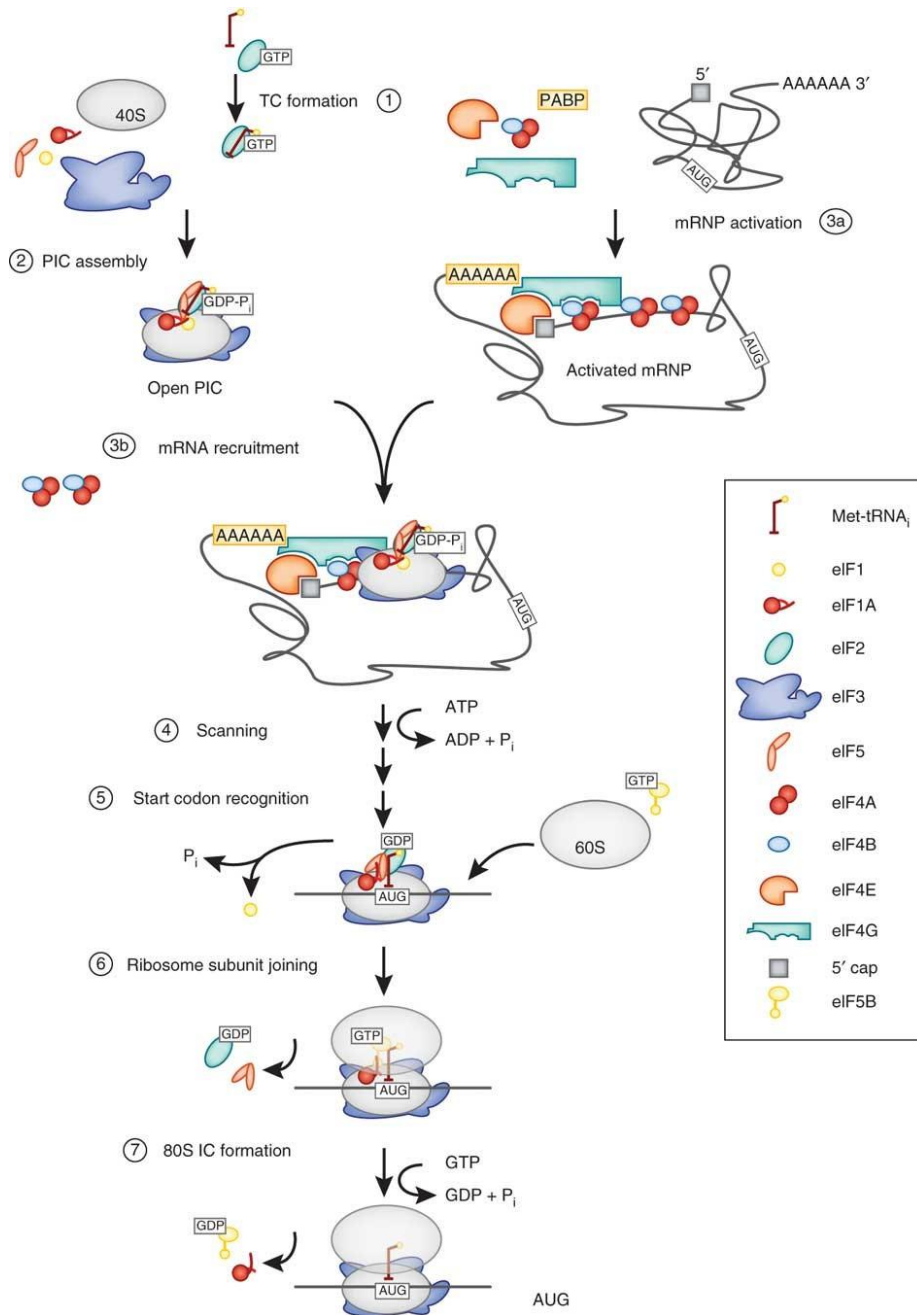


Figure 1.1: Translation Initiation Pathway Schematic in Eukaryotes: (1) Initiation begins with the formation of the TC containing eIF2•GTP and the initiator tRNA. The ternary complex is employed to the 40S subunit with the help of eIFs 1, 1A, 3 and 5 to form the PIC (2). Meanwhile, the mRNA is bound by the eIF4 factors and the PABP to form an activated mRNP (3a), which is then recruited to the PIC (3b). Once bound at the 5' end of the mRNA, the PIC scans to locate the start (AUG) codon (4). Start codon recognition triggers eIF1 release and conversion of eIF2 to its GDP-bound state, arresting the scanning process (5). eIF2•GDP and eIF5 dissociate, clearing the way for eIF5B to mediate joining of the 60S subunit (6). Subunit joining is followed by GTP hydrolysis by eIF5B and factor dissociation to form the 80S IC (7). Adapted from (Aitken & Lorsch, 2012).

mRNAs by alternative mechanisms (Chu *et al*, 2016). The microenvironment of the cell can also be greatly affected during various stress, the spatial and temporal resolution of translation control

may present further effects. The dysregulation of mRNA translation mechanisms is increasingly being exploited as a target to treat various disease pathologies (Tahmasebi *et al*, 2018; Kapur & Ackerman, 2018; Kim *et al*, 2019; Eshraghi *et al*, 2021).

One of the most critical Eukaryotic Initiation Factor that has been heavily reported to have crucial role in stress regulation is eIF2alpha (Wek *et al*, 2006; Boye & Grallert, 2020; Sidrauski *et al*, 2015). Its role has been classified in the integrated stress response along with its co-partners such as eIF4F, with its role in cap-binding and eIF4G and eIF4E for their efficient role in translation. Other mechanisms include eIF3 subunit interactions with S6K1 and mTOR and eIF5A's necessary activation through posttranslational modification, important to the mediation of cell proliferation, apoptosis, and inflammatory response (Sharma *et al*, 2016; Silvera *et al*, 2010).

During cellular stress, one or more kinases phosphorylate eIF2alpha leading to reduced concentration of eIF2-guanosine triphosphate (GTP)-transfer ribonucleic acid for methionine tRNA (Met)), the ternary complex that loads tRNA (Met) onto the small ribosomal subunit to initiate protein translation. In lack of ternary complex in the eukaryotic cell, the related RNA-binding proteins TIA-1 and TIAR promote the assembly of a noncanonical preinitiation complex (PIC) that lacks eIF2-GTP-tRNA (Met). These translationally incompetent noncanonical PIC are sorted into discrete cytoplasmic domains known as Stress Granules (SGs) (Collier *et al*, 1988; Arrigo *et al*, 1988; Collier & Schlesinger, 1986; Kedersha *et al*, 1999b; Nover *et al*, 1983, 1989).

1.2.2 Stress Granules: dynamic cytoplasmic entity

Stress Granules (SGs) have been observed in multiple organisms truly stating their important role in some kind of regulatory function they have organisms like yeast (such as *Saccharomyces pombe*), protozoa (*Trypanosoma brucei*) and metazoan (such as *Homo sapiens* and *Caenorhabditis elegans*) presence of SGs have been reported earlier (Kramer *et al*, 2008; Kuo *et al*, 2020; Souquere *et al*, 2009; Groušl *et al*, 2009). They have even been observed in plants and in chloroplasts (Chodasiewicz *et al*, 2020; Jang *et al*, 2020), suggesting that they may be assembled in prokaryotes as well.

SGs are basically non-membranous cytoplasmic foci ranging in size from 0.1 to 2.0 μm , composed of non-translating messenger ribonucleoproteins (mRNPs) (Castellani *et al*, 2011; Groušl *et al*, 2009). They tend to rapidly aggregate in cellular matrix when exposed to stressful environmental conditions (Nover *et al*, 1983, 1989). Their assembly can be triggered by various kind of environmental changes including heat shock, oxidative stress, hyperosmolarity, viral infection, and UV irradiation, but at the same time they have not been reported to form under X-irradiation

or DNA-damaging agents(Kedersha & Anderson, 2007; Kedersha *et al*, 2008; Beckham & Parker, 2008). Their mRNA composition is selective— they contain transcripts encoding housekeeping genes but exclude those encoding stress-induced genes such as HSP70(Kedersha and & Anderson, 2002). SGs have been reported in both cultured cell lines and complex tissues(Grabocka & Bar-Sagi, 2016).

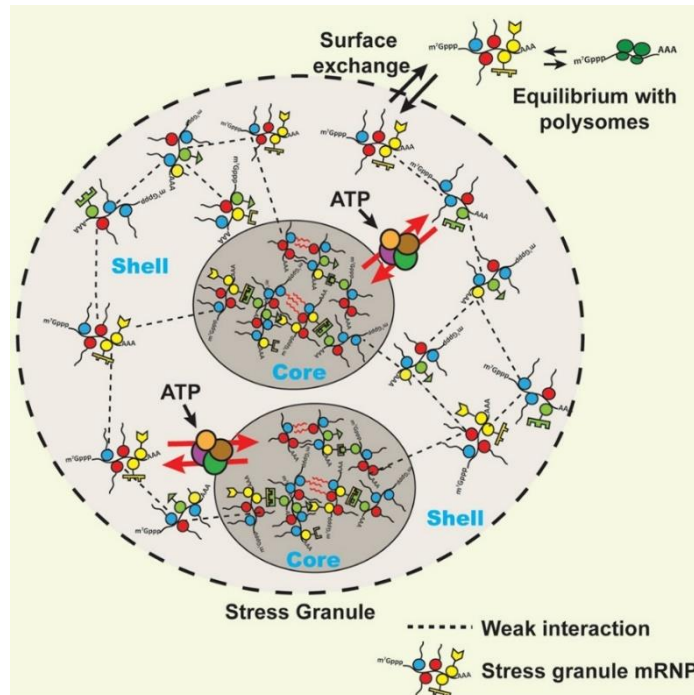


Figure 1.2: Stress Granule dynamics (adapted from S. Jain, 2016)

Stress induces phosphorylation of the translation initiation factor eIF2 α which further promotes induces SG assembly via delayed or completely stopped translation initiation in cells. However, this does not affect the elongating ribosomes, which eventually run off resulting in polyadenylated circularized mRNA transcripts which are still bound to the preinitiation machinery (comprising 40S ribosomal subunits and eIF3) (Anderson & Kedersha, 2008). These mRNAs which are abortively initiated mRNPs results in the formation of SGs. Also, when eIF4A function is blocked, translational initiation is stalled and SGs are assembled, even in the absence of eIF2 α phosphorylation(Anderson & Kedersha, 2008). Experiments where fluorescence recovery after photobleaching revealed that the half-life of stress-granule-associated RNA binding proteins is very brief, it is on the order of seconds to minutes, and via time-lapse microscopy it is even revealed that SGs can last for hours in the cellular matrix. This rapid shuttling of protein and RNA within SGs makes for a transient association with their mRNA contents(Kedersha & Anderson, 2007) . Unlike other types of RNA granule, such as germ cell granules or neuronal granules, SGs are not sites of long-term mRNP storage(Mollet *et al*, 2008). With recent development in this field it has been evidenced that the RNA recruitment can be both concentration driven due to the high local concentration of the non-translating mRNA; and also can be due the ability of several RBP to actively recruit them(Matheny *et al*, 2021).

Recent development has reviewed that stress causes RNAs, RBPs, and translational machinery to phase separate into SGs. SGs assemble through liquid-liquid phase separation (LLPS) from interactions distributed across a core protein-RNA interaction network (Molliex *et al*, 2015; Duan *et al*, 2019). In response to a rise in intracellular free RNA concentration, the central node of the network - G3BP1 functions as a molecular switch triggering RNA-dependent LLPS (Yang *et al*, 2020). When misfolded proteins are abundant, they can contaminate the healthy stress granule and alter its physical properties, causing it to non-dynamic and become more gel-like or solid. If aberrant SGs cannot be repaired, they are targeted for degradation. The failure of this quality control process is thought to underlie onset of neurodegenerative diseases (Mateju *et al*, 2017).

1.2.2.1 Biochemistry and Function of SGs

SGs' composition primarily consists of the stalled 48S complexes containing bound mRNAs derived from disassembling polysomes. These contain polyadenylated RNA bound to pre-initiation complex and factors as explained in the earlier section (such as eIF4E, eIF3, eIF4A, eIFG) and small, but no large ribosomal subunits. The first and defining class of SG components consists of stalled initiation complexes, still bound to mRNA and recruited to SGs from disassembling polysomes. This class includes mRNA transcripts, eIF3, eIF4F (comprising eIF4E, eIF4A and eIF4G), eIF4B, small ribosomal subunits and PABP-1. These core SG components are universal markers for all SGs. In addition to these core components, SGs components can vary across different cell types and also varies with the nature and duration of stress experienced by the cell. RNA-binding proteins, transcription factors, RNA helicases, nucleases, kinases and signaling molecules have been reported to accumulate in SGs, it has also been reported that recruitment of signaling proteins into SGs has an influence on cell survival (Kedersha *et al*, 2013). More recently, SGs have been shown to contain the Argonaute proteins, microRNAs, a number of mRNA-editing enzymes, and proteins required for transposon activity (Hwang *et al*, 2019; Leung *et al*, 2006).

The dynamic nature of SGs suggests that they are the major sites of mRNA triage, wherein individual mRNAs are possibly dynamically sorted for post stress functions such as storage, degradation, or translation during stress and recovery. Short-lived mRNAs bearing adenine-uridine-rich destabilizing elements in their 3' untranslated regions bind to TTP and BRF1/2, promoters of interactions between SGs and processing bodies (P-bodies) and induce mRNA decay (von Roretz *et al*, 2011). These events pose a crucial regulatory function of SGs on stability of mRNA. Beyond mRNP sorting, the recruitment of other signaling molecules into SGs suggests that they link mRNP sorting with other signaling events. Cells that express a non-phosphorylatable form of eIF2 α (S51A) cannot assemble SGs in response to arsenite induced oxidative stress and

show heightened sensitivity towards even low doses of arsenite stress (McEwen *et al*, 2005). This sensitivity can be attributed to either inefficient silencing of translation initiation or directly affects SG assembly, there is no solid confirmation for these events in literature yet. Then in some cases it was observed that the sequestration of signaling molecules which are not directly linked to RNA metabolism (such as TRAF2, RACK1 and FAST) in SGs regulate cell survival (Park *et al*, 2020).

1.2.4 Protein composition of SGs

Multiple research over the year have reported an increasing number of protein factors residing in SGs, which are constantly being characterized biochemically and genetically (Buchan & Parker, 2009) (Kosmacz *et al*, 2019; Markmiller *et al*, 2018). Earlier due to technical limitations it was challenging to capture and isolate intact membrane less granules from cytoplasm. Much recently, development of advanced techniques such as mass spectrometry-based high-throughput proteomics and proximity labeling techniques, several studies profiled the larger proteome of SGs in yeast and different mammalian cell types under various stresses and, for mammalian cell types. Greater than 100 novel protein factors were identified and extensive interactomes within mRNP granules were characterized (Niinae *et al*, 2021; Jain *et al*, 2016a; Kosmacz *et al*, 2019). Mammalian granules are more complex with stress-induced phase separation event being evolutionarily conserved in both mammalian and yeasts. Even though the majority of the proteome is granule-specific, several protein families and classifications are highly enriched in both types of mRNP granules across species. Most notably, there is very high enrichment in RBPs, with over 50% of proteins present in human SGs and yeast have RNA-binding functionality. Combined proximity labeling with mass spectrometry have provided insight into the degree of heterogeneity in the proteomes of stress-induced mRNP granules formed in different cell types and in response to different stresses. Multiple proteins have thought to be present in all SGs with emphasis on those which phase separate and nucleate to SGs formation but the protein composition of SGs vary across different conditions (Molliex *et al*, 2015; Riback *et al*, 2017). For example, comparison of SGs formed during arsenite stress with those formed during heat shock showed that 23% of protein components are stress-type-specific (Markmiller *et al*, 2018; Jain *et al*, 2016a). Along with the above mentioned, SGs also contain multiple translation repressors such as sCIRP, DDX3, FXR1/2 and Staufen1 (de Almeida Gonçalves *et al*, 2011; De Leeuw *et al*, 2007; Shih *et al*, 2011). SGs contain many components involved in translation including initiation factors (EIF2A/3/4A/4B/4G) and, notably, 40S ribosomal subunits. A second class of SG components consists of mRNA-binding proteins linked to translational silencing or mRNA stability, which are reliable SG markers but might not be universal to all SGs. Translational silencing members of this group include TIA-1 (T cell internal antigen-1) and TIAR (TIA-1-related) (Kedersha *et al*, 1999b), fragile X mental retardation protein (FMRP) and fragile X mental retardation-related protein 1 (FXR1) (de Almeida

Gonçalves *et al*, 2011). RNA decay-associated SG components include the Argonaute proteins, tristetraprolin (TTP) and BRF1 (Anderson & Kedersha, 2008), the RNA helicase RCK (Chalupníková *et al*, 2008).

Recent studies have highlighted that proteins which recognize both RNA secondary structures like G-quadruplexes (FXR1, FMR1) and the epitranscriptional RNA modification N⁶-methyladenosine (m⁶A) (YTHDF1/2/3) are found to be enriched in granules. Which highlights how these RNA structures and modifications recognized by these proteins may help determine specific in targeting of certain mRNAs to mRNP granules.

It has been now thought for past few years that some SGs may be serving as molecular scaffolds that define the SG domain, which remains relatively constant, despite the fact that most SG proteins (e.g. TIA-1, TIAR, G3BP, PABP-1 and TTP) shuttle through SGs much more rapidly as opposed to changes in SGs morphology.

1.2.5 RNA composition of SGs

SGs are composed of non-translating RNAs but only form, or become easily visible, during a stress response when a large number of mRNAs have translation initiation stopped. Studying RNA composition of SGs and its function became important not only because RNA is the major component of SGs but also because RNA itself is able to phase separate in the absence of proteins and to function as efficient scaffolds for protein complexes (Van Treeck *et al*, 2018).

The intrinsic properties of RNA that influence LLPS with G3BP, is the length and the structure of the RNA- Length longer than 250nt and single stranded promote this interactions (Yang *et al*, 2020). Further, the intermolecular RNA-RNA interactions are not essential, but can promote assembly by lowering the threshold of constituents needed for LLPS. G3BP1 association with polyA RNA significantly increases after arsenite stress, and the SG transcriptome is enriched predominantly in mRNAs and to a lesser extent non-coding RNAs (Khong *et al*, 2017; Yang *et al*, 2020). Pathogenic dipeptides increase the propensity of RNA to assemble. Thus, it refers that RNAs are assembly prone and must be carefully regulated.

SGs are formed upon ribosome run-off, which results in exposing the previously ribosome-occupied coding regions that would be expected to form RNA–RNA interactions both *in cis* and *in trans*. Long mRNAs partition highly into stress granules but only show a modest increase in the binding sites of stress granule proteins, suggesting length might contribute to the partitioning of mRNAs into stress granules through *trans*-RNA–RNA interactions. SG cores in lysates are resistant to high salt, which are known to disrupt many protein–protein,

but not RNA–RNA, interactions. And extensive RNase treatment fails to degrade the RNA within stress granule cores(Jain *et al*, 2016a; Khong *et al*, 2017; Van Treeck *et al*, 2018).

In mammalian cells, in situ staining reveals that approx. 50% of all poly(A)+ mRNA is recruited to SGs, indicating that a significant fraction of total mRNA is actively recruited to SGs(Kedersha and & Anderson, 2002). HSP70 mRNA is excluded from TIA (SG marker)-positive SGs. Whether they exclude other stress-induced transcripts that are preferentially translated during stress, such as ATF4 (activating transcription factor-4), GADD34 (growth arrest and DNA damage-34), and BiP (binding immunoglobulin protein), remains to be determined. Whereas, ‘housekeeping’ transcripts, like: glyceraldehyde 3-phosphate dehydrogenase (GAPDH) mRNA is an example of a non-stress-induced transcript. The latter have also been found to be targeted to SG during arsenite stress, including other endogenous cellular mRNAs encoding β -actin, c-MYC, insulin-like growth factor II (IGF-II)(Khong *et al*, 2017). Although only 50% of cytoplasmic poly(A) RNA and poly(A)-binding protein-1 is recruited to SGs, nearly 90% of TIA-1 is recruited to SGs; this indicates that the mRNA content of SGs is selective.

1.3 Role of mRNA modification upon stress

RNA modifications have recently become hugely diverse, especially with many post-transcriptional modifications on the mRNA, which were earlier thought to not be present at all or function was limited in their understanding. But today we know that these post-transcriptional modifications have multiple diverse functions that can regulate RNA metabolism and gene expression(Roundtree *et al*, 2017; Gilbert *et al*, 2016). These modifications have specific RNA interacting protein partners that either write, erase or catalyze the function of the specific modification. At the time of unfavorable cellular conditions, RNA modifications activate or inhibit the signaling pathways that combat stresses, including oxidative stress, hypoxia, therapeutic stress, metabolic stress, heat shock, DNA damage, and ER stress. The role of RNA modifications in response to these cellular stressors is context- and cell-type-dependent.

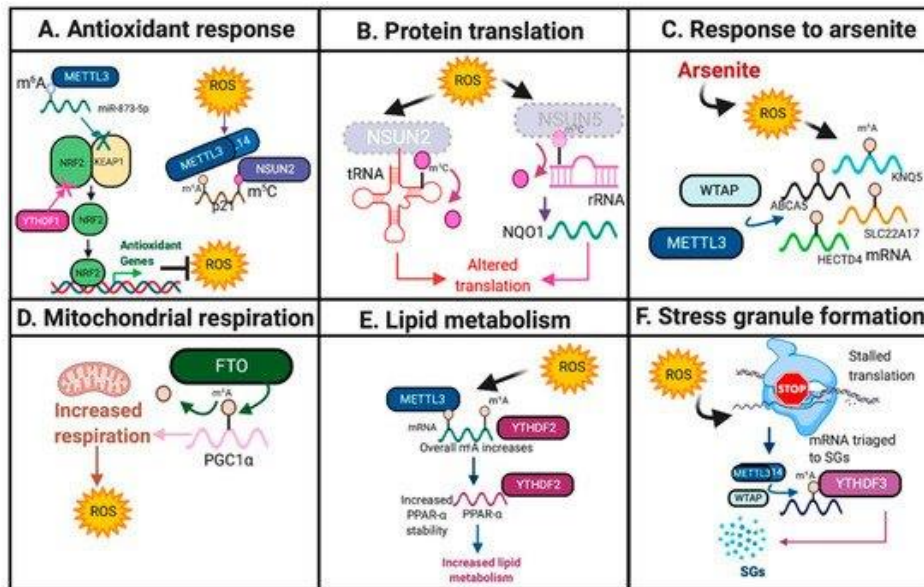


Figure 1.3: Chart showcasing the diverse pathways by which RNA modifications respond to oxidative stress. Featured pathways include: (A). Antioxidant response. (B). Protein translation. (C). Response to arsenite. (D). Mitochondrial respiration. (E). Lipid metabolism. (F). SG formation. (Adopted from (Wilkinson *et al*, 2021))

Both m⁶A and m⁵C pathways play important roles in regulating the cellular response to oxidative stress. Previous studies have suggested that METTL3(m⁶A writer) may serve a protective role against oxidative stress(Wang *et al*, 2019b), whereas hypomethylation of 28S rRNA at position C3782, leads to reduced overall protein translation in response to oxidative stress, but increased translation of proteins that promote survival and adaptation to oxidative stress, including antioxidant(Janin *et al*, 2019). Furthermore, m⁵C writers have also been implicated in the oxidative stress response(Gkatza *et al*, 2019). Using colon cancer cell lines and HeLa cells, Li and colleagues identified that NSUN2 catalyzes the deposition of m⁵C, and METTL3/METTL14 catalyze the deposition of m⁶A, in the 3' UTR of *p21*, which has been previously found to up-regulate *NRF2* in response to oxidative stress and induce cellular senescence(Villeneuve *et al*, 2009; Li *et al*, 2017).

RNA in the cell go through commonly local and global structural rearrangements that are critical for its functions.It has the ability to change structure in response to molecular effectors and environmental cues. Cellular modifiers such as metabolites, ions, and RBPs change the abundance of one or two pre-existing conformations of the RNA ensemble(Chalupníková *et al*, 2008; Li *et al*, 2017; Yongdae & P., 2017; Cherkasov *et al*, 2013; Halvorsen *et al*, 2010; Salari *et al*, 2013; Kutchko *et al*, 2015; Dallaire *et al*, 2016). Chemical modifications that vary architecture and charge in RNA molecules could disturb the dynamics of RNP granule assembly and disassembly

by altering RNA, RNA–RNA, and RNA–protein interactions (Arguello *et al*, 2017; Edupuganti *et al*, 2017).

1.3.1 m⁶A RNA and SG formation

SG formation is very important to maintain crucial stress response and re-program gene expression in the cell, this ensures maximal survival of the cellular state under stress. Recent studies have revealed two modes of triaging mRNAs into SGs following oxidative stress. For almost 55% of the mRNA fraction, the m⁶A modification mobilized due to stress conditions are near the 5' vicinity of the mRNA transcripts and serve as a key feature for these mRNA to triage to SGs (Anders *et al*, 2018). As for the mRNA fraction which gets no mobilized methylation approximately 45% of the total may associate with the SGs triggered by translation initiation halt (Buchan & Parker, 2009; Sonenberg & Hinnebusch, 2009; Kedersha *et al*, 2013).

This dynamicity of the m⁶A methylation during stress conditions or in other words the stress inducible form of m⁶A on mRNA can be read by its corresponding reader proteins and potentially lead them to SG. As mentioned earlier that approximately 45% of the mRNA which does not get this stress induced modification/methylation and are led to SG by stalled pre-initiation complex factors may serve as the already understood scaffold for SG formation and as there is no role of m⁶A modification in this kind of nucleation hence the primary nucleation of SG formation maybe completely m⁶A independent (Decker & Parker, 2012; Kedersha *et al*, 2013). This allows the secondary mRNA to arrive later in the sequence of SG assembly and decorate it on its periphery. Although m⁶A may not lead to primary nucleation of SG formation but as reported by Ries *et al*. (Ries *et al*, 2019) that m⁶A modification specifically can hasten the process of SG formation and have downstream effects on various biological functions. RNA- m⁶A modification is involved in almost the entirety of mRNA regulation in cell from affecting its stability to determination of cell fate, lipid metabolism etc. (Jiang *et al*, 2021). The most important feature which makes m⁶A unique is its reversible nature by the involvement of both methyltransferase and demethylase. Methyltransferase complex containing methyltransferase-like 3 (METTL3), METTL14 and Wilms' tumour-1–associated protein (WTAP) catalysis m⁶A methylation, whereas obesity-associated protein (FTO) and AlkB homolog 5 (ALKBH5), the demethylases, catalyze demethylation of m⁶A (Cao *et al*, 2016; He & He, 2021). Moreover, m⁶A -binding proteins with YTH domain, including cytoplasmic proteins YTHDF1, YTHDF2, YTHYTHDF3, and nuclear protein YTHDC1, have been identified to be the 'readers' of m⁶A and modulate mRNA stability and translation to mediate downstream effects (Du *et al*, 2016; Xu *et al*, 2015; Shi *et al*, 2017). More recent study has shown an enrichment of m⁶A- and m¹A-modified mRNAs in SGs. With depleted reader enzymes YTHDF1/3, enrichment of methylated and unmethylated mRNAs in SGs

was prevented, and SG formation was inhibited (Fu & Zhuang, 2020). Additionally, RNA m¹A-generating methyltransferase complex TRMT6/61A and m¹A modification of RNAs accumulate in SGs during heat shock stress (Alriquet *et al*, 2020).

1.3.2 m⁶A regulator: YTHDF protein and SG formation

m⁶A regulation as highlighted in the earlier section are undertaken by the reader proteins. m⁶A readers serve diverse roles in response to oxidative stress. Loss of clock protein BMAL1 increased ROS production in human HepG2 and mouse Hep1-6 cells, which resulted in specific METTL3-mediated m⁶A increases on the nuclear receptor peroxisome proliferator-activator α (*PPAR α*) locus, increased *YTHDF2* expression, which mediates *PPAR α* stability, and increased lipid metabolism (Luo *et al*, 2019). However, YTHDF1 and YTHDF2 may serve context-dependent functions in mediating oxidative stress, YTHDF1 may serve as a negative regulator of the KEAP1-NRF2 antioxidant pathway as *YTHDF1* knockdown in human bronchial epithelium cells (BEAS-2B) increased *NRF2* expression and antioxidant production (Shi *et al*, 2019).

Oxidative stress also induced METTL3/METTL14/WTAP-mediated m⁶A deposition on 5'UTR of SGs (SGs), which are assemblies of mRNA that are stalled within translation initiation, and form in response to stress (Anders *et al*, 2018) (Meyer *et al*, 2015). YTHYTHDF3 has been shown to mediate the triage of mRNAs into SGs in response to oxidative stress in HEK293 and U2OS osteosarcoma cells. Under permissive growth, translation of selected transcripts is enhanced by YTHDF1 which binds to select transcripts at m⁶A in their 3' UTRs (Wang *et al*, 2015). YTHDF1 binds simultaneously then to ribosomal proteins of already assembled initiating ribosomes to influence the cap-dependent translation (Li *et al*, 2017). Although YTHYTHDF3 itself can also associate with ribosomal proteins and m⁶A -modified 3' UTRs (Li *et al*, 2017; Shi *et al*, 2017), it does not compete but rather facilitates YTHDF1 binding. An unexpected feature of YTHYTHDF3 protein in triaging mRNAs to SGs offers a mechanism for dynamic control of the localization of mRNAs during stress.

1.3.3 SG Assembly and Disassembly

1.3.3.1 SG Assembly

The formation of SGs happens in two phase manner. First, the mRNA with inhibited translation initiation and stalled mRNA accumulate together (Kedersha *et al*., 2002). Then at the second step these mRNA and the mRNPs condense in the cytoplasm to form phased out distinct foci. So far from literature it can be easily said that formation of SG is at least biphasic. In most physiological cases, translation inhibition is initiated through phosphorylation of eIF2 α by one or more of the

four eIF2 α kinases: PKR, PERK/PEK, HRI and GCN2 (Anderson and Kedersha, 2009b, 2006; Kedersha et al., 2002, 1999). Consequently, the depletion of eIF2-GTP-tRNAⁱ Met ternary complexes disrupts translation initiation, which leads to polysome disassembly and concomitant recruitment of stalled 48S PICs into SGs.

The assembly of SGs is largely driven by liquid-liquid phase separation (LLPS), RNA molecules tend to self-assemble in in vitro systems (Boundedjah et al., 2012; Langdon et al., 2018; Van Treeck et al., 2018). Direct RNA-RNA interactions such as Watson-Crick base-pairing, non-canonical base-pairing, or helical stacking, therefore facilitate the formation of macromolecular condensates by LLPS. Another important aspect of interactions that lead to SG formation is intermolecular interactions between RNA modifications apart from molecular interaction of proteins to form macromolecular condensates through LLPS (Fay and Anderson, 2018; Van Treeck and Parker, 2018).

First postulated in 1940s: The Flory-Huggins model predicts that molecular crowding promotes liquid-liquid phase separation (LLPS) in the cellular cytosol (Johansson *et al*, 1999). After almost twenty years we now know that LLPS indeed occur within the crowded cytoplasm, and several membraneless compartments, also called biomolecular condensates, of various different functions have been identified both in the cytoplasm and in the nucleus (Alberti & Dormann, 2019; Yongdae & P., 2017; Yoshizawa *et al*, 2020; Johansson *et al*, 1999).

SG or any granule formation is dependent on multiple physiological factors, the score Mammalian Granule Z score (MaGS) includes total amount of proteins disorders/Intrinsic disorder regions, along with accounting for P-Score which further sheds information on π - π interactions for potential protein-protein or RNA-protein interactions. Furthermore, increased potential for post-translational modifications (PTMs), as well as RNA-binding capacity also contributes to a higher MaGS and presents another interesting feature of proteins associated with SGs.

Through recent studies it has been unraveled that the most abundant mRNA modification m⁶A is critical for SG assembly. RNA chemical modifications have the potential to alter architecture and charge in RNA molecules that could affect the dynamics of RNP granule assembly and disassembly by modifying RNA, RNA-RNA, and RNA-protein interactions. The first evidences of the contribution of RNA modifications in the dynamics of SGs was the observation that m⁶A disrupts RNA binding by G3BP1/2, ubiquitin-specific peptidase 10 (USP10), cell cycle-associated protein 1 (CAPRIN1), and RNA-binding motif protein 42 (RBM42), all proteins of SGs (Edupuganti *et al*, 2017; Arguello *et al*, 2017). And later, high-throughput RNA sequencing techniques and isolation of RNA granules are serving to appreciate the specific role of RNA modifications in SG dynamics.

1.3.3.2 SG Disassembly

Even though the mechanisms of SG assembly in response to various stressors and in different model systems have been expansively studied, less attention has been paid to the SG disassembly process. The reversibility of SGs after stress removal is an intimation on the important roles of polysome dynamics in this process, although how polysome formation affects phase separation is not known. SG recovery from cold shock-induced SGs takes place within minutes after return to normal temperature (Hofmann *et al*, 2021), however after arsenite stress, H₂O₂ treatment, sorbitol exposure, or heat shock disassembly occurs between 60-120 minutes (Cherkasov *et al*, 2013; Kedersha and & Anderson, 2002; Anderson & Kedersha, 2002; Marmor-Kollet *et al*, 2020; Huang *et al*, 2020).

Latest study by Marmor-Kollet *et al*. conducted proximity labeling of several core SG proteins, and identified subsets of proteins that associate with these core proteins during the disassembly (Marmor-Kollet *et al*, 2020). These unique subsets of proteins are termed as Disassembly Engaged Proteins (DEPs), indicates that the disassembly of SGs occurs in a controlled stepwise manner. Several SUMO ligases were identified as DEPs that are recruited to SGs during recovery from stress, and they showed that there is broad SUMOylation of SG proteins. A recent work(Huang *et al*, 2020) have shown that Ubiquitin associated protein 2like protein(UBAP2L) could be a regulator in SG disassembly and overexpression or knockdown of UBAP2L impairs the process. Though the molecular mechanism of it is still not known. SG fluidity is essential for the cell in a sense that the disassembly of the granules can govern the translation recovery of the transcripts, knowing the SG acts as a protective compartment in the cell. In the publication by Wheeler *et al*. (Wheeler *et al*, 2016) it was suggested that SG disassembly occurs through multiple steps, wherein the stalled mRNAs are titrated out of SGs, thereby causing structural instability of the protein complexes, and subsequently stepwise disassembly of the visible SGs.

The mechanisms for SG disassembly need to be widely studied, because the resolution of SGs is important for maintaining protein homeostasis. Impaired clearance of SGs results in persistent protein aggregates, which are implicated in several neurodegenerative diseases, e.g. ALS (Poljšak & Milisav, 2012; Aulas *et al*, 2012; Baron *et al*, 2013; Gal *et al*, 2016)Parkinson's disease (Repici *et al*, 2019) and Alzheimer's (Repici *et al*, 2019).

1.4 RNA and Protein Interactions

RNA-protein complexes have long known to have exert functions by having Noncoding RNA sequences, including long noncoding RNAs, small nucleolar RNAs, and untranslated mRNA regions, through direct interactions with RNA-binding proteins (RBPs). But recently identified

new RNA binding proteins that lack any sort of known RNA-binding domains have truly understated the complexity and diversity of RNA-Protein complexes. There are many RNA species at any given time in cell, human cell itself encode for more than 20,000 different mRNA and furthermore the complexity in their diversity increases many fold by processes like splicing and modification; hence the biological specificity of RNA binding proteins most possibly is affected by structure, other protein, both RNA and protein concentration in cells also the functions and mechanism of many of ncRNAs may depend on their interactions with various protein complexes in the cell. Some studies have also shown that if mis-regulated interactions between ncRNA and protein occur can also contribute to multiple human diseases.

Interaction between a specific RNA site and its protein binding pattern is majorly governed by protein's inherent affinity for the specific site on the RNA, along with this concentration of the protein and RNA also influences this interaction. The protein binding partners compete with other RNA with may contain sites also favorable for their binding along with existing competition between the proteins themselves. Once a protein binding partner binds to the mRNA it will heavily influence the context of its partner RNA leading to profound changes in further RNA-binding patterns. These inter-complex interactions are a confirmation that RNA and their protein binding partners do not conform to a binary model of specific vs non-specific, at the same time challenges to provide a model that will sufficiently cover all the inter-complex nuances of RNA-protein binding interplay.

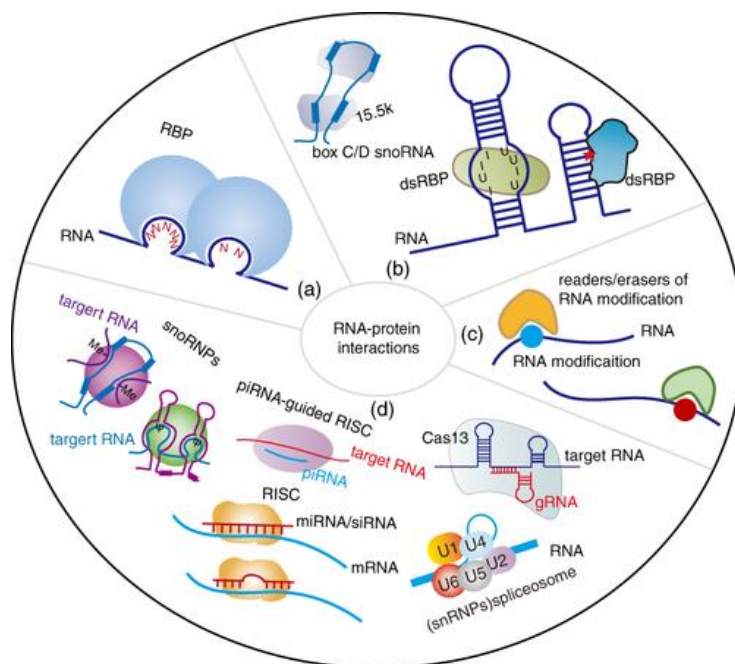


Figure 1.4: Classification of RNA–protein interactions, divided into four classes according to the characteristics of their relationships: (a) RNA motif-dependent RNA–protein interactions; (b) RNA structure-dependent RNA–protein interactions; (c) RNA modification-dependent RNA–protein interactions; and (d) RNA guide-based RNA–protein interactions. (Adopted from (Liu *et al.*, 2020))

1.5 AIM OF THESIS

Over a decade, work to understand the formation of cytoplasmic SGs have provided detailed knowledge on the principles and biophysical factors by which their assembly is regulated. SG assembly is concentration driven process (Jain *et al*, 2016a; Matheny *et al*, 2021), that are stabilized through plethora of interactions, including protein-RNA, RNA-RNA, protein-protein interactions, (Buchan & Parker, 2009; Jain *et al*, 2016b; Guillén-Boixet *et al*, 2020; Van Treeck *et al*, 2018; Liu *et al*, 2017). The most abundant modification on RNA-m6A plays a crucial role and modulates assembly of SGs and acts as a signal for triaging more than 50% of cellular transcripts into SG (Anders *et al*, 2018). SGs are viewed as protective for the transcripts during stress, thus raising the question on the fate of these transcripts following stress recovery. Thus, In Chapter 2 we address the following specific questions: (1) Do all those transcripts recover for translation pool upon stress relief? and (2) What is the potential role of stress-induced m6A methylation on some SG-sequestered transcripts on their recovery?

Furthermore, we addressed the role of m6A-reader protein YTHYTHDF3 in the process of SG assembly (**Chapter 3**). Among the other YTH-family reader proteins, this particular one is specific to SGs and suggested to act as a crucial recognition element in triaging m6A methylated mRNAs to the SGs (Anders *et al*, 2018; Fu & Zhuang, 2020; Shi *et al*, 2017; Gao *et al*, 2019).

Finally, the last part of the thesis focuses on establishing a protocol for quantification of tRNA-protein interactions (**Chapter 4**). Several pathologies are associated with tRNA mutations (Kirchner & Ignatova, 2015) and mutation in their binding partners (Abbott *et al*, 2014; Orioli, 2017), thus urging in developing a quantitative measurements and qualitative identification of tRNA and proteins in the complexes. The method developed in **Chapter 4** is specific for determining binding affinity of Charcot Marie tooth mutant glycyl-tRNA-synthetase to tRNA^{Gly} and was used already to decipher the molecular mechanism of CMT pathology (Zuko *et al*, 2021). Importantly, this immunoprecipitation-based approach is versatile and can be applied to any RNA-protein complex in both cell culture or tissue samples.

2 mRNA recovery from SGs and dynamics of m⁶A regulation of its clients

The work in this section was executed as joint collaboration with Leonardo Santos – a member of our group - who performed the bioinformatic analysis. The experimental design and the experimental data were produced by me, including the deep-sequencing data sets. All bioinformatic analysis were performed by Leonardo Santos. The work summarized in this chapter, has been submitted for publication, which is coauthored by me as first author and Leonardo Santos as second author.

2.1 m⁶A-RNA assembly and disassembly in SG

SGs (SGs) are crucial for cells to sustain and adapt to stress. SGs are dynamic cytoplasmic membrane-less condensates composed of RNA and proteins that form via liquid-liquid phase separation in response to various types of stress, including oxidative agents, heat stress, glucose deprivation (Bregues & Parker, 2007; Protter & Parker, 2016). The assembly of SGs is tightly regulated and misregulation is implicated in several human pathologies (Mathieu *et al*, 2020; Wolozin & Ivanov, 2019). SGs assemble through weak and transient protein-protein, RNA-protein and RNA-RNA interactions and when the sum of these interactions reaches a threshold, known as percolation threshold, the extensive interaction network separates the SGs from the surrounding milieu creating a liquid condensate (Banani *et al*, 2017; Guillén-Boixet *et al*, 2020; Sanders *et al*, 2020; Yang *et al*, 2020). Exposure to stress rapidly inhibits translation initiation and ceases translation and the following ribosomal run-off raises the influx of unprotected mRNAs capable of mediating RNA-protein or RNA-RNA interactions (Begovich & Wilhelm, 2020). Approximately 36 proteins together with RNAs provide the core of SG interaction network in establishing the percolation threshold (Yang *et al*, 2020) although much larger fraction of the cellular proteome has been detected in the mature SGs (Jain *et al*, 2016b). Earlier quantification of the RNA constituents of SGs suggested that only a small portion of the bulk cellular mRNAs assemble into SGs with longer coding sequences (CDS) and UTRs that are mostly inefficiently translated (Khong *et al*, 2017). Other studies propose that the majority of the cellular mRNAs can condensate into SG and the most prevalent mRNA modification, the m⁶A, enhances their phase-separation potential and partitioning into SG through interactions with YTHDF proteins (Ries *et al*, 2019; Anders *et al*, 2018).

In healthy cells, SGs are transient and disassemble following stress relief. Two major pathways of SG removal have been proposed: autophagy-dependent and autophagy-independent (Wang *et al*, 2019a; Gwon *et al*, 2021; Buchan & Parker, 2009). The former is suggested for clearance of SGs under long-lasting chronic stress, whereas the latter is consistent with recycling of SGs in response

to short or acute stress exposure with mRNAs reentering translation after stress removal (Gwon *et al*, 2021; Anderson & Kedersha, 2009). The disassembly mechanism may also vary dependent on stress. G3BP1, a core SG protein required to maintain the assembly of SGs, is ubiquitinated in SGs assembled under heat stress, but not in those formed under oxidative stress (Maxwell *et al*, 2021). While ubiquitination is not required for heat shock-induced SG condensation, it is essential for their disassembly (Gwon *et al*, 2021; Maxwell *et al*, 2021). In yeast, SGs formed under nutrient deprivation disassemble in a metabolite-dependent manner by controlling the dynamic assembly and disassembly of the pyruvate kinase Cdc19, the core SG seeding component that assembles into amyloid aggregates and promotes SG formation (Cereghetti *et al*, 2021). While we are beginning to understand the SG disassembly and the variety of tightly controlled clearance, it remains unclear whether mRNAs deposited in SGs completely recover for translation following stress relief.

In this study, we identified the mRNAs recovering for translation using RNA-seq. Nearly 90% of the mRNAs sequestered in the SGs following acute stress exposure recovered for translation. In a previous study, we discovered that SGs constitute of two different types of mRNAs, unmodified or pervasively m⁶A-modified (Anders *et al*, 2018). Monitoring the fate of modified and non-modified mRNAs, here, we observed that the methylated mRNAs fully recovered for translation (96%) whereas from the non-modified a substantial fraction was lost (84%). The m⁶A may display some advantage to the mRNAs in their recovery for translation likely due to the m⁶A-driven structural stabilization in the near vicinity of the m⁶A modification.

2.2 Materials and Methods

2.2.1 Cell Lines, Growth Conditions and Immunostaining

U2OS cells stably expressing GFP-tagged G3BP1, a SG marker (Ohn *et al*, 2008), were used to perform the immunofluorescence experiment. HEK293 cells expressing N-terminally FLAG tagged TIA1, another SG marker (Damgaard & Lykke-Andersen, 2011) were used to perform all the sequencing experiments which is called HEK-TIA1 above. Both cell lines were grown in DMEM medium at 37°C, 5% CO₂. To induce oxidative stress, 500 μM sodium arsenite (AS) was used for 30 min. For stress recovery, experiment, fresh medium was added after 30 min and the cells were collected at different time points.

For immunostaining, cells were grown on coverslips. For imaging, cells were washed twice with PBS, fixed for 15 min with 4% Paraformaldehyde at room temperature, and permeabilized using 0.5% saponin. Subsequently blocking was done using 1% BSA in PBST for 1 hr at RT. Primary antibody was added to the blocking buffer (m⁶A Antibody, SySy) in 1:200 dilution and incubated

for another 1 hr at RT and then washed three times with PBS. Secondary antibody AlexaFluor 568 was diluted in blocking buffer (1:200) and added for 1 hr at RT.

All images were acquired on Leica-TCS-SP5 confocal microscope, on one Z-plane. Images were processed by ImageJ with FIJI plugin.

2.2.2 Polysome Profiling, RNA Isolation and RNA-seq Library Preparation

10-15 Million cells were pelleted at 850xg and resuspended in 500 µl polysome lysis buffer (10 mM Tris-HCl (pH 7.4), 5 mM MgCl₂, 100 mM KCl, 1% Triton X-100, 2 mM DTT and 100 µg/ml cycloheximide). Cells were shear opened with 26-gauge needle by passing the lysate 8-times. 400 µL of lysate was loaded onto 5-ml sucrose gradient (50% to 15% sucrose dissolved in 50 mM HEPES-KOH, pH 7.4, 50 mM MgCl₂, 100 mM KCl, 2 mM cycloheximide, 2 mM DTT) and separated by ultracentrifugation at 148,900xg (Beckman, Ti55 rotor) for 1.5 hours at 4°C.

Polysome fractions were collected and RNA was extracted by adding 0.1 volume of 10% SDS, one volume of acidic phenol-chloroform (5:1, pH 4.5) preheated to 65°C and further incubated at 65°C for 5 min. The sample was cooled on ice for 5 min and centrifuged at 21,000xg for 5 min to separate different phases. Equal volume of acid phenol-chloroform was added to the aqueous phase, separated by centrifugation and supplemented with an equal volume of chloroform:isoamyl alcohol (24:1). Upon separation, the aqueous phase was supplemented with 0.1 vol 3M NaOAc (pH 5.5) and an equal volume of isopropanol. Samples were precipitated for 3 h at -20°C. RNA was pelleted at 21,000xg at 4°C, and the dried pellets resuspended in DEPC-H₂O. The pure RNA was fragmented in alkaline fragmentation buffer (0.5 vol 0.5 M EDTA, 15 vol 100 mM Na₂CO₃, 110 vol 100 mM NaHCO₃) and subjected to cDNA library preparation as described (Kirchner *et al*, 2017a).

2.2.3 Sequencing analysis

Sequenced reads were trimmed by *fastx-toolkit* (0.0.13.2; quality threshold: 20) and depleted from the adapter sequences using *cutadapt* (1.8.3; minimal overlap: 1 nt). Only reads uniquely mapping to the human reference genome (GRCh38.p13) using STAR (Dobin *et al*, 2013) (2.5.4b) allowing one mismatch (--outFilterMismatchNmax 1 --outFilterMultimapNmax 1) were considered. Mapped reads were normalized as reads per kilobase per million mapped reads (RPKM).

CLIP-seq and m⁶A-seq were downloaded from (Anders *et al*, 2018) and used to determine the SG clients and methylated mRNAs, respectively. The analyses were performed as described earlier (Anders *et al*, 2018). DRACH motifs were predicted using HOMER algorithm (Heinz *et al*, 2010).

The PARS data sets were downloaded and analyzed as described (Wan *et al*, 2013). Briefly, trimmed reads were uniquely aligned to the human reference transcriptome (ENSEMBLE GRCh38.p13) using Bowtie (1.2.2) allowing one mismatch. Mapped reads were positioned to the 5' most nucleotide. Reads were normalized accordingly to the size of the corresponding libraries as reads per million (RPM). The PARS score is computed as described (Del Campo *et al*, 2015), which is defined as the \log_2 ratio between the normalized reads (RPM) from the RNase V1-treated and the S1 nuclease-treated samples. RNase V1 cleaves double-stranded RNAs and nuclease S1 single stranded.

2.2.4 m⁶A peak detection

m⁶A modification sites were identified as described previously (Mao *et al*, 2019). Briefly, we compared the coverage immunoprecipitated (IP) fraction to the total input sample. First, the coverage of each individual transcript was calculated using full-length mapped reads. Peak-over-median (POM) was determined by the ratio between the mean read coverage to the median read coverage of each sliding window, using 50 nucleotide window (25nt step) and a minimum window read coverage threshold of 10. The minimum POM threshold was set to 3 and overlapping windows (minimal 1nt overlapped) were merged into one larger window. The input sample was analyzed following the same steps. The shared windows between IP and input were excluded from the downstream analysis. Following, the peak-over-input (POI) was calculated by the ratio of IP POM to the input sample POM. The minimum POI threshold was set to three, indicating an m⁶A modification.

The theoretical DRACH motif were identified in the reference transcriptome using HOMER (<http://homer.ucsd.edu/homer/>) (Heinz *et al*, 2010). Only peaks assigned to regions containing at least one DRACH motif were considered as true m⁶a modification sites and kept to the following analysis. All identified modification sites were assigned to specific mRNA segments: 5' UTR, CDS and 3' UTR. Each region was separately spliced into equal number of bins with comparable length to generate the metagene plots. We calculated ratio between experimentally detected modified DRACH motif and the theoretical DRACH motif identified for each individual transcript. The metagene profiles was generated by averaging the methylation distribution profile of each individual transcripts. Lastly, due to differences in the sequencing depth, the metagene profile was once again averaged by the mean of each sample distribution (mean density) .

2.2.5 Data Availability.

RNA-seq of the translation fraction- RNAs generated in this study have been deposited in the Gene Expression Omnibus (GEO) under the accession number GEO: GSE189099. PAR-CLIP and m⁶A-Seq data sets were downloaded from the BioSample data base under accession number SRP121376. PARS data set was downloaded from GEO database under the accession number GSE70485.

2.3 Results

2.3.1 Biphasic process of SG Assembly and Disassembly

To dissect the dynamics of m⁶A modification upon arsenite stress and its relief, we used U2OS-G3BP1 cells which are GFP tagged. Time course of SG formation in U2OS-G3BP1 cells exposed for different time points (0, 15, 30 mins) to 500 μ M AS was followed and subjected to immunostaining. Similarly, after a 30minutes 500 μ M AS treatment, cells relieved by adding fresh medium and at different time points (0, 15, 30, 60, 90 mins) it was collected for immunostaining. During SG assembly, the signal of the scaffolding G3BP1 appeared much earlier than the m⁶A-containing shell following stress exposure (Figure 2.1A). At 15 mins of stress exposure the cells, already exhibit G3BP1 foci formation; whereas only at 30 mins the m⁶A decorate the granules. Next when the cells prepare to resolve the granules upon stress relief, it dissipates the m⁶A RNA as early as 15 to 30minutes but the core clearance takes much longer (Figure 2.1B). We can conclude that following acute oxidative stress, i.e. exposure with 500 μ M arsenite (AS), SGs are readily formed thereby, the m⁶A signal depicting the m⁶A modified mRNAs is somewhat enriched as a rim at the surface of the SGs. Upon stress relief, the peripherally decorated m⁶A leaves the SGs at an early time point, leaving behind the core proteins. The SG dissipation is a gradual process but an early occurrence of m⁶A -RNA escape raises a question as to whether these go back into translation facilitating recovery?

Similarly, in another cell line (i.e. HEK293 cells stably expressing another SG marker TIA1-GFP (Damgaard & Lykke-Andersen, 2011)), the m⁶A modified mRNAs first leave SGs (Figure 2.1C). Together, these results suggest a two-stage disassembly process of the SGs, with m⁶A modified mRNAs leaving the SG first.

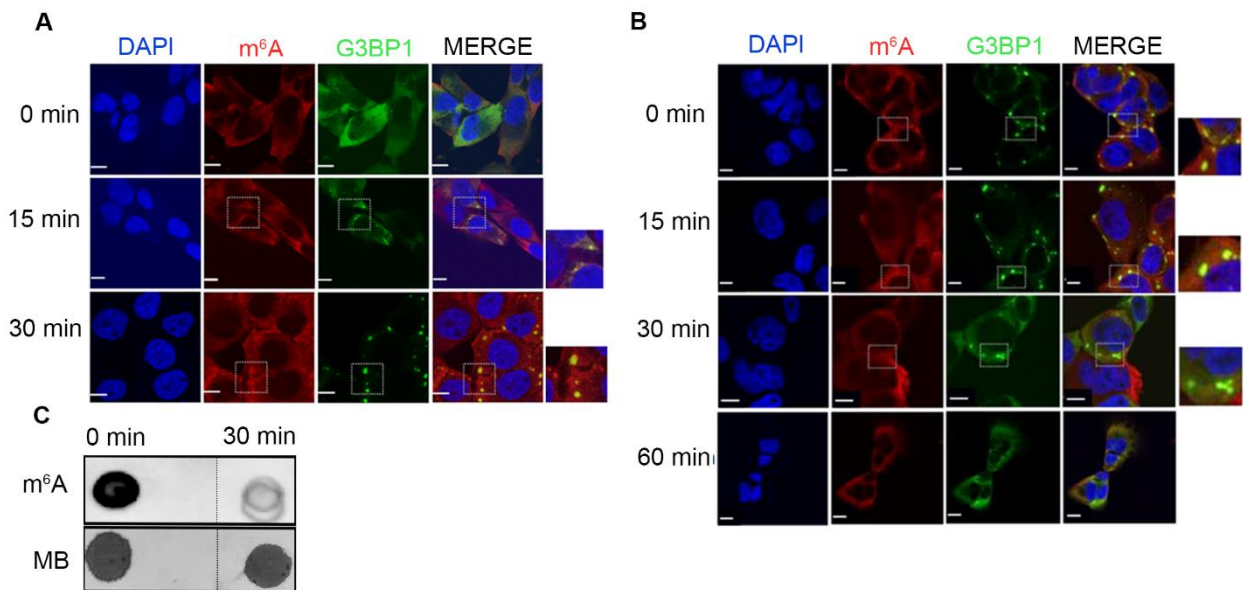


Figure 2.1: m⁶A-signal colocalizes later with SGs and upon stress relief dissipates first followed by clearance of the cores at a later time scale.

A) Time course of SG formation of U2OS-G3BP1-GFP cells exposed to 500 μM AS. At 15 min a thin rim of m⁶A signal around the G3BP1-positive SG foci was detectable, which increased at 30 min. SGs were visualized through G3BP1-GFP (green), m⁶A-modified mRNAs with m⁶A antibody (red), nuclei were counterstained with DAPI (blue). Insets on the left, zoomed in area depicted on the merged image. Scale bar, 10 μm. B) Time-course of SG disassembly in U2OS-G3BP1-GFP cells pre-exposed to 500 μM AS for 30 min and allowed to recover in permissive growth conditions. Zero min denotes the time point of the medium exchange and withdrawal of AS. SGs were visualized by G3BP1-GFP (green), m⁶A-modified mRNAs with m⁶A antibodies (red), nuclei were counterstained with DAPI (blue). Insets on the left, zoomed in area depicted on the merged image. Scale bar, 10 μm. C) The amount of m⁶A modified mRNAs decrease in SGs isolated at from HEK293-TIA1-GFP cells 30 min post-exposure to 500 μM AS. Zero time point denotes the medium exchange and withdrawal of AS. MB, methylene blue staining total mRNA. Thin vertical lanes denote excised lanes with samples unrelated to this experiment

2.3.2 SG-protected mRNAs recover nearly completely for translation

We next sought to determine whether both m⁶A modified and unmodified mRNAs pools that were sequestered in the SGs recover for translation upon stress relief. We compared translation profiles using sucrose gradients. Acute stress (500 μM AS) leads to complete inhibition of translation, i.e. complete loss of heavy polysomal fraction (Figure 2.2A). At the time point the m⁶A signal dissipated from the SG (30 min relief), some heavier polysomal fractions appear reporting of some translation activities albeit very poor. Active translation was resumed after the complete SG dissociation (4h, Figure 2.2A), but to much lower extent than the translation of the unstressed cells, suggesting that much longer times are needed for complete recovery from stress.

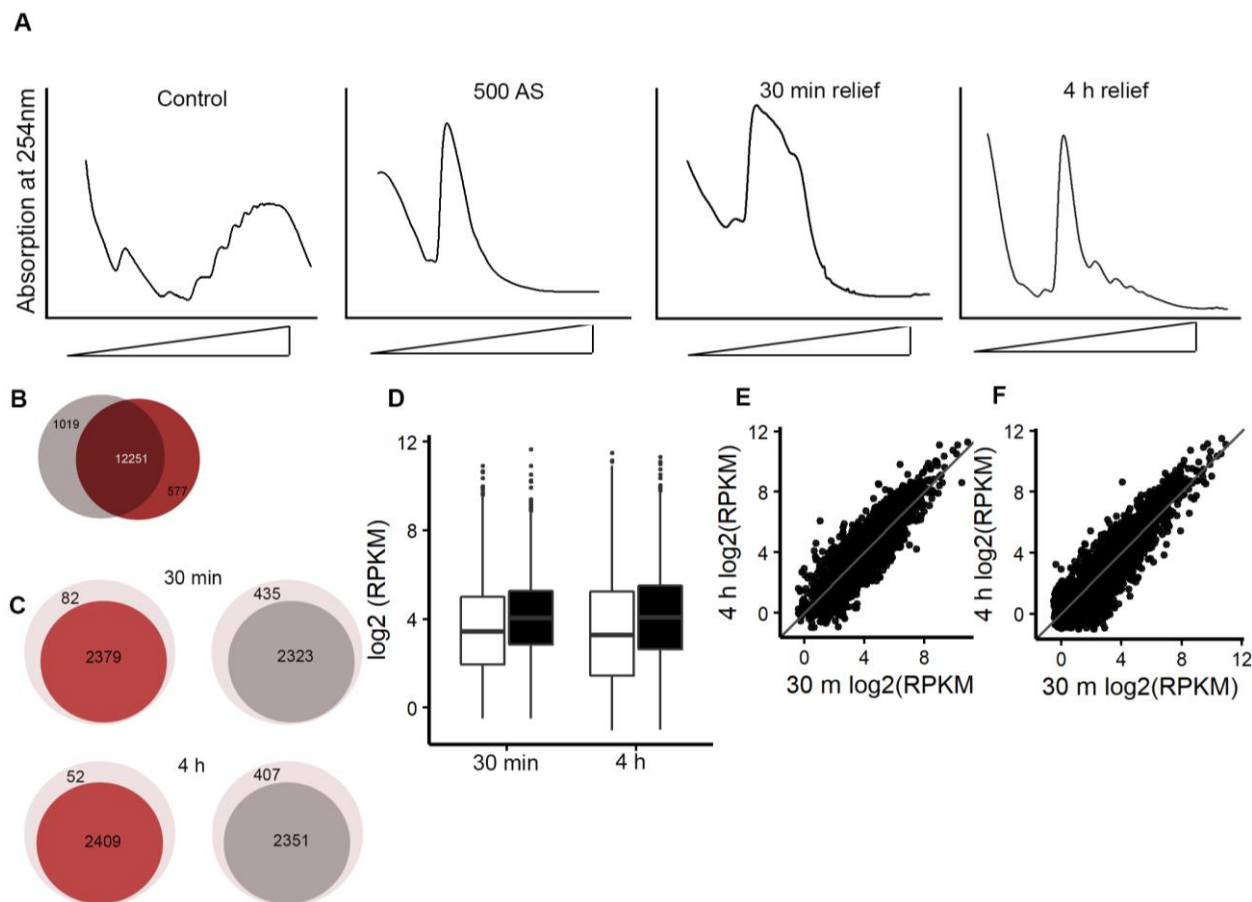


Figure 2.2: Nearly all mRNAs deposited in SGs are translated upon stress relief.

A) Polysome profiles following stress recovery of HEK-TIA1 cells. Cells were pre-exposed for 30 min to stress (500 μ M AS) and samples were collected at 30 min and 4 h of stress relief (i.e. after medium exchange and AS removal). B) mRNAs identified in the polysome fraction at 30 min (grey) and 4 h (red) following stress relief. C) m⁶A modified SG mRNAs (red) and non-methylated SG mRNAs (grey) detected in the polysome fraction at the two time points following stress relief. 5,219 mRNAs were identified in the SGs with 2,461 m⁶A modified and 2,758 non-modified (Anders et al, 2018). D) Boxplot of the abundance (RPKM) of m⁶A-modified (black) and non-methylated (white) mRNAs in the polysome fraction at different time points of recovery from stress as determined from the RNA-seq. $p = 4.82 \times 10^{-22}$ and $p = 1.17 \times 10^{-27}$; Mann–Whitney test between methylated mRNAs and non-methylated transcripts at 30 min and 4 h, respectively. E, F) Scatter plot comparing the abundance of m⁶A-methylated (E) and non-methylated (F) transcripts in the polysomal fraction at 30 min and 4 h following stress relief

Next, we collected the polysomal fractions at 30 min and 4 h, extracted the total RNA by hot-acid phenol and subjected the recovered mRNAs to RNA-seq. A total of 13,207 and 12,828 mRNAs were detected for 30 min and 4 h samples, respectively; the identified mRNA clients were largely overlapping (Figure 2.2B). In our earlier study, using CLIP-seq and m⁶A-seq we identified all SG sequestered mRNA comprising two nearly equal pools of m⁶A modified and non-modified (Anders *et al*, 2018). We took these two groups of m⁶A-modified SG mRNAs and non-modified

SG mRNAs and compared each of them to the mRNAs identified in the polysomal fractions. Strikingly, the majority of transcripts identified previously to be protected in the SGs were found in the translated fraction following stress relief (Figure 2.2C), corroborating the notion of the protective effect on mRNAs SGs exert during stress (Hofmann *et al*, 2012; Decker & Parker, 2012). Both methylated and non-methylated transcripts were nearly equally present in the translating pool either 30 min or 4 h after stress relief (Figure 2.2E, F). A higher fraction of methylated mRNAs (96% at 30 min and 97% at 4 h) recovered from the SGs compared to the non-methylated transcripts (84% at both 30 min and 4 h) (Figure 2.2C). In addition, in the polysome fraction mRNAs that were methylated in SGs were significantly more abundant than the non-methylated ones (Figure 2.2D). These results suggest that m⁶A modification may display some advantage to the mRNAs in their recovery for translation. The effect could be direct effect on the mRNA stability as shown earlier (Mauer *et al*, 2017)(Wang *et al*, 2014) or indirect and the higher transcript abundance may correlate with the higher probability of being methylated.

2.3.3 Stress induced m⁶A profile on mRNA regulates its abundance in SGs

From previous study (Anders *et al*, 2018), we discovered that RNA-m⁶A modification is important for the triaging of RNA into SGs. Stress induced methylation of mRNA during arsenite treatment, results in an increased m⁶A signal and also additional mRNAs with m⁶A peaks around the 5'UTR and start codon. SG (SG) have more than 50% of its transcript clients m⁶A modified which exhibits an overall distinct m⁶A distribution pattern compared to control condition. About 96% of all mRNAs with increased m⁶A signals during oxidative stress were detected as SG clients. (Anders *et al*, 2018). SGs are crucial element for cells adapting to stress conditions. And knowing about the important role of m⁶A -RNA modification in the process of transcript triaging to SG, we next asked how the SG clients are affected upon co-transcriptional inhibition leading to dysregulation of m⁶A deposition during stress?

From literature we know that, RNA m⁶A modification occurs co-transcriptionally and is dependent on the transcribing RNA polymerase II (Slobodin *et al*, 2017). This study tries to understand how mild co-transcriptional inhibition affects the m⁶A content upon stress condition parallel to enhancement of m⁶A content. Suggesting a negative correlation between transcription elongation and m⁶A deposition.

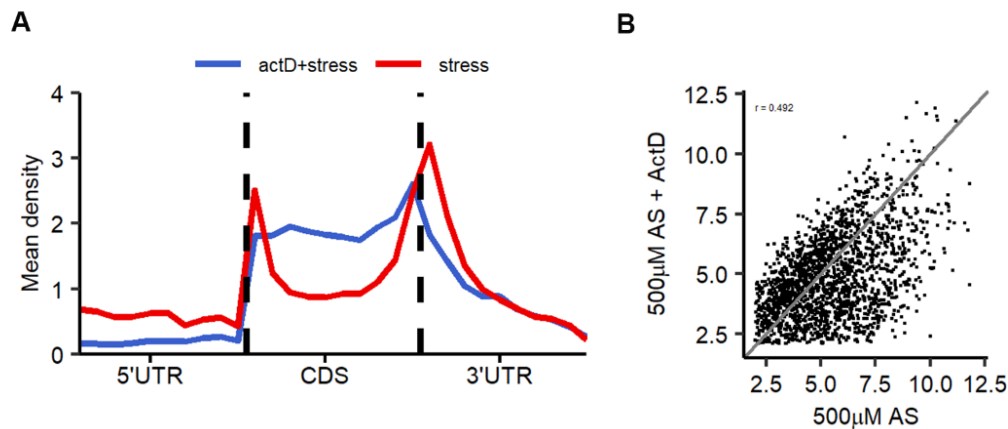


Figure 2.3: Transcription inhibition alters methylation pattern of SG clients and reduces its abundance

A) Metagene profiles of m⁶A distribution across methylated transcript regions of SG mRNAs upon 500 μ M AS stress (red) and upon stress with transcription inhibited with Actinomycin D (blue). $p = 1.08e-05$ for 5' UTRs and $p = 3.77 \times 10^{-2}$ for 5' vicinity of the CDSs; Mann–Whitney test between Stress condition treated and untreated with Act-D. The mean density distribution was calculated by dividing each distribution by its mean value. Transcript regions were binned for comparable lengths. B) Scatter plot showing the abundance of transcripts in the SG under 500uM AS stress and upon actinomycin D treatment and Stress. $R=0.492$

We were interested to understand how co-transcriptional changes may affect m⁶A deposition on transcripts during stress and further look into its effect on the SG clients. For transcription inhibition, Actinomycin-D in mild dosage was used in a co-treatment with arsenite stress. Through global profiling of the RNA methylome (m⁶A sequencing), we analyzed the distribution of m⁶A peaks in different transcript segments of the SG mRNA set, binned to equal lengths for comparison. As shown in figure 2.3A, the methylation profile changes significantly over the transcripts upon such inhibition. The enrichment of m⁶A signal, at the 5'UTR and near start codon associated with arsenite stress, is lost. There is a reduction in the m⁶A deposition overall in the 5' UTR region and also the CDS region has gained methylation. Most interestingly, the signature 3'UTR - m⁶A signal for stability(Meyer *et al*, 2012)- is also reduced. This result suggests an overall change in dynamics of m⁶A deposition during arsenite stress, observed upon inhibiting co-transcriptional m⁶A regulation.

Since the m⁶A mediated stability signal in such condition is being altered, hence we asked whether the m⁶A signal is crucial for the maintenance of the SG transcriptome. We compared the SG mRNAs level upon oxidative stress (500 μ M Arsenite), both with and without Act-D treatment through RNA sequencing. And the effect of the loss of m⁶A led to lower abundance of mRNA clients detected in the SGs (Figure 2.3B). The abundance was measured by the RPKM values of the transcripts present in the isolated SGs in two conditions: only AS stress and co-treatment of

AS and Act-D. The results strongly support that stress induced m⁶A methylation on a sub-set of mRNAs is a crucial factor for the SGs to protect them from degradation and stabilize them.

2.3.4 SG clients exhibit only modest effect upon stress induced methylation dysregulation during recovery

We went one step ahead to ask what happens after stress relief, when the SG transcriptome is altered? To determine whether influencing the stress induced m⁶A methylation of RNA have an effect in influencing the fate of the mRNAs protected in the SGs after stress relief, we performed RNA sequencing of the translated fraction upon 30min and 4h relief with co-treatment of Act-D. From the microscopy experiment (Figure 2.1B) we know that the methylated SG transcripts dissipated at an earlier time point of stress relief thus raising the question whether the m⁶A signal is crucial for leading them to its fate or not?

We compared the abundance of methylated and non-methylated transcripts upon Act-D treatment. Although the number of transcripts identified in the translating fraction upon stress relief is comparable to the cells not treated with Act-D (Figure 2.4B), at 30min of stress relief the methylated clients showed a higher abundance in the polysome fraction (Figure 2.4A). Interestingly, at 4h following stress relief the abundance of methylated clients showed no difference between Act-D treated or non-treated cells (Figure 2.4A). On the other hand, methylated transcripts increase their translating abundance after 4h of stress relief.

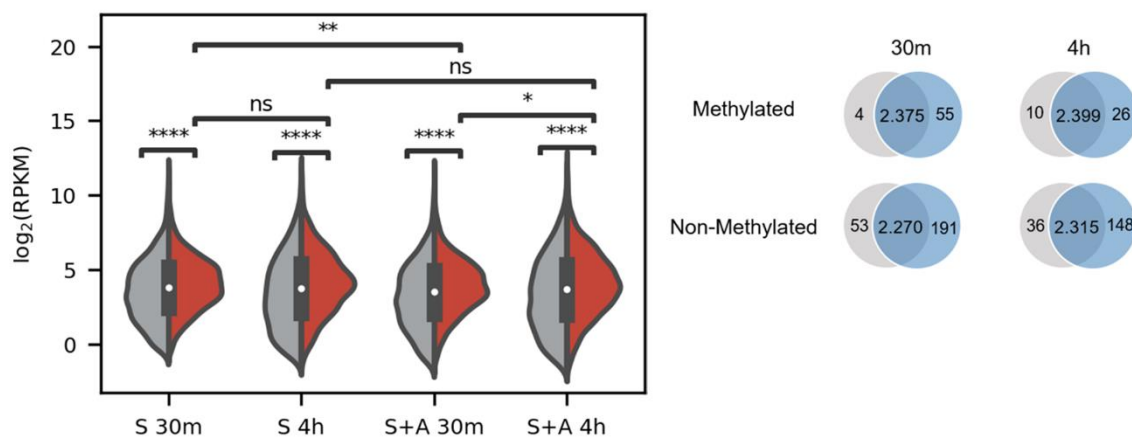


Figure 2.4: Abundance of transcripts in translation fraction at different time point after stress relief (30m and 4h) treated and untreated with Actinomycin D. A) Distribution of the abundance of the unmethylated (grey) and methylated (red) SG transcripts in the translation fraction upon relief with and without Actinomycin-D co-treatment with stress. *, p < 0.05, Mann-Whitney test. B) Transcript fraction detected in polysome sequencing after 30m and 4h of stress relief with cell treated (blue) and untreated (grey) with Actinomycin D

We first detected higher levels of transcripts in the translated fraction for methylated than the non-methylated clients after 30min of stress relief (Figure 2.4). The increased abundance of methylated clients in polysome fraction is also detected after 4h of stress relief. Non-methylated transcripts were equally abundant over the period of 30minutes to 4hours of stress relief. Taken together, the results indicate that lower abundance of methylated SG clients (Figure 2.3B) results in their lower abundance in the translated fraction (Figure 2.4A). The unchanged level of transcripts (methylated) at 4h following stress relief with and without Act-D treatment, indicates a higher level of recovery and at this time point the abundance of transcripts in the translated fraction, is independent of their abundance in the SGs.

2.3.5 Physical Basis of differential m⁶A methylation SG-mRNA clients

We observe that the stability is important, and a higher percentage of m⁶A stabilized RNA goes back into translation. To determine how does the cell select SG clients for methylation, we examined the properties of SG enriched methylated and non-methylated mRNAs. Gene Ontology (GO) analysis shows no preference to a functional group to be modified or not. It seems to be a more generic process and not limited to a subset of mRNAs. Hence, we sought to investigate the physical characteristics of methylated clients favoring the modification. The transcript length of methylated SG clients is slightly longer compared to the non-methylated transcripts (Figure 2.5A).

Methylated mRNAs were slightly longer (average length of 3.2 kb) compared to the non-methylated transcripts with an average length of 2.5 kb (Figure 2.5).

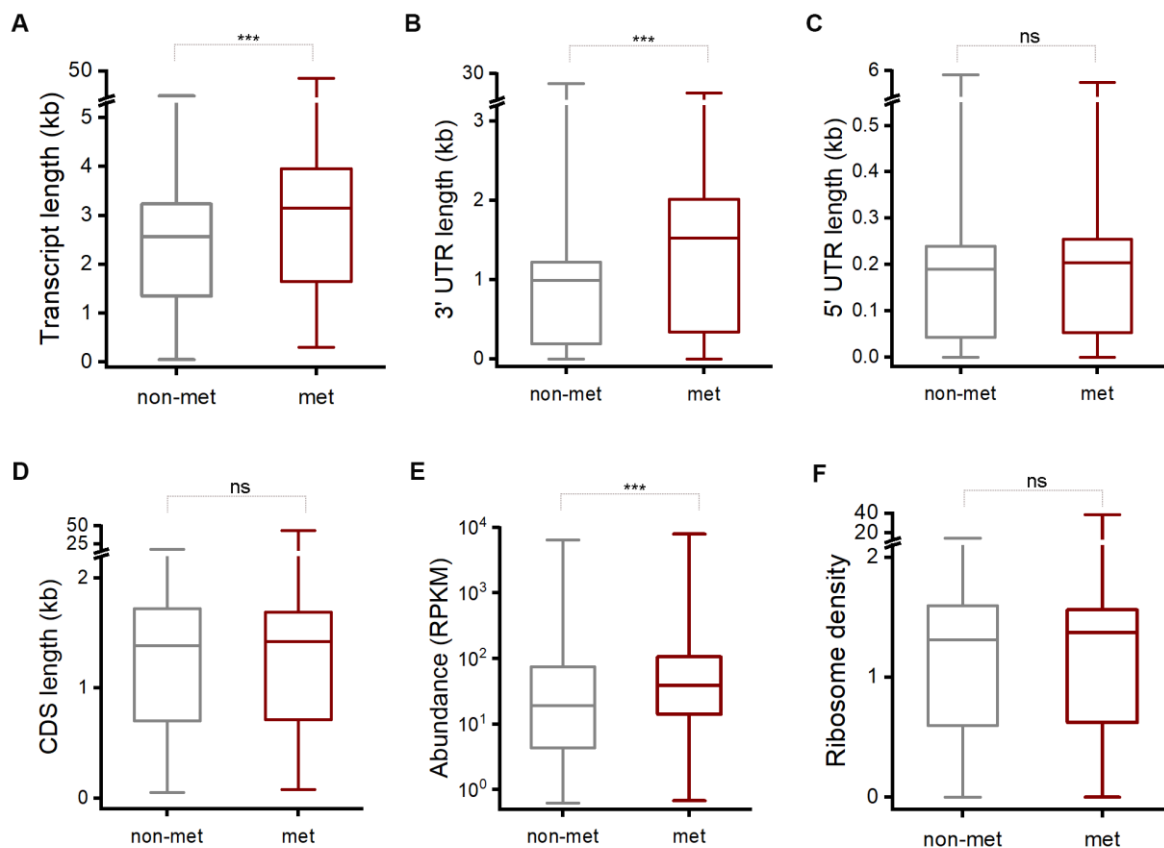


Figure 2.5: Physical basis of differential m⁶A methylation of SG mRNAs.

A-F) Box plot of whole transcript length (A), 3'UTRs (B), 5'UTRs (C) and CDC (D).

(E) Transcript abundance (F) Ribosome density, of the methylated versus non-methylated SG clients. ns, non-significant; **, $p > 0.01$; ***, $p > 0.001$ (Student's t test)

The difference in the 3'UTR length is majorly determining this difference (Figure 1.4B). The 3' UTR modulates the transcript affinity to RNA-binding proteins (RBPs) (Ke *et al*, 2015)(Chu *et al*, 2020). Following, we measured the transcript abundance of each group separately under normal growth condition. RNA-seq results suggests that, additionally to their longer mRNAs, the methylated transcripts are also more abundant in normal condition (Figure 2.5) which may imply a direct effect of the m⁶A modification on stability. Alternatively, the effect might be indirect and the higher abundance of the transcripts may correlate with the higher probability of being methylated.

Collectively, results indicate that the methylation occurs in a concentration dependent manner, i.e. more abundant transcripts are more susceptible to being methylated. Once methylated, these transcripts are captured by the SGs and avoid degradation upon oxidative stress.

2.3.6 mRNA is unstructured at m⁶A, but more structured in the near vicinity of m⁶A modification

Our observation that m⁶A modification may provide an advantage for the mRNAs to recover from SGs raised the question as to whether this could be due to structural stabilization of the transcript. m⁶A -modification regulates mRNA stability (Wang *et al*, 2014) and also has an impact on binding to several regulatory proteins (Lin & Gregory, 2014). To assess the m⁶A effect on the intrinsic propensity of mRNA to form secondary structure, we considered a published parallel analysis of RNA structure (PARS) (Dominissini *et al*, 2016). Across tissues and cell types of one organism, methylation patterns are constitutively maintained and regulatory secondary structures conserved (Dierks *et al*, 2021; Shepard & Hertel, 2008; Pedersen *et al*, 2006; Meyer *et al*, 2015), we used the PARS analysis with a very good depth of a model human cell line, HepG2, in which the total mRNA has been digested with double strand-specific RNase V1 or single strand-specific S1 nuclease and both subjected to deep sequencing (Dominissini *et al*, 2016). We computed the PARS score for each nucleotide (i.e. log₂ ratio between the normalized reads from the RNase V1-treated and the S1 nuclease-treated samples) for the two transcript groups with m⁶A modification and non-modified in the SG mRNAs (Figure 6A). For comparison, we plotted the PARS score within the vicinity of m⁶A in the group of methylated mRNAs and from the non-modified mRNA set we selected regions of predicted DRACH motifs because of their sequence similarity to the methylated DRACH motifs. A positive PARS score indicates higher propensity of the nucleotide to be involved in secondary structure, and vice versa, lower PARS score indicates no involvement of the nucleotide in secondary structure. The m⁶A methylation alone markedly decreased the PARS score at the modified A nucleotide (Figure 6B,C), suggesting decrease of structure propensity at the m⁶A nucleotide and corroborating earlier observations (Mao *et al*, 2019; Dominissini *et al*, 2016). However, it should be noted that the m⁶A effect was not significant as the A nucleotide in nonmethylated DRACH motifs exhibited a high intrinsic propensity to be rather unstructured, i.e. very low PARS score (Figure 2.6B, C). This effect was not limited to the mRNAs found in the SGs, but was uniform for all putative DRACH motifs in the transcriptome (Figure 2.6E, D). Intriguingly, we observed a significant increase in the structure propensity of the nucleotides (i.e. increase of the PARS score) in the immediate vicinity of m⁶A compared to the DRACH motifs of unmodified mRNAs (Figure 2.6). Together, this analysis suggests that while N⁶ modification decreases structure at the modified A nucleotide, it enhances structuring at nucleotides in the immediate vicinity of the mRNA, this in turn likely increases the stability of mRNA at least locally.

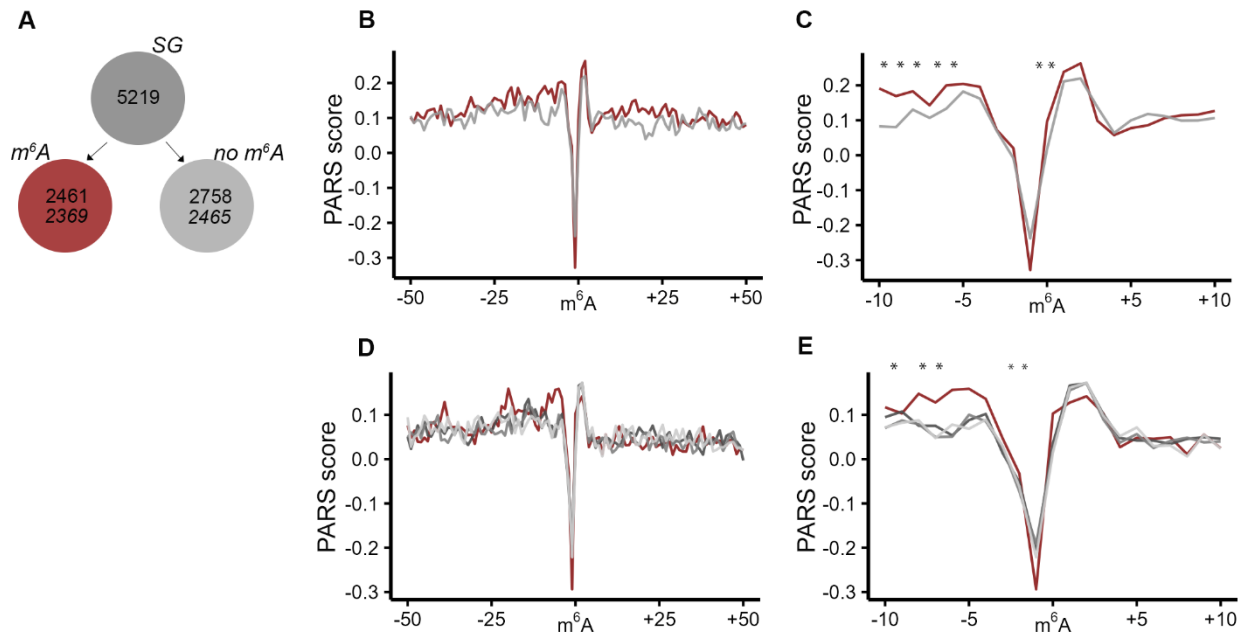


Figure 2.6: mRNAs exhibit higher structural propensity in the m⁶A vicinity.

A) From the SG mRNA clients nearly all methylated (red) and non-methylated (grey) mRNAs were detected in the PARS data set (italicized numbers). B) Aggregated PARS score plotted centered at the m⁶A including 50 nt up- and downstream of the SG methylated transcripts.

C) Zoom in into 10nt window up- and downstream of the m⁶A. Red, m⁶A-modified mRNAs; gray, non-modified mRNAs. *, p < 0.05, Mann-Whitney test.

D) Aggregated PARS score plotted centered at the m⁶A including 50 nt up- and downstream of all cellular transcripts. Since in the whole cellular transcriptome the m⁶A-modified mRNA set (red) was much smaller than the non-modified mRNA, the latter was randomly split into three groups (three shades of gray) of a similar size to the m⁶A-modified ones.

E) Zoom in into 10 nt window up- and downstream of the m⁶A. Color code as in panel A. *, p < 0.05, Mann-Whitney test.

2.4 Discussion

RNA partitioning into SGs are governed by the translation status of the cell (Tyler *et al.*, 2021). Transcriptomic studies have revealed the principle of RNA accumulation in mammalian and yeast SGs (Khong *et al.*, 2017). There is a diverse kind of mRNA that accumulates in SG and the abundance of the transcript does not drive its accumulation, suggesting that every mRNA in the cell could be present in the SGs and is not limited to any specific subset. Poor translation efficiency of the transcripts and longer length correlate with its targeting to SGs. Alternatively, RNA modification influences the binding of the RBPs and thus can alter its partitioning. The localization of mRNA to SGs may be a protective function by the cell (Protter & Parker, 2016), yet it remains unclear whether mRNAs deposited in SGs recover for translation following stress relief. In a previous study, we discovered two different modes of triaging mRNAs into SGs following

exposure to oxidative stress (Anders *et al*, 2018). A larger fraction of the mRNAs is pervasively methylated, mostly in the 5' vicinity of the CDS, which serves as a signal for triaging them from the translation pool to SGs (Anders *et al*, 2018). In my thesis study we also tried to understand the basis of such differential methylation of the SG -mRNA clients.

Here, we address an important aspect of the dynamics of SG disassembly, namely the recovery of mRNAs from SGs. We observed a gradual recovery of the SG-sequestered mRNAs with methylated mRNAs being first to leave the SGs. Combining fractionation of translating ribosomes with RNA-Seq identification of mRNAs in translated pools, we detected that the majority of the SG mRNAs recover for translation, with modest but significant higher recovery of m⁶A-modified mRNA compared to non-methylated ones i.e. 95% vs 84%, respectively. This nearly complete recovery of SG-sequestered mRNAs supporting the idea of the protective function of SGs (Protter & Parker, 2016). Deep sequencing-based structural PARS analysis reveal that at the N⁶ modification punctually enhances the tendency of the modified adenine to be more single-stranded corroborating earlier observations(Liu *et al*, 2017; Mao *et al*, 2019; Liu *et al*, 2015). By contrast, m⁶A renders the structural propensity of the nucleotides in its nearby vicinity and we found them with enhanced ability to participate in secondary structures.

m⁶A can destabilize RNA duplex by 1.4 kcal/mol (Kierzek & Kierzek, 2003)and alter locally mRNA structure, thereby exposing RNA binding motifs and facilitating binding (Liu & Pan, 2016; Mao *et al*, 2019). In some other contexts, however, m⁶A can contribute to stabilization of secondary structures. For example, m⁶A-U pair facilitates RNA secondary structure via canonical Watson-Crick geometry and by stabilizing adjacent basepair by adding a favorable hydrophobic interaction (Sternglanz & Bugg, 1973). Thus, m⁶A modifications may act as conformational switch or structural remodeler and through stabilizing or destabilizing local secondary mRNA structures may modulate interactions with RBPs.

In this study, we identified the mRNAs recovering for translation using RNA-seq. Nearly 90% of the mRNAs sequestered in the SGs recovered for translation. In a previous study, we discovered that SGs constitute of two different types of mRNAs, unmodified or pervasively m⁶A-modified (Anders *et al*, 2018). Monitoring the fate of modified and non-modified mRNA, here we observed that the methylated mRNAs fully recovered for translation (96%) compared to the non-modified (84%). The m⁶A may display some advantage to the mRNAs in their recovery for translation likely due to the m⁶A-drive structural mRNA stabilization in the near vicinity of the m⁶A modification.

In the SG mRNA group, the m⁶A modification is the highest in the vicinity of the stop codon and 3'UTRs (Anders *et al*, 2018). Higher structuring at 3'UTRs, likely mediated by m⁶A modification

in this region, correlates with poor targeting by miRNA mediated RNA degradation and higher stability of the modified mRNAs (Liu *et al*, 2014; Zhao *et al*, 2005).

Recent more precise gene-level quantification of m⁶A positions suggest a strong contribution of m⁶A modification to mRNA stability and mRNA half-life and link it directly to steady-state mRNA levels(Dierks *et al*, 2021). mRNAs with longer half-life times are more pervasively m⁶A modified(Dierks *et al*, 2021). Thus, based on the observation for a much higher or nearly complete recovery of m⁶A-modified mRNAs for translation compared to non-modified mRNAs, it is conceivable to propose that the m⁶A provides an advantage to the mRNAs in their recovery for translation by likely increasing the half-life and stability through m⁶A-driven mRNA structuring in the close vicinity of the modification site.

The dynamic behavior of this RNA-m⁶A-modification with stress and relief, provoked us to further understand what happens if the methylation is prevented, specially the stress induced m⁶A deposition at the 5' vicinity of the transcript. With Actinomycin-D(Act-D) co-treatment at a very mild dose, we inhibited co-transcriptional m⁶A RNA methylation and as a result of which the m⁶A peaks markedly reduced at the 5' region of the SG transcripts at 500μM Arsenite stress. As a result of inhibited transcription that affected the m⁶A deposition, we observed a poor correlation between the abundance of the SG clients. Thus, suggesting that m⁶A regulation upon stress determined the transcript composition in the SG. Unfortunately, the effect of m⁶A dysregulation was not observed upon stress relief. There was a significant modest decrease in abundance of the translating transcripts of methylated SG clients when transcription was inhibited during arsenite stress. This affect was lost later at 4 hr of relief condition.

Overall, we can conclude that m⁶A is a crucial signal for the SG transcript composition and their abundance. During translation recovery, the m⁶A methylated clients show increased abundance than the unmethylated transcripts indicating a stability factor from the m⁶A signal. Most of the transcripts from the SG was identified in the translation pool, reasserting the protective function of the SG. In a condition of dysregulated m⁶A signaling during arsenite stress by inhibiting co-transcriptional methylation, there was only modest effect on the fate of transcripts from SG to translation, majority of the transcripts methylated and non-methylated were present in the translated fraction. But, the detected abundance of these transcripts, were reduced whereas there was little or no effect on the non-methylated transcripts from SGs. Finally, our further analysis suggests the stability conferred to the m⁶A -methylated SG transcripts is due to the potential of forming stable folded structures at near vicinity of the modified base. The results of our study urges for future investigation on the structural changes of the transcriptome upon stress and also stress relief condition in eukaryotic cells.

3 Influence of YTHDF3 domains on its association with SGs

3.1 m⁶A reader YTHDF proteins regulate key processes in the cell

Recently, various studies have documented connection between m⁶A and cellular differentiation for different cell types (Lee *et al*, 2019; Cui *et al*, 2017; Barbieri *et al*, 2017). Through these studies it is evident that m⁶A has an essential role to modulate mRNA fate and cellular physiology. The biological function of the m⁶A-modified transcripts are mediated generally by reader proteins., belonging to the YT521-B homology Domain-containing Family (YTHDF) family of m⁶A - binding protein (Shi *et al*, 2017). There is a poor understanding of the complex network of interactions between the YTHDF1,2,3 proteins and the m⁶A sites. For all the readers RNA-bound structure has been stated and each of the amino acids that bind m⁶A and the adjacent nucleotides is conserved (Figure 3.1). Still they exhibit specific cellular function, most likely because the structures determined only considers the YTH domain and no other accessory interactions that occur with the other regions of the DF proteins.

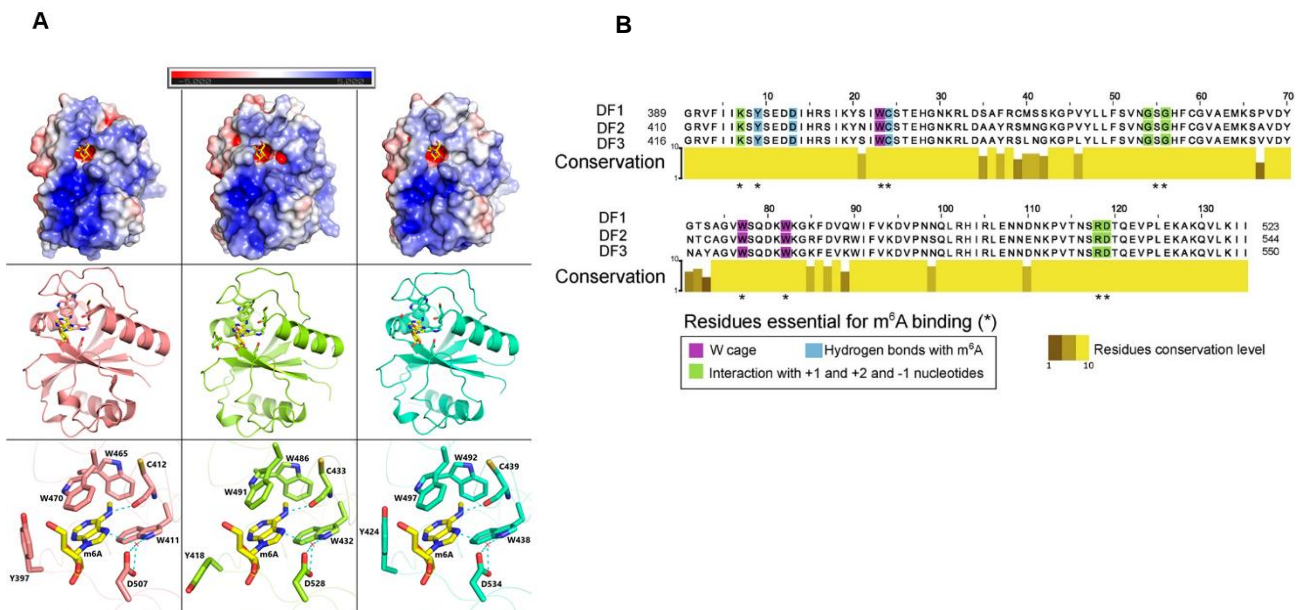


Figure 3.1: YTH domains of human DF proteins show similar potential at the RNA recognition and high sequence homology. A) Similar electrostatic potential at the RNA recognition surface (top), overall fold (middle), and interactions with m⁶A (bottom). (Left) DF1, PDB code 4RCJ; (middle) DF2, PDB code 4RDN; (right) YTHDF3, PDB code 6ZOT (Adopted from (Li *et al*, 2020)). B) The YTH domain of DF1, DF2 and YTHDF3 exhibit high sequence homology. Shown is a detailed representation of the aligned amino acid sequence for the YTH domains of DF1, DF2 and YTHDF3. (Adopted from (Zaccara & Jaffrey, 2020)) Pink indicates the three tryptophan

residues that form the aromatic cage surrounding m⁶A. Blue and Green indicate amino acids that make extra points of interaction between the YTH domain and the nucleotides next to m⁶A.

Recent structural study including X-ray crystallography and molecular dynamics shows that the three reader proteins share identical interactions with the m⁶A containing RNA (Li *et al*, 2020). As shown in figure 3.1B, amino acids essential for the m⁶A binding based on the DF1- m⁶A RNA and DF2- m⁶A RNA crystal structures (Xu *et al*, 2015; Li *et al*, 2014) are highlighted. Shown below in a yellow color code scheme is the level of conservation of every amino acid among the three YTHDF proteins with a range from 1 (low conservation) to 10 (high conservation) as predicted by the Clustal Omega alignment algorithm (Madeira *et al*, 2019). Most residues (88%) are fully conserved residues across all DFs proteins (Figure 3.1B). Importantly, amino acids essential for recognizing m⁶A and its adjacent residues are fully conserved. (Zaccara & Jaffrey, 2020).

In this work, we investigated the role of the disordered region of these proteins and their ability to form interactions with SGs. From previous studies we know that YTHYTHDF3 is associated with SG formation upon arsenite stress (Anders *et al*, 2018), the protein YTHDF2 localize in p-bodies and regulate RNA degradation (Du *et al*, 2016) and YTHDF1 directly influence the efficiency of translation of m⁶A containing mRNAs (Wang *et al*, 2015). Because we were interested to study the specificity of YTHYTHDF3 to associate with the RNA granule-SGs, we decided to compare in contrast to YTHDF2 protein which on the other hand associates with another type of RNA granule – the p-bodies. It was noted that in fact the intrinsically disordered region (IDR) in the readers have dissimilarity, both at the nucleotide sequence and also at its propensity of constituting prion-like domains (PRLD). PRLDs are basically low complexity domain (LCD), with compositionally biased regions, found usually in RBPs that help them to condense into functional liquids which can phase transit (Harrison & Shorter, 2017; Piovesan *et al*, 2021; Shorter, 2017; Maharana *et al*, 2018; Guo *et al*, 2018). Hence, we created mutants of YTHDF3 protein without the YTH-domain and the PRLD, to separately assess their contribution to mRNA localization in SGs and further its influence on m⁶A -RNA phase separation. Finally, we elucidated whether the specificity of the YTHDF3 protein depends on the composition of the disordered region, which may play an essential role in interacting with the proteins in the SGs other than directly through the m⁶A-mRNA.

3.2 Materials and Methods:

3.2.1 Cell Lines, Growth Conditions

U2OS cells stably expressing GFP-tagged G3BP1, a SG marker (Ohn *et al*, 2008), were used to perform the immunofluorescence experiment. Both cell lines were grown in DMEM medium at 37°C, 5% CO₂. To induce oxidative stress, 500 μM sodium arsenite (AS) was used for 30 min.

3.2.2 Cloning and expression of YTHYTHDF3, YTHDF2, YTHYTHDF3 mutants

Commercially available vectors consisting whole length YTHDF2 and YTHYTHDF3 gene was used to sub-clone into mammalian expression vector pcDNA3.1. Cloning by PCR technique was used to generate flag tagged mutants: YTH deleted mutant (deleted amino acid 384 to 585) and PRLD deleted mutant (deleted amino acid 304-351). These mutants were validated by sanger sequencing.

3.2.3 Transfection

Wild-type or mutant variants of YTHDF were transfected using polyethyleneimine (linear, MW 40.000 Da, Polysciences). Fresh media was added after 6hours of transfection and then used for immunostaining.

3.2.4 Immunostaining

For immunostaining, cells were grown on coverslips. For imaging, cells were washed twice with PBS, fixed for 15 min with 4% Paraformaldehyde at room temperature, and permeabilized using 0.5% saponin. Subsequently blocking was done using 1% BSA in PBST for 1 hr at RT. Primary antibody was added to the blocking buffer (m⁶A Antibody, SySy) in 1:200 dilution and incubated for another 1 hr at RT and then washed three times with PBS. Secondary antibody AlexaFluor 568 was diluted in blocking buffer (1:200) and added for 1 hr at RT.

All images were acquired on Leica-TCS-SP5 confocal microscope, on one Z-plane. Images were processed by ImageJ with FIJI plugin.

3.3 Results

3.3.1 YTHDF3 colocalizes to SGs upon arsenite stress condition

To distinguish the localization of YTHDF3 compared to DF2 reader protein, we adopted to the technique of immunostaining to visualize its localization upon oxidative stress. We probed with antibody against the flag tagged reader protein YTHDF2 and YTHYTHDF3 to visualize its localization upon arsenite stress, by method of immunostaining to recapitulate the previous results. We used U2OS-G3BP1-GFP tagged cells (Ohn *et al*, 2008) to expose them to 500μM arsenite

stress for 30 mins and immune-stained with antibodies against YTHDF2 and YTHYTHDF3 protein. In normal growth control conditions, YTHYTHDF3 appeared diffused in the cell, whereas upon stress it forms puncta in the cell. The YTHDF 3 foci formed upon stress, completely co-localized with the SGs (Figure 3.2).

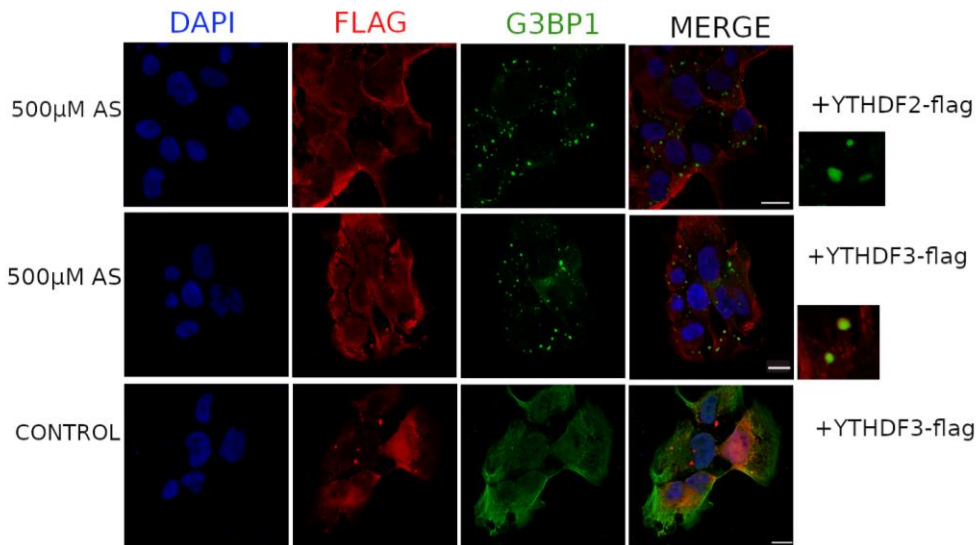


Figure 3.2: Reader protein YTHYTHDF3 co-localizes to SGs upon 500 µM Arsenite stress

SG is marked by G3BP1 tagged GFP and the ectopically expressed reader protein is probed by flag antibody stained in blue. Scale=10 µm

In accordance with the literature, the reader protein YTHDF 2 generally associated to degradation of RNA (Du *et al*, 2016), was completely absent in the SGs. From previous study (Anders *et al*, 2018) it was distinguished that reader protein YTHYTHDF3 among the other two readers has a selective role to triage the transcripts with the stress-induced m⁶A mRNA to SGs during arsenite stress. Both the reader proteins belong to the YTH-domain family proteins, and their sequence similarity suggest them to have a similar function but it is not the case. These proteins consist of IDR and also PLR regions within, which are often essentially crucial to form cytoplasmic granules in the cell that also regulates the granule's liquid like properties. Hence the next step was to understand its structural constitution investigating towards its specificity to SGs.

3.3.2 Structural analysis of YTHDF3 protein

To look at the sequence specificity of the disordered region YTHDF3 protein, we used online available tools for the study. PLAAC (Prion-Like-Amino acid Composition) (Lancaster *et al*,

2014) searches for probable prion subsequences with a protein sequence and it is based on hidden-Markov model algorithm. Using this tool, the likelihood of the prion like domain region in YTHDF3 protein was determined.

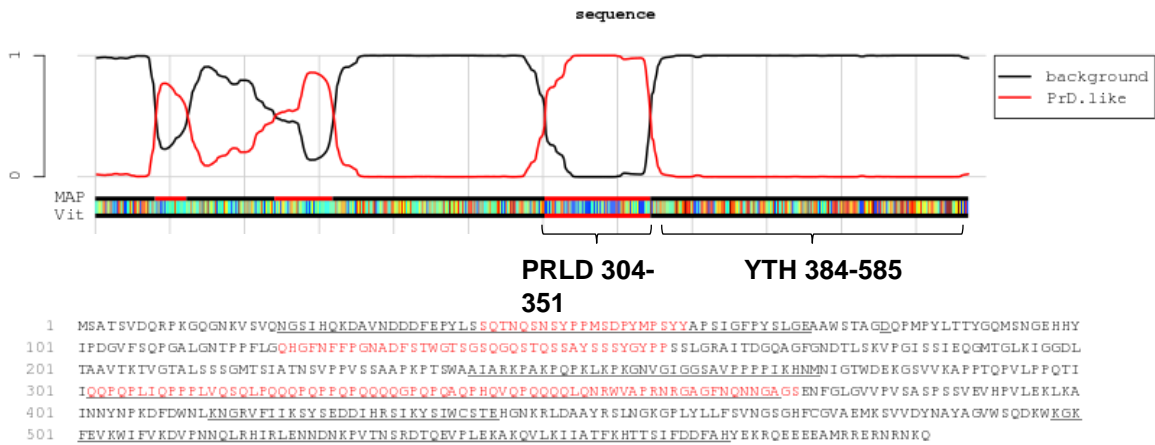


Figure 3.3: Structural prediction for potent Prion-like domain in YTHYTHDF3 protein.

The plot (red line) represents the PRLD propensity along the sequence length of the protein. Below shown is the amino acid sequence of the full-length YTHYTHDF3 protein.

As shown in Figure 3.3, the protein consists of the YTH domain 384 to 585 amino acid at the C' terminal, with a N' terminal IDR. Within the IDR a continuous stretch of PRLD region 304-351 amino acid present is a specific feature of YTHDF3 which has no similarity with the other DF proteins. The composition of the LCD within IDR has differences in the composition and also in its distribution across the proteins (Figure 3.4) and therefore we elucidated their role by creating YTHDF3 variant with deleted PRLD/LCD region and for comparison we used full-length protein along with a variant- deleted YTH domain.

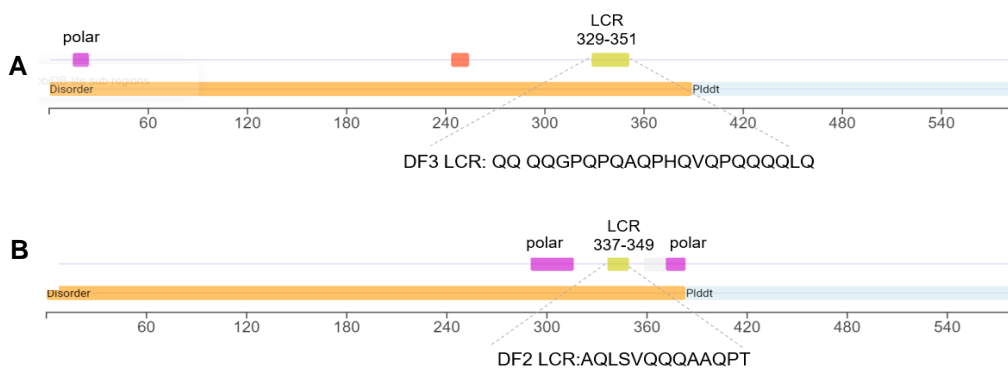


Figure 3.4: Diagrammatic representation of YTHYTHDF3(A) and YTHDF2(B) protein structure prediction obtained from MobiDB (Piovesan *et al*, 2021). The orange bar shows the

disordered region and the yellow bar shows the specific low-complexity region within it. In YTHDF3 the LCR region stretches longer and the distribution relative to the other region.

3.3.3 Reader YTHDF3-domain specificity to SG association

To dissect the role of the YTHYTHDF3 protein domains for its contribution to localize to SGs, we created YTHYTHDF3 protein variants in mammalian expression vector pcDNA3 consisting C' terminal flag tag. These constructs were created by site-directed mutagenesis and transfected in U2OS-G3BP1-GFP tagged cells. The cells were treated with 500 μ M arsenite for 30minutes and then used to perform fluorescent-immunostaining using antibody against flag tag to visualize the transfected variant protein and m⁶A antibody against RNA- m⁶A. The m⁶A -RNA is stained in red and the DF-flag tagged protein is stained in blue.

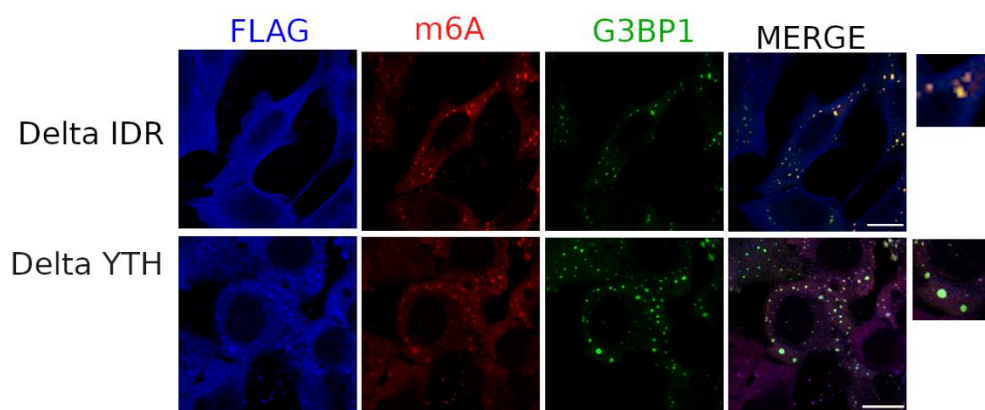


Figure 3.5: YTHDF3- Δ IDR mutants fails to localize to SGs.: The mutants are probed by flag tag antibody, stained in blue; m⁶A -RNA is stained in red and SG is marked by G3BP1-GFP tagged. Scale= 10 μ m

Upon arsenite stress exposure, the flag tagged YTHDF3 protein with deleted IDR shows much reduced localization to the SGs. The flag tagged YTHDF3 protein with deleted YTH domain show a different behavior, it clearly shows colocalization to the SGs. The YTHDF3-YTH deleted mutant shows clear puncta upon stress, of both small and big sizes that completely localizes with the m⁶A RNA to the SGs. This however, reflects that m⁶A binding of YTHDF3 only partially facilitate its association to the SGs and accessory interactions mediated by PRLD-IDR region with protein component of the SGs is also crucial. It is known that IDR facilitate high order functional aggregates(Latysheva *et al*, 2015; Babu, 2016; Wu & Fuxreiter, 2016) and from the above results we get a similar idea for the role of YTHDF3 in SG formation.

3.4 Discussion

The transcriptome-wide study on the binding properties for the DF paralogs reported earlier (Shi *et al.*, 2017) indicated the potential of the different DF protein paralogs to bind different m⁶A sequence motifs. Previous study from our laboratory (Anders *et al.*, 2018) has suggested how YTHDF3 protein is involved in mediating the m⁶A modified transcript localization to the SGs. It was an open question to understand how the YTHDF3 paralogue discriminate those m⁶A SG clients from the rest and whether this activity is solely m⁶A -binding dependent.

Through immunostaining experiment to study the localization DF2 and YTHDF3 in the cell upon stress we have a clear indication that YTHDF3 is specific to SG (Figure 2)(Anders *et al.*, 2018) whereas DF2 is specific to p-bodies(Wang *et al.*, 2014). Both these readers have some unique and common targets of methylated RNA partners and when present equivalently in a certain cell type there is a profound redundancy (Lasman *et al.*, 2020; Shi *et al.*, 2017). But the prevailing model derived from previous knowledge of: 44% m⁶A mRNAs bind a single DF paralogue, 32% bind to two DF proteins and 24% m⁶A RNA bind all three DF paralagues; suggested that different DFs regulate distinct physiological process. The specific interaction of the YTHDF3 to SGs could be a specific function of this paralogue, playing a critical role upon oxidative stress in the cell.

To elucidate further, we hypothesized that if there is a contribution beyond m⁶A binding then it can be led by its intrinsically disordered region and the prion-like domain. Hence, by the use of reader mutants with deleted IDR and YTH domain separately, the localization was affected when the mutant lacked the IDR (Figure 3.5). The YTHDF3-YTH deleted mutant showed formation of distinct round foci which colocalized to SGs along with m⁶A RNA. The YTHDF3-IDR deleted mutant showed reduced foci formation and also reduced localization to the SGs. This strongly suggests that the role of IDR to form hydrophobic interactions with other proteins in the SG play an important role and may be the causation for YTHDF3 specificity to SGs, facilitating or increasing the phase separation properties.

While we were proceeding with the design and setup experiment for in-vitro phase separation studies, two back-to-back publications were published (Fu & Zhuang, 2020; Zaccara & Jaffrey, 2020). Earlier study(Ries *et al.*, 2019) discusses the role of m⁶A in providing a mechanism of regulated phase separation and its level in different pathological condition will determine the context of the phase separated transcriptome. And further suggests this regulation be dependent on the efficiency of LLPS of the YTHDF proteins, thus determining the fate of the m⁶A-RNA. This has now been evidenced by the recent publication(Fu & Zhuang, 2020) where they clearly show that YTHDF play an important role in SG formation. Knockdown of YTHDF1/3 led to reductive influence in SG formation in U2OS cells upon arsenite treatment. Notably, they also

found both the N-terminal IDR and C-terminal m⁶A-binding YTH domains are important for helping SG formation. They found both the N-terminal IDR and C-terminal m⁶A-binding YTH domains to be important for promoting SG formation. m⁶A-binding activity of YTHDF proteins also appears to be helpful for SG formation. And in the other paper by S. Jaffrey (Zaccara & Jaffrey, 2020), they suggest something totally contrasting to the prevailing model, where each YTHDF paralog binds to distinct subsets of mRNAs, their study shows that the YTHDF paralogs bind proportionately to each m⁶A site throughout the transcriptome. All m⁶A sites bind all DF proteins in an essentially indistinguishable manner and contribute to mRNA destabilization. This hints that further additional work by other groups is required for development and understanding of the role of the YTHDF protein in context of regulating m⁶A RNA in both cellular stress and permissive growth condition.

4 Immunoprecipitation Assay to Quantify Amounts of tRNA associated with their Interacting Proteins in Tissue and Cell Culture

In this chapter I present a novel approach developed to assess bound tRNA to its cognate aminoacyl-tRNA-synthetase (AARS) protein. More specifically, the approach was originally developed to determine the interaction of tRNAs paring to Gly codons (tRNA^{Gly}) with their cognate glycyl-tRNA-synthetase (GlyRS) in both cell culture samples and mouse tissues. This work was performed in collaboration with the team of Dr Erik Storkebaum (Radboud University, The Netherlands) and is published as:

tRNA overexpression rescues peripheral neuropathy caused by mutations in tRNA synthetase; Amila Zuko, Moushami Mallik†, Robin Thompson..., Sarada Das, Divita Kulshrestha, Robert W. Burgess, Zoya Ignatova, Erik Storkebaum, 2021, Science (80-) 373: 1161–1166. In this publication, I performed the analysis of the tRNAGly: GARS complexes, an analysis which contributed significantly to determination of the molecular mechanism of Charcot-Marie-Tooth (CMT) peripheral neuropathy.

The approach itself is summarized in a protocol paper:

Immunoprecipitation Assay to Quantify Amounts of tRNA associated with their Interacting Proteins in Tissue and Cell Culture. Sarada Das, Amila Zuko, Robin Thompson, Erik Storkebaum, Zoya Ignatova. 2022, Bio-protocol, in press.*

4.1 Methods to study RNA and Protein Interactions

RNA-protein interaction could be studied from either the prospect of RNA or protein's, as elaborated in earlier section that their interplay is so intertwined with each other's interaction where every possible interaction leading to change in further binding patterns. Methods can then be devised around the molecule the interaction start off with either be RNA-centric or Protein-centric, wherein binding partners of the specific molecule can be looked into respectively. As understood by the complex nature of these studies, there are drawbacks and advantages of the method chosen for a study.

There are two ways to look at it: RNA centric Methods: with an RNA of interest, used to study proteins that associate with that RNA

RNA centric methods can be briefly listed as follows and shown in figure 4.1.

4.1.1 In vitro methods:

End-biotinylated-RNA pulldown. RNA is synthesized with biotin at the 5' or 3' end and combined with streptavidin. Recombinant or cellular-extract proteins bind to RNA. After being washed, the beads are boiled to elute and identify RNA-bound proteins.

Aptamer-tagged-RNA capture methods. The RNA of interest is in vitro-transcribed with an RNA tag. The RNA tag binds RNA to a resin support. Proteins in the cellular extract bind to RNA. Protein microarray. RNA is in vitro-transcribed with Cy5. The RNA is then added to a human protein microarray spotted with ~9,400 proteins.

4.1.2 In vivo cross-linking methods.

Cross-linking-based methods use either UV or formaldehyde cross-linking. Biotinylated oligonucleotide probes are hybridized to the RNA of interest, and the RNA and cross-linked proteins are purified for downstream analysis. In vivo non-cross-linking method (RaPID). Proximity proteomics has recently been applied for the RNA-centric study of RNA-protein interactions in living cells without the use of any form of cross-linking

. Protein centric method:

When the interaction study baits the protein of interest, and RNAs that interact with this protein of interest is characterized. The approach starts with direct purification of the protein or use a selective chemical modification in a way that relies on its association with the protein of interest. The overwhelming majority of studies that identify RNAs bound to a given protein do so by purifying the protein of interest. The most common approach in this case is to make use of the long-known fact that protein will chemically cross-link to nucleic acid in vivo when hit by UV light at approximately 254 nm.

Methods that involve UV cross-linking followed by purification of the protein of interest and identification of bound RNAs are broadly termed cross-linking immunoprecipitation (CLIP) methods, with those that use high-throughput sequencing (HITS) forming the CLIP-seq family of methods.

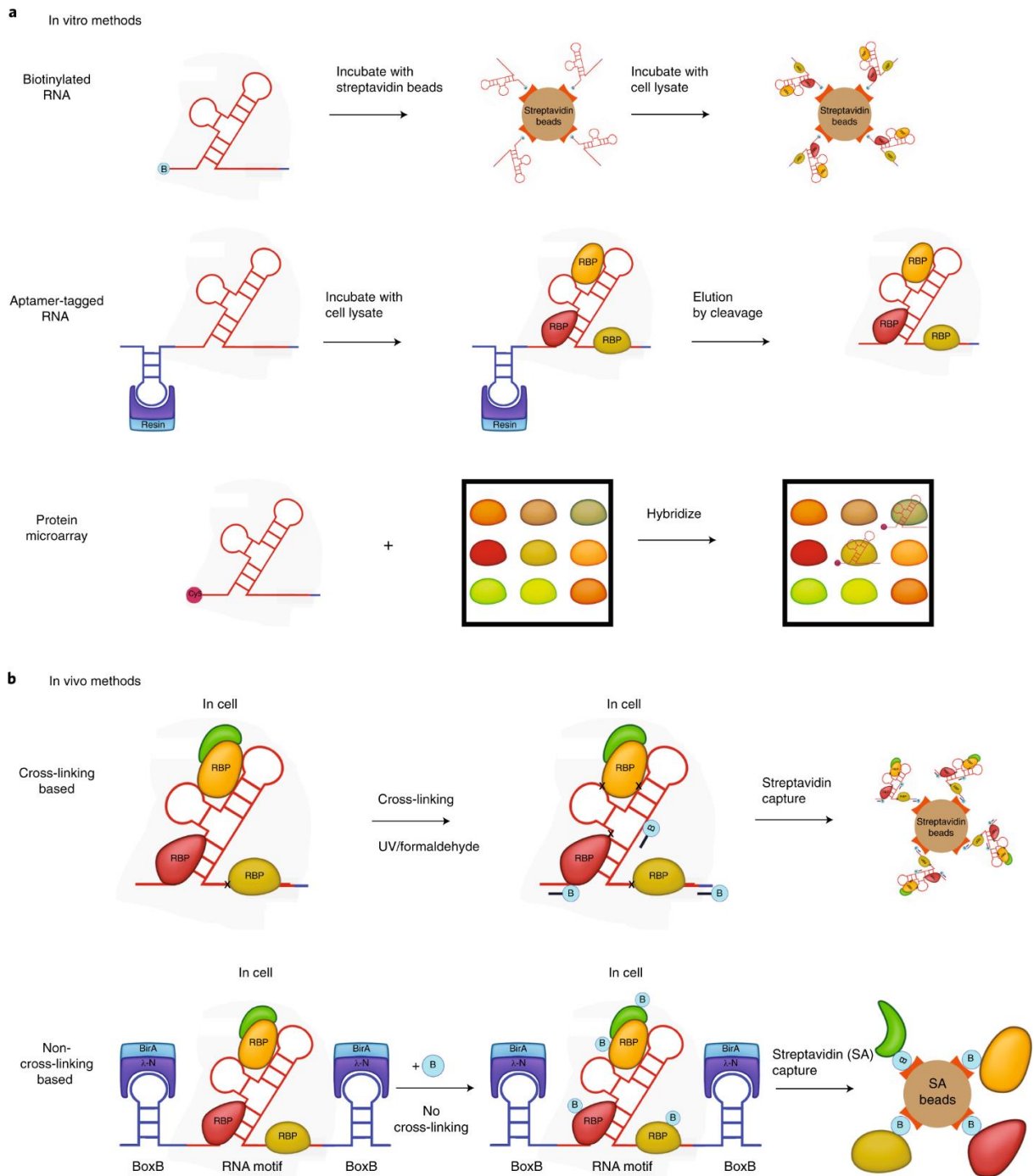


Figure 4.1: Schematic for the known RNA centric method to study RNA-protein interactions.(Adopted from (Ramanathan *et al*, 2019))

4.2 Methods to study tRNA-Protein interaction

tRNA-Protein interaction occurs throughout the process of protein translation where tRNA binds to several protein and RNA molecules, some that discriminate based on tRNA specificity (aminoacyl-tRNA synthetases (aaRSs), mRNA) and some that interact with every tRNA (elongation factor Tu (EF-Tu)). Mutation in genes of such interactors lead to pathological conditions (Abbott *et al*, 2014) and thus making it important to study them with both qualitative

and quantitative RNA centric approach to obtain the underlying mechanisms.

The current common methods for detection and quantitation of tRNA include northern blotting, RNA sequencing or custom Taqman-based PCR assays. Northern blotting doesn't give us a quantitative results but this is possible by RNA sequencing and PCR based methods. With the latest advancement in high-throughput sequencing of tRNA, we could achieve a quantitative output for bound tRNA but still the current sequencing method has not been able to give an unbiased quantitative measurement of the isoacceptors (Kimura *et al*, 2020; Orioli, 2017; Warren *et al*, 2021). In such case, there is a need of a method of tRNA detection to study tRNA-protein interactions that serve to be both quantitative and qualitative measurement.

4.2.1 tRNA immunoprecipitation approach

Transfer-RNAs (tRNAs) are highly abundant species and along their biosynthetic and functional path they establish interactions with a plethora of proteins. The high number of nucleobase modifications in tRNAs renders conventional RNA quantification approaches unsuitable to study protein-tRNA interactions and their associated functional roles in the cell. We present an immunoprecipitation-based approach to quantify tRNA bound to its interacting protein partner(s). The tRNA-protein complexes are immunoprecipitated from cells or tissues and tRNAs are identified by Northern blot and quantified by tRNA-specific fluorescent labeling. The tRNA interacting protein is quantified by automated Western blot and the tRNA amount is presented per unit of the interacting protein. This simple and versatile protocol can be easily adapted to any other tRNA binding proteins.

tRNAs are ubiquitous molecules representing 4-10% of all cellular RNAs. tRNAs undergo complex biogenesis in which they interact with different protein entities, including tRNA-splicing proteins, tRNA-base modifying enzymes, tRNA-charging enzymes, 3'-end modification and repair enzymes and various nucleases generating active tRNA fragments or completely degrading tRNAs (Betat & Mörl, 2015; Kirchner & Ignatova, 2015; Fernández-Millán *et al*, 2016; Barciszewska *et al*, 2016; Schmidt & Matera, 2020; Tosar & Cayota, 2020). tRNAs are crucial component of the translation machinery and are charged at the 3' ends with their cognate amino acid catalyzed by an aminoacyl-tRNA-synthetase. Mutations in tRNAs or genes encoding tRNA-interacting partners are linked to complex human pathologies with intricate heterogeneity at cell and tissue level that modulate the disease penetrance. Thus, it is of urgent need to develop a method for quantitative detection of tRNA-binding-protein interactions that can be widely used to study disease-related alterations of tRNA interactome in living cells and tissues.

Traditional methods to detect RNA-protein interactions include RNA immunoprecipitation (RIP) and crosslinking and immunoprecipitation (CLIP), both of which use antibodies to

immunoprecipitate RNA-protein complexes followed by identification of RNAs by sequencing. Unlike mRNA, the sequencing of tRNAs, despite recent advances (Behrens *et al*, 2021; Zheng *et al*, 2015), is still with a restricted quantitative resolution towards many tRNA isoacceptors likely because of their complex modification pattern (Kimura *et al*, 2020). Combining immunoprecipitation (IP) of the RNA-protein complexes with tRNA-tailored detection (Figure 1), we have developed a new twist of the classic IP methods that is suitable for quantifying tRNA-protein interactions in living cells. In a recent study, we have used this approach to quantify alterations in the tRNA binding to mutated glycyl-tRNA-synthetase (GlyRS) implicated in Charcot-Marie-Tooth (CMT) disease (Zuko *et al*, 2021). In a CMT-mouse model *Gars*^{C201R/+}, we observed stronger association of tRNAs^{Gly} with the mutant GlyRS, thus depleting the glycyl-tRNA^{Gly} pool and causing ribosome stalling at Gly codons (Zuko *et al*, 2021). The tRNA-IP methodology identifies and quantifies tRNAs bound to GlyRS in native conditions in tissues. The experimental setting can be easily adapted to other aminoacyl-tRNA-synthetases or any tRNA-binding proteins to quantify interactions in native conditions, in both cell culture and tissue.

4.3 Methodology

The starting material can be any tissue of interest, or mammalian cell culture endogenously expressing, stably transfected or epictopically expressing the tRNA-interacting protein of interest. If possible, it is recommended to test and optimize the protocol with easily accessible material, e.g. cell culture, before performing experiments in tissue. For quantitative assessment, it is important to perform the experiment in multiple independent biological replicates, i.e. at least ≥ 4 to enable statistical assessment. All steps should be performed in RNase-free environment.

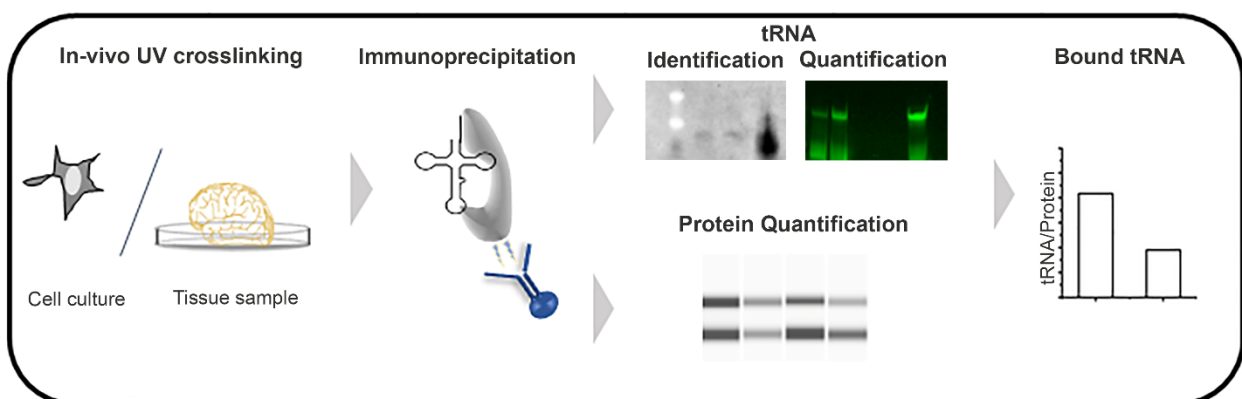


Figure 4.1: Schematic of the tRNA-Immunoprecipitation approach.

4.3.1 Sample Preparation

In-vivo UV crosslinking to stabilize transient tRNA-protein interactions in cell culture here HEK293T cells, hereafter named only HEK): For one experiment, approximately 20 million cells

are required, however for scarcely available cell culture material as little as 6 million cells can be used. HEK293 cells were used to perform this experiment, which is maintained in DMEM medium supplemented with 10% FBS and 2.5mM L-glutamine at 37°C in 5% CO₂. To prepare the cells for UV-crosslinking, the medium is aspirated and cold 1x PBS was added gently. Placed the cell culture plate on ice and illuminate with the UV light source (254 nm) of a crosslinker at 150 mJ/cm² radiation. In parallel, cells treated the same way without UV crosslinking was used as a control. The cell culture dish is kept on ice, to gently aspirate the PBS solution and added 800 µl of pre-cooled cell lysis buffer(20 mM Tris-HCl ,pH 7.4,15 mM NaCl,1% NP-40,0.1% Triton® X-100,1X Protease Inhibitor) Harvested the cells by scraping and transferred them into a pre-cooled 1.5 ml Eppendorf tube. With a 26-gauge, the lysate is passed through 8-times to further shear open the cells and facilitate lysis. To obtain a clear lysate centrifuge at 16,000xg for 10 min at 4°C. This is the starting material for the IP

In-vivo UV Crosslinking to stabilize transient tRNA-protein interactions in tissue samples: To choose the most appropriate tissue for the experiment, one can refer to the Human Protein Atlas. In our experiment, we use brain tissue from 3- to 6-weeks of age CMT model mice (Gars^{C201R/+}; (Achilli et al, 2009)) and compared it to the wildtype littermate mice (i.e. mice expressing WT GlyRS (C57Bl/6J)). One hemisphere of the mouse brain tissue was enough to obtain a sufficient amount of tRNA and GlyRS in the IP. Freshly dissected brain tissue sample is flash frozen in liquid nitrogen and powdered in a pre-cooled CellCrusher tissue pulverizer. The powdered tissue is transferred into a 3.5 cm cell culture dish placed on ice. The dish placed on an ice bath is irradiated by UV light source inside a UV crosslinker at 400 mJ/cm² radiation. To Note: Dependent on the tissue availability a non-crosslinked control could be used. To the tissue sample, 500 µl of cold tissue lysis buffer(20 mM Tris-HCl pH 7.4,15 mM NaCl,1% NP-40,0.1% Triton® X-100,0.5% SDC,1x Protease inhibitor) is added and mechanically sheared by pipetting up and down using pre-cooled wide-bore pipette tips (or 1000 µl-pipette tips with cut end). Addition an additional 500 µl of cold lysis buffer to the lysed tissue is needed and further agitated at 4°C for 1 h. To obtain a clear lysate, centrifuge at 16,000xg for 10 min at 4°C. This was the starting material for the IP .

4.3.2 Preparation of magnetic beads and antibody coupling

Select magnetic beads according to the immunoglobulin (Ig) type of the antibody to be used for the IP.

For HEK cell lysate:Protein G-coupled Dynabeads® were used here, 20 µl of the beads for each antibody coupling reaction. Two times washed beads with 500 µl cold 1x PBS were used and resuspended them in 50 µl cell lysis buffer. The beads were incubated with 2 µg of the antibody

on a tube rotator for 45 min at room temperature. Leave on ice while preparing the lysates.

For brain tissue lysate: Protein G-coupled Dynabeads® were used here, 50 µl of the beads for each coupling reaction. Prepared the beads by washing them two times with 500µl cold 1x PBS solution and resuspended in 100 µl of tissue lysis buffer. The beads were incubated with the antibody on a tube rotator for 45 min at room temperature. Leave on ice while preparing the lysates. For our experiment in both cell culture and mouse tissue, we used a mixture of two different anti-GlyRS antibodies, which we mixed in equal amounts (i.e. 1 µg each). Using a mixture of antibodies from different suppliers enhances the IP reproducibility between various supplier charges.

4.3.3 Immunoprecipitation (IP)

To determine the efficiency of the antibodies, the pulldown was first performed with more accessible material (e.g. cell culture), thereby optimizing the amount of the beads with coupled antibody and the IP incubation time. For incubation time we recommend starting with 1 hr, or a few hours up to overnight incubation. The optimal incubation time is the one at which the antibodies maximally retain the desired target with minimal to no non-specific RNA bands detectable on ethidium bromide stained denaturing polyacrylamide gel.

For HEK293 cell lysate: The clear lysate obtained after crosslinking from the above steps, was transferred to the prepared beads, along with 20U of RNase inhibitor. This reaction was incubated for 2 h at 4°C on rotation. Using a magnetic separator, the immunoprecipitated tRNA-GlyRS bound to the antibody-coupled beads was separated. The supernatant is carefully discarded, which is followed by bead washing steps with 1X wash buffer (20 mM Tris-HCl pH 7.4, 100 mM NaCl, 1% NP-40, 0.1% Triton® X-100), twice. Finally the beads are resuspended in 500µl wash buffer. From this IP reaction (with beads), withdraw 10µl and kept separately for protein quantification (as explained in the next steps below). A hot acid-phenol extraction of the remaining IP sample is performed directly on the beads, to denature the protein (here GlyRS) and elute bound tRNAs. Finally, dissolve the recovered tRNA in 5 µl sterile nuclease-free water.

For brain tissue lysate: The clear lysate obtained after crosslinking from the above steps, was transferred to the prepared beads, along with 20U of RNase inhibitor. This reaction was incubated for overnight at 4°C on rotation. Using a magnetic separator, the immunoprecipitated tRNA-GlyRS bound to the antibody-coupled beads was separated. The supernatant is carefully discarded, which is followed by bead washing steps with 1X wash buffer, twice. Finally the beads are resuspended in 500µl wash buffer (20 mM Tris-HCl pH 7.4, 100 mM NaCl, 1% NP-40, 0.1% Triton® X-100, 2% SDC). From this IP reaction (with beads), withdraw 10µl and kept separately for protein quantification (as explained in the next steps below). A hot acid-phenol extraction of

the remaining IP sample is performed directly on the beads, to denature the protein (here GlyRS) and elute bound tRNAs. Finally, dissolve the recovered tRNA in 5 μ l sterile nuclease-free water.

4.3.4 Identification and quantification of the bound tRNAs in the IP.

tRNA identification by Northern blot

An *in vitro* transcribed tRNA of interest-is required as a positive control. Here, tRNA^{Gly}GCC was prepared by a standard T7-RNA polymerase run-off transcription reaction using DNA template. Two partly overlapping DNA primers were designed that cover the full-length tRNA^{Gly}GCC, and 5' to the forward primer the T7 promoter site (Table 1).

Table 4.1: Example of DNA primers for *in vitro* T7 promoter-driven synthesis of tRNA^{Gly}GCC. The forward primer contains 5' upstream of the tRNA transcription start site the T7 promoter (underlined).

Forward	5'-TAATACGACTCACTATAGCATCGGTGGTTCAGTGGTAGAATGCTCGCCTGCCACGCGGGC-3'
Reverse	5'-TGGTGCATCGGCCGGAATCGAACCCGGGCCCGCCGCGTGGCAGGCGAGCATTCTA-3'

To prepare the IP (step C-a7) for Northern blot analysis, the sample is heated at 95°C for 3 min and placed it on ice. Samples are loaded on a 10% denaturing polyacrylamide gel and ran at 10 Watt for 30 min. *In vitro* synthesized tRNA is also loaded on the gel as a positive control (Figure 2A and 3A). The RNA from the gel was transferred onto a Hybond-N blotting membrane in pre-cooled 0.5x TAE buffer at 4°C at 10V overnight. Immobilized the RNA to the membrane by application of UV light (365 nm, 9999.9 mJ/cm²). Followed by hybridization of the membrane with Atto565-labeled DNA oligo probe (5 μ l of 100 μ M probe) recognizing the tRNA of interest at 28°C overnight in hybridization buffer. Thereafter, blots are washed three times with 6x SSC (supplemented with 0.1% SDS), followed by one wash with 6x SSC, one wash with 2x SSC, and a final wash with 0.2x SSC. Imaging was done on a ChemiDocTMMMP Imaging system.

If the tRNA-binding protein binds all tRNA isoacceptors of one tRNA family (that are all tRNAs recognizing different codons for a given amino acid, and thus aminoacylated with the same amino acid), we recommend using a mixture of probes to all isoacceptors. Here, we used two probes, including one with degenerate nucleotide sequence that recognizes all three tRNA^{Gly} isoacceptors (Table 2).

Table 4.2: Sequences of the Atto565-labeled DNA probes used in the Northern blot experiment. One probe contains degenerate bases, thus recognizing both tRNA^{Gly}CCC and tRNA^{Gly}GCC. The probes are labeled at their 5' ends with Atto565.

Probe	Sequence
tRNA ^{Gly} TCC	5'-CCCGGGTCAACTGCTTGGAAGGCAGCTAT-3'
tRNA ^{Gly} CCC/GCC	5'-GYCTCCCGCGTGGSAGGCGAG-3'

4.3.4.2 Quantification of the tRNA bound to GlyRS by fluorescent tRNA labeling

The IP (step C) yields enough RNA for tRNA detection by Northern blot and fluorescent quantification. Since the Northern blot is performed only for tRNA identification, we recommend performing it in a single biological replicate and load the entire remaining extracted tRNA amount in multiple wells onto the gels and use them as multiple technical replicates in the fluorescent quantification. To label the immunoprecipitated bound-tRNA, a fluorescently labeled RNA: DNA hairpin oligonucleotide specific to tRNA with the following sequence: 5'-CGCACUGCdTdTXdTdTdGdCdAdGdTdGdCdGdTdGdGdN-3'. (X denotes a dT nucleotide labeled either with Cy3 or Atto647; the 5' should have a monophosphate) was used. The labelling reaction consists of the labelling mix : 1 µl 10x T4 ligation buffer (NEB, #M0202), 1.5 µl DMSO, 0.5 µl Cy3-labeled 25-mer oligonucleotide (90 µM), 0.5 µl T4 DNA ligase and 1.5 µl H₂O. The fluorescently labeled RNA:DNA hairpin oligonucleotide is designed to basepair to the unique unpaired 3'-NCCA end of the tRNAs and is used to specifically label tRNAs as described previously (Kirchner *et al*, 2017b).

Combining 5 µl of extracted tRNAs with 5 µl of the above labeling mix, it is kept to incubate for 1h at 25°C in the dark to protect the fluorophores. The ligation mixture is then heated at 95° C for 3 min and placed on ice immediately. The mixture is loaded and ran on a 10% denaturing-polyacrylamide gel at 10 W for 30 min in the dark. Visualization of the tRNA was performed on a ChemiDoc™MP Imaging System in the respective fluorescent channel and a good quality image is saved for further quantification of the fluorescent tRNA bands. (A representative image is shown in Figure 2B and 3B).

4.3.5 Quantification of the GlyRS protein in the IP.

The 10µl of the IP sample kept before the RNA extraction, is now used at this step to separate the beads with bound antibody and protein-tRNA complexes from the liquid phase with the use of a magnetic separator. Added 10 µl of 1x SDS buffer(50 mM Tris-HCl pH 6.8,2% SDS) to the beads and incubate at 50°C for 10 min by gentle shaking. Collect the solution in a fresh Eppendorf tube – this eluent consists of the bound tRNA-interacting protein. The eluent was then subjected to the

Jess automatic Western blot system – a capillary-based automated Western blot instrument – to quantify the protein (Figure 2C and 3C).

A conventional Western blot can also be used instead, though the automated Jess system offers much higher sensitivity. We used purified human wildtype GlyRS protein at varying concentrations to establish a standard curve. Wildtype GlyRS was cloned into pET28 vector and expressed in Escherichia coli Rosetta strain. GlyRS sequence was extended by two purification tags; 6xHis and SUMO tag. The protein was purified to homogeneity using two consecutive chromatography steps, i.e. Ni-NTA-based affinity purification, followed by cleavage of both tags and purification by size-exclusion chromatography. The detailed purification protocol is described in (Zuko et al, 2021).

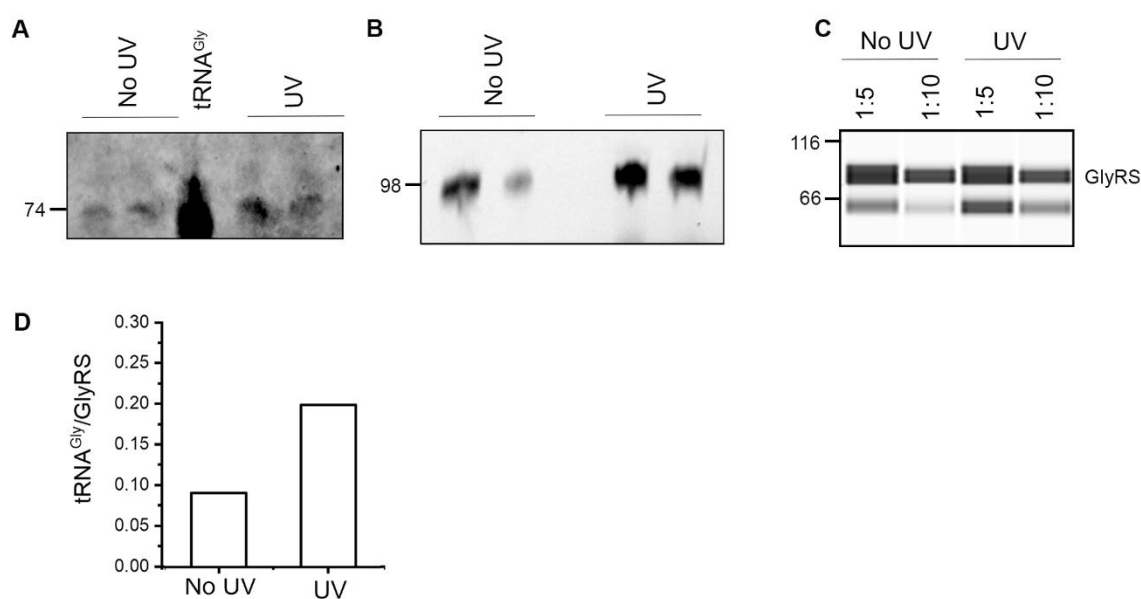


Figure 4.2: Quantification of tRNA bound to GlyRS in HEK cells. A) Detection of tRNA^{Gly} bound to GlyRS by Northern blot using Atto565-labeled probes recognizing all three tRNA^{Gly} isoacceptors. *In vitro* transcribed tRNA^{Gly}GCC was loaded as a positive control and has a size of 74bp. UV and Non-UV cells treated with UV and with no UV treatment, respectively. B) Quantification of tRNA^{Gly} bound to GlyRS with Cy3-labelled fluorescent stem-loop RNA/DNA oligonucleotide. The ligated tRNA product was monitored on a 10% denaturing polyacrylamide gel. Florescently labeled extended tRNAs have a size of 98 bp. C) Immunoblot of of the IP analyzed by Jess automated Western blot and probed with antibodies recognizing GlyRS. Different dilutions of the IP reactions were analyzed. Protein weight markers are shown on the left in kDa. D) Quantification of tRNA bound to GlyRS.

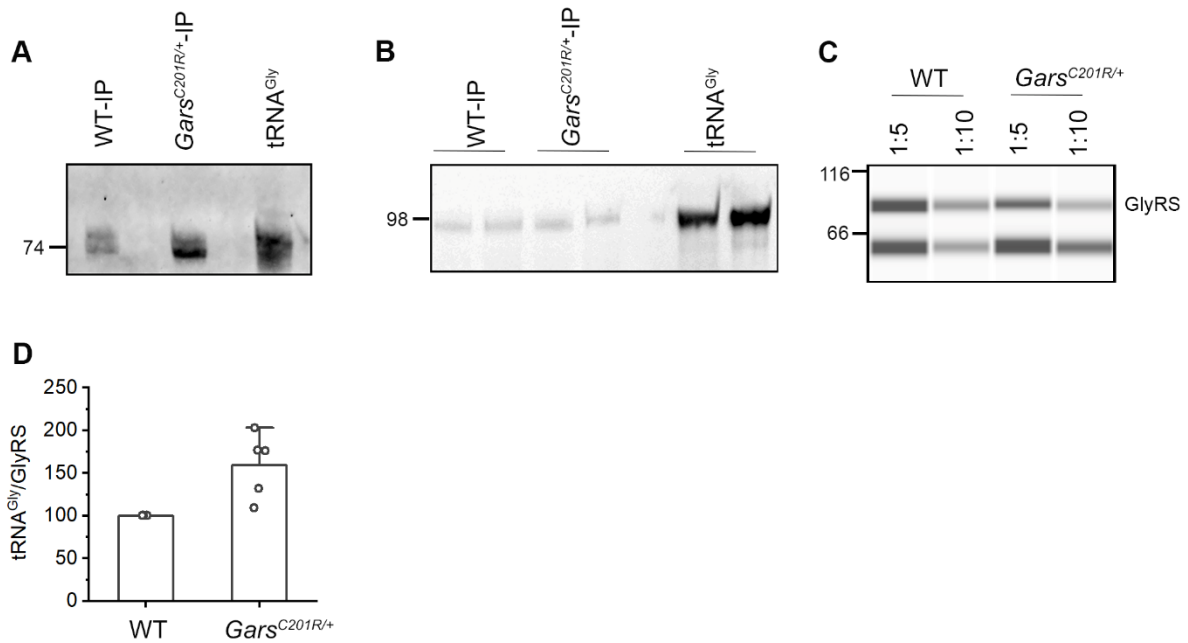


Figure 4.3: Quantification of tRNA bound to GlyRS in brain tissue from *Gars*^{C201R/+} mice (C201R-IP) and wildtype littermate (WT-IP). A) Detection of tRNA^{Gly} bound to mutant and wildtype GlyRS by Northern blot using Atto565-labelled probes recognizing all three tRNA^{Gly} isoacceptors. *In vitro* transcribed tRNA^{Gly}GCC was loaded as a positive control and has a size of 74bp. B) Quantification of tRNA^{Gly} bound to GlyRS with Cy3-labelled fluorescent stem-loop RNA/DNA oligonucleotide. The ligated tRNA product was loaded on a 10% denaturing polyacrylamide gel. Fluorescently labeled extended tRNAs are with a size of 98 bp. C) Immunoblot of the IPs analyzed by Jess automated Western blot and probed with antibodies recognizing GlyRS. Different dilutions were analyzed. Protein weight markers are shown on the left in kDa. D) Quantification of tRNA bound to GlyRS and normalized to the tRNA/GlyRS ratio of wildtype mice which is set as 100%. Data are shown as mean \pm SEM (n=5 independent biological replicates).

4.4 Data analysis

The intensity of the tRNA band was quantified from the gel in (Figure 4.2A and 4.3A), using Image J software. It was ensured that the samples to be compared are loaded onto the same gel and that the image is taken in grayscale. Use the same area when calculating the intensities and average it from multiple technical replicates. Blank intensity from the gel should be used to subtract the gel background.

From the Jess electrogram report, the peak area corresponding to the protein of interest was used to determine the concentration using the standard curve with purified protein samples. Further, divide the tRNA amount by that of the protein. For comparison reasons, if comparing two conditions or the effect of a mutation, normalize to the ratio to that of the wildtype control, whose ratio is set to 1. We used such additional normalization enabling assessment of the increase of the

bound tRNA to CMT-mutant GlyRS (Figure 4.2E and 4.3E).

4.5 Discussion

RNA-protein interaction studies are crucial to understand their role towards homeostasis in the cell. Many cellular processes revolve around such interactions, where non-coding RNAs like: tRNA, rRNA, small nuclear RNA and also untranslated mRNA regions make associations with RNA binding proteins (Hentze *et al*, 2018; Ramanathan *et al*, 2019). Their role is not limited to just a few domains of cellular life but expands to various dynamic processes like splicing, transcription and translation. They function also to maintain each other's life cycle in the cell. Studies on them provide valuable insights into their binding modes and functional implications.

tRNAs are highly abundant short non-coding RNA species and during their biosynthesis and functional path establish interactions with a variety of proteins. Well studied tRNA-protein complexes in the cell is that of with ribosomal proteins (Abdurashidova *et al*, 1991). This interaction regulates translation and both structural and biochemical studies since a long time have enabled to establish a near to complete knowledge about them (Fei *et al*, 2011; Abdurashidova *et al*, 1991; Ofengand *et al*, 1986).

Specific interaction of tRNA and its cognate AARS is essentially crucial for accurate translation of the genetic code. Changes in the cellular environment can affect such interactions leading to poor tRNA aminoacylation and further alter translation regulation (Zaborske *et al*, 2009). Recent studies have revealed role of several AARs in pathology associated with genetic mutation. Since they are housekeeping genes, it is linked to complex human diseases (Yao & Fox, 2013; Kim *et al*, 2011). The field in general lacks studies on how such mutation in the tRNA binding proteins have a mechanistic link towards the disease phenotype. For better understanding of the molecular mechanisms of such dysregulation at the level of tRNA-protein interaction, this method for quantitative detection of tRNA-binding-proteins interactions can be widely used to study such disease-related alterations of various tRNA-protein complexes in living cells and tissues.

The method relies on the principle of in-vivo-immunoprecipitation where we immunoprecipitated GlyRS from brains of *Gars*^{C201R/+} and WT littermate mice and quantified the amount of tRNA^{Gly} bound to GlyRS. Basically it is an immunoprecipitation-based approach to quantify stoichiometry between tRNA and its protein interacting partners. The tRNA-protein complexes are immunoprecipitated from cells or tissues and tRNAs are identified by Northern blot and quantified by a tRNA-specific fluorescent labeling. The tRNA interacting protein is quantified by automated Western blot and the tRNA amount is presented per unit of the interacting protein. The

simple and versatile protocol can be easily adapted to any other tRNA binding proteins.

The CLIP assay uses UV-irradiation method to fix RNA-protein complexes in living cells or tissues. This version of the protocol was standardized for eukaryotic cells and hence required optimization for tissue samples. To optimize glycine-tRNA synthetase protein specific pull-down, we initially used HEK293 cells. There are several factors on which an immunoprecipitation assay is dependant on and three major parameters to consider for optimization are: type and amount of beads used to bait the Protein-RNA complex , the amount of antibody against the target protein, and the antibody incubation period with the lysate. Once the protocol was standardized for cells, we then standardized it for mice tissue samples. For the method with mouse tissue samples, we used brain tissue. And we immunoprecipitated and extracted bound tRNA in considerable amounts for validation and quantification. Combining immunoprecipitation assay and in-gel fluorescence, we have developed a method to quantify AARS bound tRNA from in-vivo condition.

The method developed was successfully used to qunatitatively decipher the binding of tRNA^{Gly} to the CMT disease mutant glycine-tRNA-synthetase (GlyRS) implicated in Charcot-Marie-Tooth disease, compared to wild type synthetase protein in a study conducted in collaboration with Dr Erik Storkebaum(Zuko *et al*, 2021) . This study demonstrated how slow tRNA^{Gly} release by CMT-mutant GlyRS sequester a large fraction of cellular tRNA^{Gly} and thus deplete it for translation. With the current method developed we added in-vivo experimental evidence to support the study. The greatest advantage of this method is that with a very reasonable amount of starting material: cells or tissue, we obtain good output for both validation and quantification of specififc bound tRNA to the protein in closest accuration.

5 General Discussion

5.1 SG assembly, disassembly with respect to m⁶A modified RNA

The process of SG assembly is well studied and explored (Gilks *et al*, 2004; Kedersha *et al*, 1999a; Ohn *et al*, 2008; Banani *et al*, 2017; Jain *et al*, 2016b; Mazroui *et al*, 2006; Yang *et al*, 2020; Protter & Parker, 2016). SG consisting both RNA and protein, the assembly is complicated requiring systematic progression. To add to this field our lab previously studied the localization of m⁶A methylated RNA with respect to SG assembly and gained the understanding of the role of m⁶A as a signal for the process of RNA triaging to SGs (Anders *et al*, 2018). In this current study, we looked at the m⁶A -RNA assembly procedure along with studying the m⁶A RNA disassembly procedure upon stress recovery.

Through immunostaining we observed that the SG assembly with respect to the m⁶A -RNA, is a biphasic process. SG assembly in general is a biphasic process, where leading aggregation and SG nucleation occurs when heterogeneous 48S-bound transcripts are bound by RBDs that possess homotypic aggregation potentials, such as G3BP, TIA-1 etc. This is followed by the secondary aggregation where transcripts forms oligomers with RBD and nucleates to the SG thus increasing its size (Anderson & Kedersha, 2008). The m⁶A methylated RNA associates at a second step to the SG nucleation and forms a stable interaction with it upon 30 mins arsenite stress (section 2.3.1). This biphasic mode of the m⁶A RNA to come and interact with the SG in the second step, exhibit a likeliness that m⁶A -RNA association is dependent on the first step and may serve to give physical support in the outer shell of the SG.

Our study investigates the same during stress relief, that is the movement of m⁶A modified RNA from the SG as the cell recovers from stress. Immunostaining method was again the key method to follow this kinetics and from which we report that the m⁶A RNA dissipates from the SG at a much earlier time point compared to the core of the SG. The core of the SG takes long as 90mins which is in accordance to the literature (Wheeler *et al*, 2016). The early release of the mRNA could be because the SG act as protective compartment, and the accumulated mRNA needs to go back into the cellular milieu from this protective compartment upon recovery.

We also tried to look at the mechanistic understanding of the specificity of YTHDF3 protein targeted to SG upon arsenite stress (Anders *et al*, 2018). The different transcriptome-wide binding properties reported for the DF paralogs reflects distinguished function for each (Shi *et al*, 2017; Du *et al*, 2016; Xu *et al*, 2015; Wang *et al*, 2015). We hypothesized that the biophysical differences could be an attribute contributing to the functional difference of YTHDF3, here to have a role in triaging m⁶A RNA to SGs, compared to other reader protein like: DF2 (Anders *et al*, 2018). Mutants of YTHDF3 were cloned

with deleted YTH domain and deleted PRLD region, thus influencing their biophysical property. These were used to follow their behavior in associating with the SGs in vivo upon stress. Interestingly, there was a difference in their localization to the SG. The YTH deleted mutant showed complete localization to the small and big size granules along with the m⁶A -RNA. But the mutant with deleted PRLD showed poor localization to the SG. This suggests that the hydrophobic interaction exhibited by the PRLD region of this RNA binding protein plays a critical role during its assembling on the SGs. This points for an investigation towards its probable role to enhance the phase separation of the m⁶A RNA by the support of protein-protein interactions.

Amid, it came to light that the reader protein indeed enhances the phase separation potential of RNA during SG assembly (Fu & Zhuang, 2020) and is also crucial for the process during oxidative stress. More interestingly they did suggest that both the disordered domain and the folded family domain-YTH is equally crucial for SG assembly. Another study (Zaccara & Jaffrey, 2020) highlighted that YTHDF1/2/3 show equal potential to be part of the SG. The two contradicting observations reflects a need for additional studies with different experimental approach to obtain better clarification on the relation between YTHDF protein and SGs related to m⁶A RNA for better understanding of their fundamental biological impact.

5.2 Difference in translation recovery of methylated and unmethylated SG clients

The RNA composition of SGs is quite diverse and does not follow the principle of abundance dependent behavior (Khong *et al*, 2017). The physical principle and targeting efficiency of mRNA accumulation in SGs correlates with major parameters being, inefficient translation and the length of cds and 3'UTR of the transcript that can play a role in efficient binding to RBP. But, while mRNA-binding proteins can clearly play a role in the overall assembly of SGs whether they dictate the specific mRNAs localized to SGs remains unknown.

We tried to solve whether the transcripts that enter the SG show a difference in behavior during translation recovery upon stress relief. To study this, we took to the approach of polysome profiling followed by RNA sequencing of the translating fraction upon stress relief. In the SGs there are more than 50% transcripts that are m⁶A methylated, with stress-induced m⁶A methylation (Anders *et al*, 2018). The criteria for methylation was also determined based on correlation analysis of the physical properties of the methylated versus unmethylated groups of SG transcripts (section 2.3.5). We observed that the main parameter for cells selecting transcripts for methylation was mostly based on the abundance and the 3'UTR, cds length. The methylated SG transcripts leaves the

granule at an early time point during relief and to understand comparative behavior of these two groups: methylated and unmethylated SG transcripts, their abundance was compared from the polysome fraction upon early and late time points of relief.

It was noted that after 30 mins of relief when the m⁶A RNA has completely left the SG, the abundance of the methylated mRNA in the translating pool shows higher abundance than the unmethylated ones (section 2.3.2). Most of the transcripts identified in the SG shows its abundant presence in the polysome suggesting that translation recovery happens within this 30mins of the relief. There was a significant difference in the value of abundance of SG transcripts between the methylated and unmethylated groups, suggesting that m⁶A imparts some kind of additional protection during oxidative stress condition. This advantage was however not relevant for longer period of relief.

RNA-m⁶A is a co-transcriptional modification (Zhou *et al*, 2019). Upon mild-inhibition of transcription using Actinomycin-D(Act-D), the m⁶A regulation is disturbed which is mirrored by its effect on the m⁶A metaprofile of transcripts upon arsenite stress (section 2.3.3). This also influenced the abundance of the SG methylated transcripts suggesting the m⁶A plays a key determining factor to signal RNA into SGs for its security. If the abundance in the SG is affected then it ultimately leads us to think that the recovery may also get potentially affected. But from our sequencing results of the translating fraction at early time (30 min) and late time point (4 hr) of relief, there was no change in the genes identified upon Act-D co-treated or untreated with arsenite stress. Only a modestly higher level of the methylated transcripts was identified at the early time point of relief with no Act-D treatment.

The m⁶A methylated SG transcripts was higher abundant in the process of translation recovery that led us to explore the stability imparted by it. Various RNA modification has been studied and known to affect the physical properties of the transcript and consequently regulate cellular and biological processes(Nachtergaele & He, 2018; Roundtree *et al*, 2017; Dimitrova *et al*, 2019; Delaunay & Frye, 2019). The key feature focused here was the effect on the secondary structure by the m⁶A modification to impart stability. Comparing the PARS scores of nucleotide region in vicinity to the modified adenosine, there was a higher secondary structure propensity, mostly 10 nucleotides upstream. This help us to conclude that the m⁶A influences the physical characteristic of the methylated group of transcripts in the SGs and imparts a stability feature that

In sum, the work presented here explored the dynamicity of m⁶A RNA upon oxidative stress with SG assembly and disassembly. The work highlights the fate of the SG transcripts methylated and unmethylated subsets in terms of translation recovery upon stress relief, indicating a higher percentage of methylated transcripts back in the translation pool of the cell. Additionally, our work

also reports how the m⁶A may provide an additional advantage to the transcripts by stabilizing folded RNA.

5.3 Method development for tRNA-protein interaction

Through the translation process, tRNA recognizes several protein and RNA molecules, some that discriminate based on tRNA specificity AARSs, mRNA and some that interact with every tRNA (elongation factor Tu (EF-Tu)). Mutation in genes of such interactors leads to human diseases, and thus, making it important to study them by both qualitative and quantitative approaches. To gain insight into the molecular mechanisms of dysregulations at the level of tRNA-protein interactions, we developed a method for quantitative detection of tRNA-binding-proteins interactions. The method relies on the principle of in-vivo-immunoprecipitation where we immunoprecipitated GlyRS from brains of *Gars*^{C201R/+} and WT littermate mice and quantified the amount of tRNA^{Gly} bound to GlyRS. The tRNA-protein complexes are immunoprecipitated from cells or tissues and tRNAs are identified by Northern blot and quantified by a tRNA-specific fluorescent labeling. The tRNA interacting protein is quantified by western blot and the tRNA amount is presented per unit of the interacting protein. The simple and versatile protocol can be easily adapted to any other tRNA binding proteins.

There exists innumerable potential molecular tRNA species, epitomized by their post-transcriptionally modified forms, by the presence of isoacceptors and isodecoders as well as the formation of complexes between tRNA or tRNA fragments and various proteins. This makes it even more challenging to obtain a quantitative measurement between the isoacceptor and isodecoders. With the latest advancement in high-throughput sequencing of tRNA, we could achieve a quantitative output for bound tRNA but still the current sequencing method has not been able to give an unbiased quantitative measurement of the isoacceptors (Kimura *et al*, 2020; Orioli, 2017; Warren *et al*, 2021). In such case, our method will serve the desired tool for both quantitative and qualitative measurement of tRNAs.

This approach was successfully used to distinguish the binding of tRNA^{Gly} to the CMT disease mutant glycine-tRNA-synthetase (GlyRS) implicated in Charcot-Marie-Tooth disease, compared to wild type synthetase protein (Zuko *et al*, 2021). This study demonstrated CMT-mutant GlyRS sequesters a large fraction of cellular tRNA^{Gly} and thus depleting them for translation. With the current method developed we added in-vivo experimental evidence supporting this mechanism. The greatest advantage of this approach is that with a practical amount of starting material we obtain good output for both validation and quantification of specific tRNAs bound to the protein from both cell culture and tissue samples.

REFERENCES

1. Abbott JA, Francklyn CS & Robey-Bond SM (2014) Transfer RNA and human disease . *Front Genet* 5: 158 (<https://www.frontiersin.org/article/10.3389/fgene.2014.00158>) [PREPRINT]
2. Abdurashidova GG, Tsvetkova EA & Budowsky EI (1991) Direct tRNA-protein interactions in ribosomal complexes. *Nucleic Acids Res* 19: 1909–1915
3. Achilli F, Bros-Facer V, Williams HP, Banks GT, AlQatari M, Chia R, Tucci V, Groves M, Nickols CD, Seburn KL, *et al* (2009) An ENU-induced mutation in mouse glycyl-tRNA synthetase (GARS) causes peripheral sensory and motor phenotypes creating a model of Charcot-Marie-Tooth type 2D peripheral neuropathy. *Dis Model Mech* 2: 359–373
4. Aitken CE & Lorsch JR (2012) A mechanistic overview of translation initiation in eukaryotes. *Nat Struct Mol Biol* 19: 568–576
5. Alberti S & Dormann D (2019) Liquid–Liquid Phase Separation in Disease. *Annu Rev Genet* 53: 171–194
6. de Almeida Gonçalves K, Bressan GC, Saito Â, Morello LG, Zanchin NIT & Kobarg J (2011) Evidence for the association of the human regulatory protein Ki-1/57 with the translational machinery. *FEBS Lett* 585: 2556–2560
7. Alriquet M, Calloni G, Martínez-Limón A, Delli Ponti R, Hanspach G, Hengesbach M, Tartaglia GG & Vabulas RM (2020) The protective role of m1A during stress-induced granulation. *J Mol Cell Biol* 12: 870–880
8. Ananthan J, Goldberg AL & Voellmy R (1986) Abnormal proteins serve as eukaryotic stress signals and trigger the activation of heat shock genes. *Science (80-)* 232: 522–524
9. Anders M, Chelysheva I, Goebel I, Trenkner T, Zhou J, Mao Y, Verzini S, Qian SB & Ignatova Z (2018) Dynamic m⁶A methylation facilitates mRNA triaging to stress granules. *Life Sci Alliance* 1: 1–12
10. Anderson P & Kedersha N (2002) Stressful initiations. *J Cell Sci* 115: 3227–3234
11. Anderson P & Kedersha N (2008) Stress granules: the Tao of RNA triage. *Trends Biochem Sci* 33: 141–150
12. Anderson P & Kedersha N (2009) RNA granules: post-transcriptional and epigenetic modulators of gene expression. *Nat Rev Mol Cell Biol* 10: 430–436
13. Aprile-Garcia F, Tomar P, Hummel B, Khavaran A & Sawarkar R (2019) Nascent-protein ubiquitination is required for heat shock–induced gene downregulation in human cells. *Nat Struct Mol Biol* 26: 137–146
14. Arguello AE, DeLiberto AN & Kleiner RE (2017) RNA Chemical Proteomics Reveals the N6-Methyladenosine (m⁶A)-Regulated Protein–RNA Interactome. *J Am Chem Soc* 139: 17249–17252
15. Arrigo AP, Suhan JP & Welch WJ (1988) Dynamic changes in the structure and intracellular locale of the mammalian low-molecular-weight heat shock protein. *Mol Cell Biol* 8: 5059–5071
16. Aulas A, Stabile S & Velde C Vande (2012) Endogenous TDP-43, but not FUS, contributes to stress granule assembly via G3BP. *Mol Neurodegener* 7: 1–15
17. Aylett CHS & Ban N (2017) Eukaryotic aspects of translation initiation brought into focus. *Philos Trans R Soc London Ser B, Biol Sci* 372
18. Babu MM (2016) The contribution of intrinsically disordered regions to protein function, cellular complexity, and human disease. *Biochem Soc Trans* 44: 1185–1200
19. Banani SF, Lee HO, Hyman AA & Rosen MK (2017) Biomolecular condensates: organizers of cellular biochemistry. *Nat Rev Mol Cell Biol* 18: 285–298
20. Barbieri I, Tzelepis K, Pandolfini L, Shi J, Millán-Zambrano G, Robson SC, Aspris D, Migliori V, Bannister AJ & Han N (2017) Promoter-bound METTL3 maintains myeloid leukaemia by m⁶A-dependent translation control. *Nature* 552: 126–131
21. Barciszewska MZ, Perrigue PM & Barciszewski J (2016) tRNA--the golden standard in molecular biology. *Mol Biosyst* 12: 12–17

22. Baron DM, Kaushansky LJ, Ward CL, Sama RRK, Chian R-J, Boggio KJ, Quaresma AJC, Nickerson JA & Bosco DA (2013) Amyotrophic lateral sclerosis-linked FUS/TLS alters stress granule assembly and dynamics. *Mol Neurodegener* 8: 1–18
23. Beckham CJ & Parker R (2008) P bodies, stress granules, and viral life cycles. *Cell Host Microbe* 3: 206–212
24. Begovich K & Wilhelm JE (2020) An In Vitro Assembly System Identifies Roles for RNA Nucleation and ATP in Yeast Stress Granule Formation. *Mol Cell* 79: 991-1007.e4
25. Behrens A, Rodschinka G & Nedialkova DD (2021) High-resolution quantitative profiling of tRNA abundance and modification status in eukaryotes by mim-tRNAseq. *Mol Cell* 81: 1802-1815.e7
26. Betat H & Mörl M (2015) The CCA-adding enzyme: A central scrutinizer in tRNA quality control. *Bioessays* 37: 975–982
27. Boye E & Grallert B (2020) eIF2 α phosphorylation and the regulation of translation. *Curr Genet* 66: 293–297
28. Brengues M & Parker R (2007) Accumulation of polyadenylated mRNA, Pab1p, eIF4E, and eIF4G with P-bodies in *Saccharomyces cerevisiae*. *Mol Biol Cell* 18: 2592–2602
29. Bresson S, Shchepachev V, Spanos C, Turowski TW, Rappsilber J & Tollervey D (2020) Stress-Induced Translation Inhibition through Rapid Displacement of Scanning Initiation Factors. *Mol Cell* 80: 470-484.e8
30. Buchan JR & Parker R (2009) Eukaryotic Stress Granules: The Ins and Outs of Translation. *Mol Cell* 36: 932–941
31. Del Campo C, Bartholomäus A, Fedyunin I & Ignatova Z (2015) Secondary Structure across the Bacterial Transcriptome Reveals Versatile Roles in mRNA Regulation and Function. *PLoS Genet* 11: e1005613
32. Cao G, Li H-B, Yin Z & Flavell RA (2016) Recent advances in dynamic m6A RNA modification. *Open Biol* 6: 160003
33. Castellani RJ, Gupta Y, Sheng B, Siedlak SL, Harris PLR, Coller JM, Perry G, Lee H, Tabaton M & Smith MA (2011) A novel origin for granulovacuolar degeneration in aging and Alzheimer's disease: parallels to stress granules. *Lab Invest* 91: 1777–1786
34. Cereghetti G, Wilson-Zbinden C, Kissling VM, Diether M, Arm A, Yoo H, Piazza I, Saad S, Picotti P, Drummond DA, *et al* (2021) Reversible amyloids of pyruvate kinase couple cell metabolism and stress granule disassembly. *Nat Cell Biol* 23: 1085–1094
35. Chalupníková K, Lattmann S, Selak N, Iwamoto F, Fujiki Y & Nagamine Y (2008) Recruitment of the RNA helicase RHAU to stress granules via a unique RNA-binding domain. *J Biol Chem* 283: 35186–35198
36. Cherkasov V, Hofmann S, Druffel-Augustin S, Mogk A, Tyedmers J, Stoecklin G & Bukau B (2013) Coordination of translational control and protein homeostasis during severe heat stress. *Curr Biol* 23: 2452–2462
37. Chodasiewicz M, Sokolowska EM, Nelson-Dittrich AC, Masiuk A, Beltran JCM, Nelson ADL & Skirycz A (2020) Identification and characterization of the heat-induced plastidial stress granules reveal new insight into Arabidopsis stress response. *Front Plant Sci* 11
38. Chu J, Cargnello M, Topisirovic I & Pelletier J (2016) Translation Initiation Factors: Reprogramming Protein Synthesis in Cancer. *Trends Cell Biol* 26: 918–933
39. Chu Y, Kilikevicius A, Liu J, Johnson KC, Yokota S & Corey DR (2020) Argonaute binding within 3'-untranslated regions poorly predicts gene repression. *Nucleic Acids Res* 48: 7439–7453
40. Collier NC, Heuser J, Levy MA & Schlesinger MJ (1988) Ultrastructural and biochemical analysis of the stress granule in chicken embryo fibroblasts. *J Cell Biol* 106: 1131–1139
41. Collier NC & Schlesinger MJ (1986) The dynamic state of heat shock proteins in chicken embryo fibroblasts. *J Cell Biol* 103: 1495–1507
42. Cui QI, Shi H, Ye P, Li L, Qu Q, Sun G, Sun G, Lu Z, Huang Y & Yang C-G (2017) m6A RNA methylation regulates the self-renewal and tumorigenesis of glioblastoma stem cells. *Cell Rep* 18: 2622–2634

43. Dai C (2018) The heat-shock, or HSF1-mediated proteotoxic stress, response in cancer: from proteomic stability to oncogenesis. *Philos Trans R Soc B Biol Sci* 373: 20160525
44. Dallaire P, Tan H, Szulwach K, Ma C, Jin P & Major F (2016) Structural dynamics control the MicroRNA maturation pathway. *Nucleic Acids Res* 44: 9956–9964
45. Damgaard CK & Lykke-Andersen J (2011) Translational coregulation of 5' TOP mRNAs by TIA-1 and TIAR. *Genes Dev* 25: 2057–2068
46. Decker CJ & Parker R (2012) P-bodies and stress granules: possible roles in the control of translation and mRNA degradation. *Cold Spring Harb Perspect Biol* 4: a012286
47. Delaunay S & Frye M (2019) RNA modifications regulating cell fate in cancer. *Nat Cell Biol* 21: 552–559
48. Dierks D, Garcia-Campos MA, Uzonyi A, Safra M, Edelheit S, Rossi A, Sideri T, Varier RA, Brandis A, Stelzer Y, *et al* (2021) Multiplexed profiling facilitates robust m6A quantification at site, gene and sample resolution. *Nat Methods* 18: 1060–1067
49. Dimitrova DG, Teyssset L & Carré C (2019) RNA 2'-O-methylation (Nm) modification in human diseases. *Genes (Basel)* 10: 117
50. Dobin A, Davis CA, Schlesinger F, Drenkow J, Zaleski C, Jha S, Batut P, Chaisson M & Gingeras TR (2013) STAR: ultrafast universal RNA-seq aligner. *Bioinformatics* 29: 15–21
51. Dominissini D, Nachtergaele S, Moshitch-Moshkovitz S, Peer E, Kol N, Ben-Haim MS, Dai Q, Di Segni A, Salmon-Divon M, Clark WC, *et al* (2016) The dynamic N1-methyladenosine methylome in eukaryotic messenger RNA. *Nature* 530: 441–446
52. Du H, Zhao Y, He J, Zhang Y, Xi H, Liu M, Ma J & Wu L (2016) YTHDF2 destabilizes m6A-containing RNA through direct recruitment of the CCR4–NOT deadenylase complex. *Nat Commun* 7: 1–11
53. Duan Y, Du A, Gu J, Duan G, Wang C, Gui X, Ma Z, Qian B, Deng X, Zhang K, *et al* (2019) PARylation regulates stress granule dynamics, phase separation, and neurotoxicity of disease-related RNA-binding proteins. *Cell Res* 29: 233–247
54. Edupuganti RR, Geiger S, Lindeboom RGH, Shi H, Hsu PJ, Lu Z, Wang S-Y, Baltissen MPA, Jansen PWTC, Rossa M, *et al* (2017) N6-methyladenosine (m6A) recruits and repels proteins to regulate mRNA homeostasis. *Nat Struct Mol Biol* 24: 870–878
55. Eshraghi M, Karunadharma PP, Blin J, Shahani N, Ricci EP, Michel A, Urban NT, Galli N, Sharma M & Ramírez-Jarquín UN (2021) Mutant Huntingtin stalls ribosomes and represses protein synthesis in a cellular model of Huntington disease. *Nat Commun* 12: 1–20
56. Fei J, Richard AC, Bronson JE & Gonzalez RL (2011) Transfer RNA-mediated regulation of ribosome dynamics during protein synthesis. *Nat Struct Mol Biol* 18: 1043–1051
57. Fernández-Millán P, Schelcher C, Chihade J, Masquida B, Giegé P & Sauter C (2016) Transfer RNA: From pioneering crystallographic studies to contemporary tRNA biology. *Arch Biochem Biophys* 602: 95–105
58. Finkel T & Holbrook NJ (2000) Oxidants, oxidative stress and the biology of ageing. *Nature* 408: 239–247
59. Fu Y & Zhuang X (2020) m6A-binding YTHDF proteins promote stress granule formation. *Nat Chem Biol* 16: 955–963
60. Gal J, Kuang L, Barnett KR, Zhu BZ, Shissler SC, Korotkov K V, Hayward LJ, Kasarskis EJ & Zhu H (2016) ALS mutant SOD1 interacts with G3BP1 and affects stress granule dynamics. *Acta Neuropathol* 132: 563–576
61. Gao Y, Pei G, Li D, Li R, Shao Y, Zhang QC & Li P (2019) Multivalent m6A motifs promote phase separation of YTHDF proteins. *Cell Res* 29: 767–769
62. Gilbert W V, Bell TA & Schaening C (2016) Messenger RNA modifications: form, distribution, and function. *Science (80-)* 352: 1408–1412
63. Gilks N, Kedersha N, Ayodele M, Shen L, Stoecklin G, Dember LM & Anderson P (2004) Stress granule assembly is mediated by prion-like aggregation of TIA-1. *Mol Biol Cell* 15: 5383–5398
64. Gkatza NA, Castro C, Harvey RF, Heiß M, Popis MC, Blanco S, Bornelöv S, Sajini AA, Gleeson JG, Griffin JL, *et al* (2019) Cytosine-5 RNA methylation links protein synthesis to

- cell metabolism. *PLoS Biol* 17: e3000297
65. Grabocka E & Bar-Sagi D (2016) Mutant KRAS enhances tumor cell fitness by upregulating stress granules. *Cell* 167: 1803–1813
 66. Grousl T, Ivanov P, Frydlová I, Vasicová P, Janda F, Vojtová J, Malínská K, Malcová I, Nováková L & Janosková D (2009) Robust heat shock induces eIF2 α -phosphorylation-independent assembly of stress granules containing eIF3 and 40S ribosomal subunits in budding yeast, *Saccharomyces cerevisiae*. *J Cell Sci* 122: 2078–2088
 67. Guillén-Boixet J, Kopach A, Holehouse AS, Wittmann S, Jahnel M, Schlüßler R, Kim K, Trussina IREA, Wang J, Mateju D, *et al* (2020) RNA-Induced Conformational Switching and Clustering of G3BP Drive Stress Granule Assembly by Condensation. *Cell* 181: 346–361.e17
 68. Guo L, Kim HJ, Wang H, Monaghan J, Freyermuth F, Sung JC, O’Donovan K, Fare CM, Diaz Z & Singh N (2018) Nuclear-import receptors reverse aberrant phase transitions of RNA-binding proteins with prion-like domains. *Cell* 173: 677–692
 69. Gwon Y, Maxwell BA, Kolaitis R-M, Zhang P, Kim HJ & Taylor JP (2021) Ubiquitination of G3BP1 mediates stress granule disassembly in a context-specific manner. *Science* 372: eabf6548
 70. Halvorsen M, Martin JS, Broadaway S & Laederach A (2010) Disease-associated mutations that alter the RNA structural ensemble. *PLoS Genet* 6: e1001074
 71. Harrison AF & Shorter J (2017) RNA-binding proteins with prion-like domains in health and disease. *Biochem J* 474: 1417–1438
 72. Haselkorn R & Rothman-Denes LB (1973) Protein synthesis. *Annu Rev Biochem* 42: 397–438
 73. He PC & He C (2021) m6A RNA methylation: from mechanisms to therapeutic potential. *EMBO J* 40: e105977
 74. Heckathorn SA, Mueller JK, LaGuidice S, Zhu B, Barrett T, Blair B & Dong Y (2004) Chloroplast small heat-shock proteins protect photosynthesis during heavy metal stress. *Am J Bot* 91: 1312–1318
 75. Heinz S, Benner C, Spann N, Bertolino E, Lin YC, Laslo P, Cheng JX, Murre C, Singh H & Glass CK (2010) Simple combinations of lineage-determining transcription factors prime cis-regulatory elements required for macrophage and B cell identities. *Mol Cell* 38: 576–589
 76. Hentze MW, Castello A, Schwarzl T & Preiss T (2018) A brave new world of RNA-binding proteins. *Nat Rev Mol cell Biol* 19: 327–341
 77. Hofmann S, Cherkasova V, Bankhead P, Bukau B & Stoecklin G (2012) Translation suppression promotes stress granule formation and cell survival in response to cold shock. *Mol Biol Cell* 23: 3786–3800
 78. Hofmann S, Kedersha N, Anderson P & Ivanov P (2021) Molecular mechanisms of stress granule assembly and disassembly. *Biochim Biophys Acta - Mol Cell Res* 1868: 118876
 79. Huang C, Chen Y, Dai H, Zhang H, Xie M, Zhang H, Chen F, Kang X, Bai X & Chen Z (2020) UBAP2L arginine methylation by PRMT1 modulates stress granule assembly. *Cell Death Differ* 27: 227–241
 80. Hwang YE, Baek YM, Baek A & Kim D-E (2019) Oxidative stress causes Alu RNA accumulation via PIWIL4 sequestration into stress granules. *BMB Rep* 52: 196
 81. Jain S, Wheeler JR, Walters RW, Agrawal A, Barsic A & Parker R (2016a) ATPase-modulated stress granules contain a diverse proteome and substructure. *Cell* 164: 487–498
 82. Jain S, Wheeler JR, Walters RW, Agrawal A, Barsic A & Parker R (2016b) ATPase-Modulated Stress Granules Contain a Diverse Proteome and Substructure. *Cell* 164: 487–498
 83. Jang G-J, Jang J-C & Wu S-H (2020) Dynamics and functions of stress granules and processing bodies in plants. *Plants* 9: 1122
 84. Janin M, Ortiz-Barahona V, de Moura MC, Martínez-Cardús A, Llinàs-Arias P, Soler M, Nachmani D, Pelletier J, Schumann U, Calleja-Cervantes ME, *et al* (2019) Epigenetic loss of RNA-methyltransferase NSUN5 in glioma targets ribosomes to drive a stress adaptive translational program. *Acta Neuropathol* 138: 1053–1074

85. Jiang X, Liu B, Nie Z, Duan L, Xiong Q, Jin Z, Yang C & Chen Y (2021) The role of m6A modification in the biological functions and diseases. *Signal Transduct Target Ther* 6: 74
86. Johansson H-O, Brooks DE & Haynes CA (1999) Macromolecular crowding and its consequences. *Int Rev Cytol* 192: 155–170
87. Kapur M & Ackerman SL (2018) mRNA Translation Gone Awry: Translation Fidelity and Neurological Disease. *Trends Genet* 34: 218–231
88. Ke S, Alemu EA, Mertens C, Gantman EC, Fak JJ, Mele A, Haripal B, Zucker-Scharff I, Moore MJ, Park CY, *et al* (2015) A majority of m6A residues are in the last exons, allowing the potential for 3' UTR regulation. *Genes Dev* 29: 2037–2053
89. Kedersha N & Anderson P (2002) Stress granules: sites of mRNA triage that regulate mRNA stability and translatability. *Biochem Soc Trans* 30: 963–969
90. Kedersha N & Anderson PBT-M in E (2007) Mammalian Stress Granules and Processing Bodies. In *Translation Initiation: Cell Biology, High-Throughput Methods, and Chemical-Based Approaches* pp 61–81. Academic Press
91. Kedersha N, Ivanov P & Anderson P (2013) Stress granules and cell signaling: more than just a passing phase? *Trends Biochem Sci* 38: 494–506
92. Kedersha N, Tisdale S, Hickman T & Anderson PBT-M in E (2008) Chapter 26 Real-Time and Quantitative Imaging of Mammalian Stress Granules and Processing Bodies. In *RNA Turnover in Eukaryotes: Nucleases, Pathways and Analysis of mRNA Decay* pp 521–552. Academic Press
93. Kedersha NL, Gupta M, Li W, Miller I & Anderson P (1999a) RNA-binding proteins TIA-1 and TIAR link the phosphorylation of eIF-2 α to the assembly of mammalian stress granules. *J Cell Biol* 147: 1431–1442
94. Kedersha NL, Gupta M, Li W, Miller I & Anderson P (1999b) RNA-binding proteins TIA-1 and TIAR link the phosphorylation of eIF-2 alpha to the assembly of mammalian stress granules. *J Cell Biol* 147: 1431–1442
95. Khong A, Matheny T, Jain S, Mitchell SF, Wheeler JR & Parker R (2017) The Stress Granule Transcriptome Reveals Principles of mRNA Accumulation in Stress Granules. *Mol Cell* 68: 808-820.e5
96. Kierzek E & Kierzek R (2003) The thermodynamic stability of RNA duplexes and hairpins containing N6-alkyladenosines and 2-methylthio-N6-alkyladenosines. *Nucleic Acids Res* 31: 4472–4480
97. Kim JK, Cho J, Kim SH, Kang H-C, Kim D-S, Kim VN & Lee JH (2019) Brain somatic mutations in MTOR reveal translational dysregulations underlying intractable focal epilepsy. *J Clin Invest* 129: 4207–4223
98. Kim S, You S & Hwang D (2011) Aminoacyl-tRNA synthetases and tumorigenesis: more than housekeeping. *Nat Rev Cancer* 11: 708–718
99. Kimura S, Srisuknimit V & Waldor MK (2020) Probing the diversity and regulation of tRNA modifications. *Curr Opin Microbiol* 57: 41–48
100. Kirchner S, Cai Z, Rauscher R, Kastelic N, Anding M, Czech A, Kleizen B, Ostedgaard LS, Braakman I & Sheppard DN (2017a) Alteration of protein function by a silent polymorphism linked to tRNA abundance. *PLoS Biol* 15: e2000779
101. Kirchner S & Ignatova Z (2015) Emerging roles of tRNA in adaptive translation, signalling dynamics and disease. *Nat Rev Genet* 16: 98–112
102. Kirchner S, Rauscher R, Czech A & Ignatova Z (2017b) Microarray-based quantification of cellular tRNAs. *Protoc io*
103. Kosmacz M, Gorka M, Schmidt S, Luzarowski M, Moreno JC, Szlachetko J, Leniak E, Sokolowska EM, Sofroni K, Schnittger A, *et al* (2019) Protein and metabolite composition of Arabidopsis stress granules. *New Phytol* 222: 1420–1433
104. Kramer S, Queiroz R, Ellis L, Webb H, Hoheisel JD, Clayton C & Carrington M (2008) Heat shock causes a decrease in polysomes and the appearance of stress granules in trypanosomes independently of eIF2 α phosphorylation at Thr169. *J Cell Sci* 121: 3002–3014
105. Kuo C, You G, Jian Y, Chen T, Siao Y, Hsu A & Ching T (2020) AMPK-mediated

- formation of stress granules is required for dietary restriction-induced longevity in *Caenorhabditis elegans*. *Aging Cell* 19: e13157
106. Kutchko KM, Sanders W, Ziehr B, Phillips G, Solem A, Halvorsen M, Weeks KM, Moorman N & Laederach A (2015) Multiple conformations are a conserved and regulatory feature of the RB1 5' UTR. *Rna* 21: 1274–1285
 107. Lancaster AK, Nutter-Upham A, Lindquist S & King OD (2014) PLAAC: a web and command-line application to identify proteins with prion-like amino acid composition. *Bioinformatics* 30: 2501–2502
 108. Lasman L, Krupalnik V, Viukov S, Mor N, Aguilera-Castrejon A, Schneir D, Bayerl J, Mizrahi O, Peles S & Tawil S (2020) Context-dependent functional compensation between Ythdf m6A reader proteins. *Genes Dev* 34: 1373–1391
 109. Latsysheva NS, Flock T, Weatheritt RJ, Chavali S & Babu MM (2015) How do disordered regions achieve comparable functions to structured domains? *Protein Sci* 24: 909–922
 110. Lee H, Bao S, Qian Y, Geula S, Leslie J, Zhang C, Hanna JH & Ding L (2019) Stage-specific requirement for Mettl3-dependent m6A mRNA methylation during haematopoietic stem cell differentiation. *Nat Cell Biol* 21: 700–709
 111. De Leeuw F, Zhang T, Wauquier C, Huez G, Kruids V & Gueydan C (2007) The cold-inducible RNA-binding protein migrates from the nucleus to cytoplasmic stress granules by a methylation-dependent mechanism and acts as a translational repressor. *Exp Cell Res* 313: 4130–4144
 112. Leung AKL, Calabrese JM & Sharp PA (2006) Quantitative analysis of Argonaute protein reveals microRNA-dependent localization to stress granules. *Proc Natl Acad Sci* 103: 18125–18130
 113. Li F, Zhao D, Wu J & Shi Y (2014) Structure of the YTH domain of human YTHDF2 in complex with an m6A mononucleotide reveals an aromatic cage for m6A recognition. *Cell Res* 24: 1490–1492
 114. Li Q, Li X, Tang H, Jiang B, Dou Y, Gorospe M & Wang W (2017) NSUN2-mediated m5C methylation and METTL3/METTL14-mediated m6A methylation cooperatively enhance p21 translation. *J Cell Biochem* 118: 2587–2598
 115. Li Y, Bedi RK, Moroz-Omori E V & Caflisch A (2020) Structural and Dynamic Insights into Redundant Function of YTHDF Proteins. *J Chem Inf Model* 60: 5932–5935
 116. Lin S & Gregory RI (2014) Methyltransferases modulate RNA stability in embryonic stem cells. *Nat Cell Biol* 16: 129–131
 117. Lindquist S (1986) The heat-shock response. *Annu Rev Biochem* 55: 1151–1191
 118. Liu C, Rennie WA, Carmack CS, Kanoria S, Cheng J, Lu J & Ding Y (2014) Effects of genetic variations on microRNA: target interactions. *Nucleic Acids Res* 42: 9543–9552
 119. Liu N, Dai Q, Zheng G, He C, Parisien M & Pan T (2015) N6-methyladenosine-dependent RNA structural switches regulate RNA–protein interactions. *Nature* 518: 560–564
 120. Liu N & Pan T (2016) N6-methyladenosine–encoded epitranscriptomics. *Nat Struct Mol Biol* 23: 98–102
 121. Liu N, Zhou KI, Parisien M, Dai Q, Diatchenko L & Pan T (2017) N6-methyladenosine alters RNA structure to regulate binding of a low-complexity protein. *Nucleic Acids Res* 45: 6051–6063
 122. Liu S, Li B, Liang Q, Liu A, Qu L & Yang J (2020) Classification and function of RNA–protein interactions. *WIREs RNA* 11: e1601
 123. Luo Z, Zhang Z, Tai L, Zhang L, Sun Z & Zhou L (2019) Comprehensive analysis of differences of N6-methyladenosine RNA methylomes between high-fat-fed and normal mouse livers. *Epigenomics* 11: 1267–1282
 124. Madeira F, Park YM, Lee J, Buso N, Gur T, Madhusoodanan N, Basutkar P, Tivey ARN, Potter SC & Finn RD (2019) The EMBL–EBI search and sequence analysis tools APIs in 2019. *Nucleic Acids Res* 47: W636–W641
 125. Maharana S, Wang J, Papadopoulos DK, Richter D, Pozniakovskiy A, Poser I, Bickle M,

- Rizk S, Guillén-Boixet J & Franzmann TM (2018) RNA buffers the phase separation behavior of prion-like RNA binding proteins. *Science* (80-) 360: 918–921
126. Mahat DB, Salamanca HH, Duarte FM, Danko CG & Lis JT (2016) Mammalian heat shock response and mechanisms underlying its genome-wide transcriptional regulation. *Mol Cell* 62: 63–78
127. Mao Y, Dong L, Liu X-M, Guo J, Ma H, Shen B & Qian S-B (2019) m⁶A in mRNA coding regions promotes translation via the RNA helicase-containing YTHDC2. *Nat Commun* 10: 1–11
128. Markmiller S, Soltanieh S, Server KL, Mak R, Jin W, Fang MY, Luo E-C, Krach F, Yang D, Sen A, *et al* (2018) Context-Dependent and Disease-Specific Diversity in Protein Interactions within Stress Granules. *Cell* 172: 590-604.e13
129. Marmor-Kollet H, Siany A, Kedersha N, Knafo N, Rivkin N, Danino YM, Moens TG, Olender T, Sheban D & Cohen N (2020) Spatiotemporal proteomic analysis of stress granule disassembly using APEX reveals regulation by SUMOylation and links to ALS pathogenesis. *Mol Cell* 80: 876–891
130. Mateju D, Franzmann TM, Patel A, Kopach A, Boczek EE, Maharana S, Lee HO, Carra S, Hyman AA & Alberti S (2017) An aberrant phase transition of stress granules triggered by misfolded protein and prevented by chaperone function. *EMBO J* 36: 1669–1687
131. Matheny T, Van Treck B, Huynh TN & Parker R (2021) RNA partitioning into stress granules is based on the summation of multiple interactions. *RNA* 27: 174–189
132. Mathieu C, Pappu R V & Taylor JP (2020) Beyond aggregation: Pathological phase transitions in neurodegenerative disease. *Science* 370: 56–60
133. Mauer J, Luo X, Blanjoie A, Jiao X, Grozhik A V, Patil DP, Linder B, Pickering BF, Vasseur J-J, Chen Q, *et al* (2017) Reversible methylation of m⁶A in the 5' cap controls mRNA stability. *Nature* 541: 371–375
134. Maxwell BA, Gwon Y, Mishra A, Peng J, Nakamura H, Zhang K, Kim HJ & Taylor JP (2021) Ubiquitination is essential for recovery of cellular activities after heat shock. *Science* 372: eabc3593
135. Mazroui R, Sukarieh R, Bordeleau M-E, Kaufman RJ, Northcote P, Tanaka J, Gallouzi I & Pelletier J (2006) Inhibition of ribosome recruitment induces stress granule formation independently of eukaryotic initiation factor 2 α phosphorylation. *Mol Biol Cell* 17: 4212–4219
136. McEwen E, Kedersha N, Song B, Scheuner D, Gilks N, Han A, Chen J-J, Anderson P & Kaufman RJ (2005) Heme-regulated inhibitor kinase-mediated phosphorylation of eukaryotic translation initiation factor 2 inhibits translation, induces stress granule formation, and mediates survival upon arsenite exposure. *J Biol Chem* 280: 16925–16933
137. Merrick WC & Pavitt GD (2018) Protein Synthesis Initiation in Eukaryotic Cells. *Cold Spring Harb Perspect Biol* 10
138. Meyer KD, Patil DP, Zhou J, Zinoviev A, Skabkin MA, Elemento O, Pestova TV, Qian S-B & Jaffrey SR (2015) 5' UTR m⁶A Promotes Cap-Independent Translation. *Cell* 163: 999–1010
139. Meyer KD, Saletore Y, Zumbo P, Elemento O, Mason CE & Jaffrey SR (2012) Comprehensive analysis of mRNA methylation reveals enrichment in 3' UTRs and near stop codons. *Cell* 149: 1635–1646
140. Mollet S, Cougot N, Wilczynska A, Dautry F, Kress M, Bertrand E & Weil D (2008) Translationally repressed mRNA transiently cycles through stress granules during stress. *Mol Biol Cell* 19: 4469–4479
141. Molliex A, Temirov J, Lee J, Coughlin M, Kanagaraj AP, Kim HJ, Mittag T & Taylor JP (2015) Phase separation by low complexity domains promotes stress granule assembly and drives pathological fibrillization. *Cell* 163: 123–133
142. Nachtergaele S & He C (2018) Chemical modifications in the life of an mRNA transcript. *Annu Rev Genet* 52: 349–372
143. Niinae T, Ishihama Y & Imami K (2021) Biotinylation-based proximity labelling

- proteomics: basics, applications and technical considerations. *J Biochem*
144. Nover L, Scharf KD & Neumann D (1983) Formation of cytoplasmic heat shock granules in tomato cell cultures and leaves. *Mol Cell Biol* 3: 1648–1655
 145. Nover L, Scharf KD & Neumann D (1989) Cytoplasmic heat shock granules are formed from precursor particles and are associated with a specific set of mRNAs. *Mol Cell Biol* 9: 1298–1308
 146. Ofengand J, Ciesiolka J, Denman R & Nurse K (1986) Structural and functional interactions of the tRNA-ribosome complex. In *Structure, Function, and Genetics of Ribosomes* pp 473–494. Springer
 147. Ohn T, Kedersha N, Hickman T, Tisdale S & Anderson P (2008) A functional RNAi screen links O-GlcNAc modification of ribosomal proteins to stress granule and processing body assembly. *Nat Cell Biol* 10: 1224–1231
 148. Orioli A (2017) tRNA biology in the omics era: Stress signalling dynamics and cancer progression. *Bioessays* 39: 1600158
 149. Park Y-J, Choi DW, Cho SW, Han J, Yang S & Choi CY (2020) Stress Granule Formation Attenuates RACK1-Mediated Apoptotic Cell Death Induced by Morusin. *Int J Mol Sci* 21 doi:10.3390/ijms21155360 [PREPRINT]
 150. Paschen W, Proud CG & Mies G (2007) Shut-down of translation, a global neuronal stress response: mechanisms and pathological relevance. *Curr Pharm Des* 13: 1887–1902
 151. Pedersen JS, Bejerano G, Siepel A, Rosenbloom K, Lindblad-Toh K, Lander ES, Kent J, Miller W & Haussler D (2006) Identification and classification of conserved RNA secondary structures in the human genome. *PLoS Comput Biol* 2: e33
 152. Piovesan D, Necci M, Escobedo N, Monzon AM, Hatos A, Mičetić I, Quaglia F, Paladin L, Ramasamy P, Dosztányi Z, *et al* (2021) MobiDB: intrinsically disordered proteins in 2021. *Nucleic Acids Res* 49: D361–D367
 153. Poljšak B & Milisav I (2012) Clinical implications of cellular stress responses. *Bosn J basic Med Sci* 12: 122–126
 154. Protter DSW & Parker R (2016) Principles and Properties of Stress Granules. *Trends Cell Biol* 26: 668–679
 155. Ramanathan M, Porter DF & Khavari PA (2019) Methods to study RNA–protein interactions. *Nat Methods* 16: 225–234
 156. Repici M, Hassanjani M, Maddison DC, Garção P, Cimini S, Patel B, Szegő ÉM, Straatman KR, Lilley KS & Borsello T (2019) The Parkinson’s disease-linked protein DJ-1 associates with cytoplasmic mRNP granules during stress and neurodegeneration. *Mol Neurobiol* 56: 61
 157. Riback JA, Katanski CD, Kear-Scott JL, Pilipenko E V, Rojek AE, Sosnick TR & Drummond DA (2017) Stress-triggered phase separation is an adaptive, evolutionarily tuned response. *Cell* 168: 1028–1040
 158. Richter D & Isono K (1977) The mechanism of protein synthesis-initiation, elongation and termination in translation of genetic messages. *Curr Top Microbiol Immunol* 76: 83–125
 159. Ries RJ, Zaccara S, Klein P, Olarerin-George A, Namkoong S, Pickering BF, Patil DP, Kwak H, Lee JH & Jaffrey SR (2019) m⁶A enhances the phase separation potential of mRNA. *Nature* 571: 424–428
 160. Ritossa F (1962) A new puffing pattern induced by temperature shock and DNP in *Drosophila*. *Experientia* 18: 571–573
 161. von Roretz C, Marco S Di, Mazroui R & Gallouzi I (2011) Turnover of AU-rich-containing mRNAs during stress: a matter of survival. *Wiley Interdiscip Rev RNA* 2: 336–347
 162. Roundtree IA, Evans ME, Pan T & He C (2017) Dynamic RNA modifications in gene expression regulation. *Cell* 169: 1187–1200
 163. Salari R, Kimchi-Sarfaty C, Gottesman MM & Przytycka TM (2013) Sensitive measurement of single-nucleotide polymorphism-induced changes of RNA conformation: application to disease studies. *Nucleic Acids Res* 41: 44–53








164. Sanders DW, Kedersha N, Lee DSW, Strom AR, Drake V, Riback JA, Bracha D, Eeftens JM, Iwanicki A, Wang A, *et al* (2020) Competing Protein-RNA Interaction Networks Control Multiphase Intracellular Organization. *Cell* 181: 306-324.e28
165. Schmidt CA & Matera AG (2020) tRNA introns: Presence, processing, and purpose. *Wiley Interdiscip Rev RNA* 11: e1583
166. Sharma DK, Bressler K, Patel H, Balasingam N & Thakor N (2016) Role of eukaryotic initiation factors during cellular stress and cancer progression. *J Nucleic Acids* 2016
167. Shepard PJ & Hertel KJ (2008) Conserved RNA secondary structures promote alternative splicing. *Rna* 14: 1463–1469
168. Shi H, Wang X, Lu Z, Zhao BS, Ma H, Hsu PJ, Liu C & He C (2017) YTHDF3 facilitates translation and decay of N6-methyladenosine-modified RNA. *Cell Res* 27: 315–328
169. Shi Y, Fan S, Wu M, Zuo Z, Li X, Jiang L, Shen Q, Xu P, Zeng L & Zhou Y (2019) YTHDF1 links hypoxia adaptation and non-small cell lung cancer progression. *Nat Commun* 10: 1–14
170. Shih J-W, Wang W-T, Tsai T-Y, Kuo C-Y, Li H-K & Wu Lee Y-H (2011) Critical roles of RNA helicase DDX3 and its interactions with eIF4E/PABP1 in stress granule assembly and stress response. *Biochem J* 441: 119–129
171. Shorter J (2017) Liquidizing FUS via prion-like domain phosphorylation. *EMBO J* 36: 2925–2927
172. Sidrauski C, McGeachy AM, Ingolia NT & Walter P (2015) The small molecule ISRIB reverses the effects of eIF2 α phosphorylation on translation and stress granule assembly. *Elife* 4
173. Sies H (1997) Oxidative stress: oxidants and antioxidants. *Exp Physiol Transl Integr* 82: 291–295
174. Silvera D, Formenti SC & Schneider RJ (2010) Translational control in cancer. *Nat Rev Cancer* 10: 254–266
175. Slobodin B, Han R, Calderone V, Vrieling JAFO, Loayza-Puch F, Elkon R & Agami R (2017) Transcription Impacts the Efficiency of mRNA Translation via Co-transcriptional N6-adenosine Methylation. *Cell* 169: 326-337.e12
176. Solís EJ, Pandey JP, Zheng X, Jin DX, Gupta PB, Airoidi EM, Pincus D & Denic V (2016) Defining the essential function of yeast Hsf1 reveals a compact transcriptional program for maintaining eukaryotic proteostasis. *Mol Cell* 63: 60–71
177. Souquere S, Mollet S, Kress M, Dautry F, Pierron G & Weil D (2009) Unravelling the ultrastructure of stress granules and associated P-bodies in human cells. *J Cell Sci* 122: 3619–3626
178. Sternglanz H & Bugg CE (1973) Conformation of N6-methyladenine, a base involved in DNA modification: restriction processes. *Science* 182: 833–834
179. Tahmasebi S, Khoutorsky A, Mathews MB & Sonenberg N (2018) Translation deregulation in human disease. *Nat Rev Mol Cell Biol* 19: 791–807
180. Tosar JP & Cayota A (2020) Extracellular tRNAs and tRNA-derived fragments. *RNA Biol* 17: 1149–1167
181. Van Treeck B, Protter DSW, Matheny T, Khong A, Link CD & Parker R (2018) RNA self-assembly contributes to stress granule formation and defining the stress granule transcriptome. *Proc Natl Acad Sci* 115: 2734 LP – 2739
182. Tyler M, S. RB & Roy P (2021) Transcriptome-Wide Comparison of Stress Granules and P-Bodies Reveals that Translation Plays a Major Role in RNA Partitioning. *Mol Cell Biol* 39: e00313-19
183. Vihervaara A, Duarte FM & Lis JT (2018) Molecular mechanisms driving transcriptional stress responses. *Nat Rev Genet* 19: 385–397
184. Vihervaara A & Sistonen L (2014) HSF1 at a glance. *J Cell Sci* 127: 261–266
185. Villeneuve NF, Sun Z, Chen W & Zhang DD (2009) Nrf2 and p21 regulate the fine balance between life and death by controlling ROS levels. *Cell cycle* 8: 3255











186. Voellmy R (1984) The heat shock genes: a family of highly conserved genes with a superbly complex expression pattern. *BioEssays* 1: 213–217
187. Wan Y, Qu K, Ouyang Z & Chang HY (2013) Genome-wide mapping of RNA structure using nuclease digestion and high-throughput sequencing. *Nat Protoc* 8: 849–869
188. Wang B, Maxwell BA, Joo JH, Gwon Y, Messing J, Mishra A, Shaw TI, Ward AL, Quan H, Sakurada SM, *et al* (2019a) ULK1 and ULK2 Regulate Stress Granule Disassembly Through Phosphorylation and Activation of VCP/p97. *Mol Cell* 74: 742-757.e8
189. Wang J, Ishfaq M, Xu L, Xia C, Chen C & Li J (2019b) METTL3/m(6)A/miRNA-873-5p Attenuated Oxidative Stress and Apoptosis in Colistin-Induced Kidney Injury by Modulating Keap1/Nrf2 Pathway. *Front Pharmacol* 10: 517
190. Wang X, Lu Z, Gomez A, Hon GC, Yue Y, Han D, Fu Y, Parisien M, Dai Q, Jia G, *et al* (2014) N6-methyladenosine-dependent regulation of messenger RNA stability. *Nature* 505: 117–120
191. Wang X, Zhao BS, Roundtree IA, Lu Z, Han D, Ma H, Weng X, Chen K, Shi H & He C (2015) N6-methyladenosine modulates messenger RNA translation efficiency. *Cell* 161: 1388–1399
192. Warren JM, Salinas-Giegé T, Hummel G, Coots NL, Svendsen JM, Brown KC, Drouard L & Sloan DB (2021) Combining tRNA sequencing methods to characterize plant tRNA expression and post-transcriptional modification. *RNA Biol* 18: 64–78
193. Wek RC, Jiang H-Y & Anthony TG (2006) Coping with stress: eIF2 kinases and translational control. *Biochem Soc Trans* 34: 7–11
194. Wheeler JR, Matheny T, Jain S, Abrisch R & Parker R (2016) Distinct stages in stress granule assembly and disassembly. *Elife* 5: e18413
195. Wilkinson E, Cui Y-H & He Y-Y (2021) Context-Dependent Roles of RNA Modifications in Stress Responses and Diseases. *Int J Mol Sci* 22 doi:10.3390/ijms22041949 [PREPRINT]
196. Wolozin B & Ivanov P (2019) Stress granules and neurodegeneration. *Nat Rev Neurosci* 20: 649–666
197. Wu H & Fuxreiter M (2016) The structure and dynamics of higher-order assemblies: amyloids, signalosomes, and granules. *Cell* 165: 1055–1066
198. Xu C, Liu K, Ahmed H, Loppnau P, Schapira M & Min J (2015) Structural Basis for the Discriminative Recognition of N6-Methyladenosine RNA by the Human YT521-B Homology Domain Family of Proteins*. *J Biol Chem* 290: 24902–24913
199. Yang P, Mathieu C, Kolaitis R-M, Zhang P, Messing J, Yurtsever U, Yang Z, Wu J, Li Y, Pan Q, *et al* (2020) G3BP1 Is a Tunable Switch that Triggers Phase Separation to Assemble Stress Granules. *Cell* 181: 325-345.e28
200. Yao P & Fox PL (2013) Aminoacyl-tRNA synthetases in medicine and disease. *EMBO Mol Med* 5: 332–343
201. Yongdae S & P. BC (2017) Liquid phase condensation in cell physiology and disease. *Science (80-)* 357: eaaf4382
202. Yoshizawa T, Nozawa R-S, Jia TZ, Saio T & Mori E (2020) Biological phase separation: cell biology meets biophysics. *Biophys Rev* 12: 519–539
203. Zaborske JM, Narasimhan J, Jiang L, Wek SA, Dittmar KA, Freimoser F, Pan T & Wek RC (2009) Genome-wide analysis of tRNA charging and activation of the eIF2 kinase Gcn2p. *J Biol Chem* 284: 25254–25267
204. Zaccara S & Jaffrey SR (2020) A Unified Model for the Function of YTHDF Proteins in Regulating m6A-Modified mRNA. *Cell* 181: 1582-1595.e18
205. Zhao Y, Samal E & Srivastava D (2005) Serum response factor regulates a muscle-specific microRNA that targets Hand2 during cardiogenesis. *Nature* 436: 214–220
206. Zheng G, Qin Y, Clark WC, Dai Q, Yi C, He C, Lambowitz AM & Pan T (2015) Efficient and quantitative high-throughput tRNA sequencing. *Nat Methods* 12: 835–837
207. Zhou KI, Shi H, Lyu R, Wylder AC, Matuszek Z, Pan JN, He C, Parisien M & Pan T (2019) Regulation of Co-transcriptional Pre-mRNA Splicing by m6A through the Low-







Complexity Protein hnRNPG. *Mol Cell* 76: 70-81.e9



208. Zuko A, Mallik M, Thompson R, Spaulding EL, Wienand AR, Been M, Tadenev ALD, van Bakel N, Sijlmans C, Santos LA, *et al* (2021) tRNA overexpression rescues peripheral neuropathy caused by mutations in tRNA synthetase. *Science* (80-) 373: 1161–1166

List of the hazardous substances used by GHS (hazard symbols, H&P statements)

Substance	Pictogram	Signal word	Hazard statements	Precautionary statements
2-[4-(2-hydroxy-ethyl)piperazin-1-yl]ethane-sulfonic acid (HEPES)				
	Not a dangerous substance according to GHS			
2-Mercaptoethanol		Danger	301+331, 310, 315, 317, 318, 373, 410	273, 280, 302+352, 304+340,
Acetone		Danger	225, 319, 336	305+351+338, 308+310
Acrylamide/Bis-acrylamide		Danger	302+332, 315, 317, 319, 340, 350, 361f, 372	201, 305+351+338, 370+378, 403+235, 201, 261, 280, 304+340+312, 305+351+338, 308+313
Agarose				
	Not a dangerous substance according to GHS			
Ammonium acetate				
	Not a dangerous substance according to GHS			
Ammonium persulfate		Danger	272, 302, 315, 317, 319, 334, 335	220, 261, 280, 305+351+338, 342+311, 261, 280,
Ampicillin		Danger	315, 317, 319, 334, 335	305+351+338, 342+311
Bromophenol blue				
	Not a dangerous substance according to GHS			
Chloramphenicol		Warning	351	280
Chloroform		Danger	302, 331, 315, 319, 351, 361d, 336, 372	261, 281, 305+351+338

					201, 280, 301+330+331,
Dimethyl sulfoxide	Not a dangerous substance according to GHS				
					
Dimethyl sulfate		Danger	330, 341, 350		302+352, 304+340, 305+351+338, 308+310
Dithiothreitol		Warning	302, 315, 319, 335		261, 305+351+338 210, 240, 305+351+338,
Ethanol		Danger	225, 319		403+233
					280, 304+340, 312,
Ethylenediamine-tetraacetic acid		Warning	319, 332, 373		305+351+338, 337+313 261, 280,
					
Folinic acid		Danger	334, 335		305+351+338, 342+311
Formamide		Danger	315, 360D, 373		201, 314
Glycerol	Not a dangerous substance according to GHS				
Glycin		Warning	315, 319, 335		261, 305+351+338
Hydrogen peroxide (30%)		Danger	302, 318		280, 305+351+338,
Isopropyl alcohol		Danger	225, 319, 336		210, 233, 240,
LB-Agar	Not a dangerous substance according to GHS				
LB-Medium	Not a dangerous substance according to GHS				
Luminol	Not a dangerous substance according to GHS				

Magnesium acetate	Not a dangerous substance according to GHS			
Magnesium chloride	Not a dangerous substance according to GHS			
p-Coumaric acid		Warning	315, 319, 335	261, 305+351+338
PEG 8000	Not a dangerous substance according to GHS			
Phenol		Danger	301+311+331, 314, 341, 373, 411	260, 280, 301+330+331+310, 303+361+353, 304+340+310, 305+351+338
Phosphoenol-pyruvate	Not a dangerous substance according to GHS			
Potassium acetate	Not a dangerous substance according to GHS			
Potassium chloride	Not a dangerous substance according to GHS			
Potassium dihydrogen phosphate	Not a dangerous substance according to GHS			
RedSafe	Not a dangerous substance according to GHS			
Sodium acetate	Not a dangerous substance according to GHS			
Sodium azide		Danger	300+310, 373, 410	273, 280, 301+310+330, 302+352+310, 391, 501
Sodium chloride	Not a dangerous substance according to GHS			
Sodium dodecyl sulfate		Danger	228, 302+332, 315, 318, 335, 412	210, 261, 280, 301+312+330, 305+351+338+310, 370+378
Sodium hydrogen phosphate	Not a dangerous substance according to GHS			
SYBR Gold		Warning	227	210, 280, 370+378
Tetramethyl-ethylenediamine		Danger	225, 332, 302, 314	210, 280, 305+351+338, 310

Thiamine	Not a dangerous substance according to GHS			
TRIS acetate	Not a dangerous substance according to GHS			
Trisodium citrate	Not a dangerous substance according to GHS			201, 261, 264, 280, 273, 301+310,
TRIZOL		Danger	314, 335, 341, 373, 412	302+352, 303+361+353, 304+340, 305+351+338
Tween 20	Not a dangerous substance according to GHS			
Urea	Not a dangerous substance according to GHS			
Xylene cyanol FF		Warning	315, 319, 335	261, 305+351+338

Acknowledgments

With all humbleness and gratefulness, I would like to acknowledge my depth to all those who have helped me more than once during this whole period of my PhD. Firstly, I thank Prof. Zoya Ignatova for not only giving me this opportunity but guiding me with timely advice and meticulous scrutiny to put these ideas, well above the level of simplicity and into something concrete. Working with you and your team has been scientifically enriching. I also express my gratitude to Prof. Meliha Karsak, Prof. Daniel Wilson for the rich scientific discussion during the seminar and meetings, and Dr. Antonio Virgilio Failla for the immense help in the microscopy facility at UKE, Hamburg.

I owe a deep sense of gratitude to my parents, Mrs. Gouri Das and Mr. Pradip Kr Das, and my sister Ms. Priyanka Das, who have been a constant support morally with kindness, enthusiasm and believing in me that have enabled me to complete my thesis.

My gratitude to all my previous supervisor and guides: Assoc. Prof. Ravanan Palanyandi ; Assoc. Prof. Sankarganesh Arunachalam Assis. Prof. Podili Koteswaraiah; Prof. Kausik Chakraborty and Assoc. Prof. Koyeli Mapa who have been my inspiration to start my scientific career and pursue a PhD in this field.

I appreciate all the great scientific opportunities given to me by my collaborators: Dr. Yaser Hashem, Prof. Dr. Erik Storkebaum. Along with that I deeply thank my Lab members for the help and vivid discussions during seminar, coffee breaks and meeting. I specially thank Klara Szydlo, Robin Thompson, Nikhil Bharti and Leonardo Santos who have been great peers in the Lab with scientific and friendly cheers. I am also grateful to all my previous lab members who had my initial phase of transition into a new Lab space very comfortable. I express my gratitude to Dr. Suki Albers, from our Lab, to help me with the grammatical correction on my Abstract of the thesis in German language.

I thank my lovely flat mates, Silvia, Jannes and Heidi who were a support with their smallest help and chats, that acted as a mood lifter during the thesis writing time and times away from family here.

Lastly,I am very thankful to my friends here in Hamburg and India: Umesh, Monica, Anindita, Teena, Mugdha, Elicia, Negar and Bhaswar for motivation and every little encouragements throughout this time.

Eidesstattliche Versicherung

Hiermit erkläre ich an Eides statt, die vorliegende Dissertation selbst verfasst und keine anderen als die angegebenen Hilfsmittel benutzt zu haben. Ich versichere, dass diese Dissertation nicht in einem früheren Promotionsverfahren eingereicht wurde.

24.01.2022

Hamburg, den



Sarada Das